SCUOLA INTERNAZIONALE SUPERIORE DI STUDI AVANZATI
INTERNATIONAL SCHOOL FOR ADVANCED STUDIES
Neuroscience Area
Cognitive Neuroscience Curriculum

An fMRI investigation on empathy: physical and social pain, prosocial behavior and the role of the opioid system

Thesis submitted for the degree of
Doctor Philosophiæ

SUPERVISOR:
Dr. Giorgia Silani

CANDIDATE:
Giovanni Novembre

January 2015

JURY

Davide Anchisi
Dipartimento di Scienze Mediche e Biologiche
Università degli Studi di Udine

Geoff Bird
Social, Genetic, and Developmental Psychiatry Centre.
Institute of Psychiatry, Psychology, & Neuroscience, King's College London.

Giuseppe Di Pellegrino
Dipartimento di Psicologia
Università degli Studi di Bologna

Mathew Diamond
Neuroscience Area
International School for Advanced Studies (SISSA), Trieste

Raffaella Rumiati
Neuroscience Area
International School for Advanced Studies (SISSA), Trieste

ACKNOWLEDGEMENTS

Words don't come easy to me (F.R. David, 1982). Especially when it's time to say goodbye. But it's mainly the time to say thanks; hence I will make an attempt.

First of all, I really need to express my profound gratitude to my wonderful supervisor, Giorgia. I can proudly claim to be her first PhD student: for sure, many others will follow, but you know… they say "you never forget your first" (hopefully in a positive way!). I have learned many things from her, and she has always been helpful even when the beautiful and sweet Mila arrived.

I also want to thank Claus for his help in many aspects. Particularly, it was a great honor for me to collaborate with such a skilled and famous social neuroscientist.

Marco: should I thank you? Whatever I can say will never be as much as what you did for me. I have stressed you out a lot, I'm aware of that; but if I did so, it was only because I perceived your genuine willingness to help me ('*aiutami ti prego, sono ferito!*'). I will never forget how much fun we had in Nottingham and Hamburg. Thank you also for your friendship, I really hope it will still continue for a long time.

I also give special thanks to Migena, my super-sweet Master student, for her help in the experiments. I know I was not the best advisor you could have had, but I did my best and I taught you what I knew. I wish you a brilliant professional career because you deserve it.

Carlotta, do you realize what a godsend you are for me? You never take more than what you give, and I was so lucky to get some attention from you, especially in the hardest moments. Thank you!

Federica, thank you for both the funny and serious moments we spent together planning our experiment and for having hosted me in Vienna, despite not being the perfect housemates for each other. Thanks for letting me discover the avocado in the salad, so tasty!

Hey prof. Patillo! Thanks also to you for all the kinds of support you gave me in the last three years. I feel quite lucky to have met you! You're a brilliant scientist; I'm sure I will hear marvelous things about you and I will proudly say: 'That's a friend of mine!'. Good luck and let's keep in touch.

I am grateful to my wonderful friends: Alessio, Ana Flò, Carol, Cinzia, Elisabetta, Fabrizio, Fiamma, Georgette, Iga, Ina, Luca, Marilena, Massimo, Miriam, Olga, Paola, Seba, and Shima for the very special moments we shared together. I would really spend some words for each of you, but this section would become too long. However you know how special your friendships are for me.

Very special thanks to Alessandro, Ana Laura, Jenny, Laura B. and Vahid for being lovely classmates and friends, especially in the beginning, when my English was terrible and my social skills even worse. If they have improved it also thanks to you. Jenjen thanks for all the innumerable coffees we had together.

Thanks to the friends that have shared the office 231 with me: Rtwik, Sahar, Eugenio, and Yu Qiao. Thanks guys, I had very good times with you.

Thanks to Alessandro, Jenny, Laura C., Severino and Vahid for having lent their support in recording the videos for my experiment. That was precious time stolen from your own activities: really appreciated!

Finally, let me collectively thank all the people who have helped me with my work in Udine, and my life in Trieste, even with the tiniest of actions.

And… thank you Trieste! You are amazingly charming. I will be back to visit you, for sure.

No go le ciave del porton.

Verzime!

Perché non mi ami più?
Perché non mi ami più?

(Free adaptation of Triestinian folk-songs)

CONTENTS

General overview of the thesis

Sociality is a hallmark of great part of the animal kingdom. Several species display a rich variety of social behaviors such as cooperation in offspring safeguard, foraging and defense from predators, but also competition in mating selection, social dominance and territorial supremacy. According to the evolutionary theories, sociality has developed as a survival response to evolutionary processes, increasing the fitness of species showing at least behaviors of parental investment (Smelser and Baltes, 2001).

There is no question but that human societies have reached the highest complexity in terms of social behaviors. During evolution, humans have developed neuronal circuits dedicated to mental abilities that are fundamental to tie social bonds and effective interactions. Human connections, grounded also on the most advanced cognitive functions that can be found in the animal kingdom (e.g. language), come up as complex phenomena to investigate, since they show the highest degree of unpredictability and individual differences (Cziko, 1989). Despite these difficulties, in the last decades scientific research in the field of Social Neuroscience has outlined a bunch of social skills that are considered crucial to explain how humans succeed in understanding others' feeling, actions and intentions. Specifically, empathy, mentalizing and the capacity to understand other's actions are considered the basis of social cognition (Frith and Singer, 2008; Singer, 2012).

The work presented in this thesis collects three fMRI studies mainly focusing on empathy, i.e. the capacity to understand and/or share the emotional state of others (Singer and Lamm, 2009). Empathy is central to human sociality, as it allows us to resonate with others' positive and negative feeling, and consequently adjust our behavior. Not surprisingly, empathy has received a lot of attention in the last decades by neuroscientists, mostly interested to understand how neural circuits implement this ability and which contextual factors modulate their activity and, consequently, the behavioral output. In fact, to this day we know which brain regions are responsible for empathic responses, how empathy is modulated by context and person characteristics, and how empathy integrate with other social skills, e.g. mentalizing, to provide us with accurate representations of others' states (all reviewed in Bernhardt and Singer, 2012).

Meanwhile, we still ignore many other aspects: for instance, which kind of computational processes are executed by empathy´s neural substrates, how empathic responses vary according to the type of observed experience, which neurochemical mechanisms are at the core of empathic responses, or also what is the link between empathic responses and the tendency to behave altruistically (usually referred to as 'prosocial behavior').

The purpose of the work presented in this thesis is providing answers to some of these open questions.

In **Study 1** we aimed at understanding what are the neural substrates of empathy for social pain, a kind of pain that is constantly grabbing increasingly attention among social neuroscientists, and to which extent they overlap with the ones coding for physical pain. Recent research, in fact, has shown that experiencing events that represent a significant threat to social bonds activates a network of brain areas associated with the sensory-discriminative aspects of pain (Kross et al., 2011). By administering participants with a physical and a social pain task in a within-subject design we investigated whether the same brain areas are involved when witnessing social exclusion threats experienced by others and to which extent neural substrates of first-hand and vicarious experiences of the two kinds of pain overlap.

In **Study 2** we investigated brain correlates of prosocial behavior. For this purpose, we explored functional connectivity within brain networks of participants who exhibited either a self-benefit behavior or an altruistic one in a life-threatening situation simulated in a virtual environment. In particular, participants were asked to evacuate a virtual building on fire and, without being previously informed, they were faced with a decision on whether to stop and help a trapped virtual human, at the possible cost of losing their own life in the virtual experience.

In **Study 3** we used a placebo manipulation on a group of participants undergoing first-hand and vicarious painful stimulations in order to observe how the supposed enhancement of endogenous opioids release would affect their behavioral and neurophysiological responses to the painful experience. The comparison was made both with a natural history group (i.e., participants who were not target of the placebo manipulation) and a group of people who did not respond to the placebo manipulation.

Study 1: Empathy for physical and social pain[1,2]

INTRODUCTION

Two dimensions of pain

Pain is a fundamental sensory and affective state that informs us about the relevance of incoming external/internal signals and guides our behavior toward the maintenance of our own welfare and survival (Perl, 2007). Evolutionarily speaking, an efficient detection system of this state (for self and others) has developed in order to prioritize escape, recovery and healing (Williams, 2002). It is well known that a nociceptive stimulus applied to the body activates a broad network of brain areas usually referred to as the 'pain matrix' (Iannetti and Mouraux, 2010), which consists of two distinct yet interacting parts: one coding for the sensory-discriminate features of the stimulus (location, intensity and duration) and the other coding for the affective-motivational component of the painful experience (unpleasantness, negative affect; (Davis, 2000; Peyron et al., 2000). While the former involves mainly the primary and secondary somatosensory cortex (SI, SII), and the posterior insula (pINS), the latter is mainly represented in the anterior insula (aINS) and the anterior-mid part of the cingulate cortex (aMCC/pACC nomenclature according to (Vogt, 2005). Far from having only a 'physical' dimension, pain is also an experience that can occur without direct somatic stimulation. Probably we all are familiar with unpleasant situations after which we feel 'hurt' or 'in pain' even if we were not physically harmed. This kind of pain, which in the field of social psychology has been referred to as 'social pain', is instantiated by events that represent a threat to social relationships (e.g. bereavement, relationship break-up, and exclusion from social activities) and to the attachment system in general

---

[1] This research was published in peer-reviewed journal: G. Novembre, M. Zanon, G. Silani. Empathy for social exclusion involves the sensory-discriminative component of pain: a within-subject fMRI study. *Social Cognitive and Affective Neuroscience*, 2014; DOI: 10.1093/scan/nsu038.

[2] This research was partially funded by the Viennese Science and Technology Fund (WWTF, CS11-016).

(Bowlby, 1969). The use of 'physical' terms in everyday language to describe the feelings related to painful experiences provides a clue of the strong similarities between physical and social pain (see Eisenberger, 2012 for a review).

In the case of social pain, which has mostly been studied by eliciting feelings of exclusion during interactive games (Williams et al., 2000), cerebral activations have been predominantly found in the affective part of the pain matrix (aINS, aMCC, pACC, extending to the more ventral section of the cingulate cortex; Eisenberger et al., 2003; Dewall et al., 2010; Bolling et al., 2011). This suggests that the negative emotional state induced by pain of a social nature does not necessarily involve the activation of the sensory-discriminative part; therefore, excluding one of the hallmarks of the neural response to physically induced pain.

Common substrates for physical and social pain

However, the comparison of neural activations triggered by these two types of pain has so far mainly been based on independent investigations, which either assessed physical or social pain. Therefore, it remains an open question what neural mechanisms they share. One way to overcome this limitation is to measure neuronal and behavioral responses in the same individuals when undergoing the two types of pain.

To date, only one study has addressed this issue by using a within-subject design. Kross et al. (2011) observed neural responses in participants undergoing both physical painful stimulation and social threat. In the social pain task, they were exposed to photos of ex-partners with whom participants had recently experienced an unwanted breakup. Results showed that the neural activity related to the two tasks overlapped not only in the part of the pain network coding for the affective-motivational component of pain (i.e. aMCC and aINS), but also in the dorsal part of the posterior insula (dpINS) and in the parietal operculum (SII), which are areas associated with the sensory-discriminative component of pain. The authors concluded that when social pain is powerfully elicited, it is capable of activating areas that so far were linked only to painful physical experiences.

However, the experience of an unwanted break-up is a rather singular and complex event carrying a multitude of emotional and cognitive consequences. It thus remains to be shown whether everyday experiences of social exclusion activate areas associated with the somatosensory component of physical pain as well. Notably, previous fMRI studies on social exclusion have relied on the Cyberball task (Williams et al., 2000), in

which participants supposedly interact with other players in a virtual ball tossing game, indicated on screen by schematic depictions of these players. It might be argued that this setup is not naturalistic enough to induce strong and ecologically valid feelings of exclusion, due to its computer-game-like appearance. Indeed, previous studies have shown that distinct neural substrates are recruited for perception and representation of real and virtual agents (e.g. cartoons), with the former more capable of allowing mental inferences about others' states and intentions (Han et al., 2005; Mar et al., 2007). These and other findings have recently called on researchers to shift to more ecological paradigms to better approximate real-life social interactions (Kingstone et al., 2008; Risko et al., 2012). In the present study, we therefore developed a version of the Cyberball game by displaying videos of real players tossing the ball to participants, or deliberately excluding them.

Empathy for physical pain and empathy for social pain

The experience of pain has a fundamental role not only for the protection and the survival of the organism, but also for the social relationship among human beings. In fact, part of the nervous system has evolved to detect pain in other individuals, recognize their emotional state and produce behavioral responses appropriate for the social context (Decety, 2011). Given its relevance, in the past few years, functional neuroimaging studies have been mainly focusing on the observation of physical pain inflicted on others in order to provide insights into the mechanisms by which empathy is implemented in the nervous system (de Vignemont and Singer, 2006; Decety and Lamm, 2006; Bastiaansen et al., 2009; Singer and Lamm, 2009; Zaki and Ochsner, 2012).

While the neural underpinnings of empathy for physical and social pain have been extensively explored separately (Singer et al., 2004; Jackson et al., 2005; Lamm et al., 2011; for physical pain, Beeney et al., 2011; Masten et al., 2011b; Meyer et al., 2012 for social pain), it remains unclear to which extent the two experiences share common neural substrates. The most consistent finding of these studies is that empathy for physical pain recruits a core network consisting of aINS and aMCC (Lamm et al., 2011 for a recent meta-analysis). These brain structures jointly seem to be engaged in the representation of emotional states, and in the behavioral and autonomic nervous system regulation required by these states. Hence, it has been suggested that some sort of

'embodied simulation' lies at the root of empathizing with the painful experiences of others, that mainly entail the reactivation of the emotional aspects related to the painful experience (Singer and Lamm, 2009), but under some specific circumstances also the sensorial component (Avenanti et al., 2005; Hein and Singer, 2008; Keysers et al., 2010). Conversely, witnessing another person suffering from pain of a social nature results in the activation of what has been referred to as the 'mentalizing network' (Mitchell et al., 2005a; Amodio and Frith, 2006; Frith and Frith, 2006), but not of the pain network – unless the target of the social exclusion is a person affectively close to the observer, which has been shown to activate the affective-motivational component of the pain network (i.e. MCC and mid-INS; Masten et al., 2011b; Meyer et al., 2012).

One possible interpretation of this distinction between empathy for physical vs. social pain is that while the vicarious experience of physical pain relies on low-level, automatic processes that are easily and automatically activated by means of bottom-up processes such as perception-for-action coupling mechanisms (Preston and de Waal, 2002; Decety and Lamm, 2006), witnessing another person suffering from social pain may require more abstract types of reasoning due to the less aversive and less directly perceivable nature of the social stimulus itself. This will more likely require a deliberate effort of understanding the mental state of the other person rather than triggering a direct affective resonance with her (Eisenberger, 2012). It is however also possible that the experimental paradigms that have been used so far were not particularly effective in inducing sufficiently strong empathic responses for social pain, and that the observed differences between the vicarious experiences of physical and social pain are due to differences in the intensity and ecological validity of empathic experiences. In order to avoid this shortcoming, we developed a more realistic and ecologically valid version of the classical social pain paradigm (Cyberball), to address two main questions.

Aims of the study

First, in light of the results obtained by Kross and colleagues, we aimed at exploring to what extent first person experiences of physical and social pain overlap. Secondly, in addition to what has been reported by Kross and colleagues, we explored commonalities and differences related to the vicarious experience of physical and social pain.

To achieve these aims, we used a within-subject design in which brain and behavioral responses of female participants were observed during a physical pain task and a social

pain task, both including a condition in which the participant was the target of the painful experience (hitherto 'self') and a condition in which she was witnessing another person being in pain (hitherto 'other'). We hypothesized that the vicarious and first-hand experiences of social exclusion share hemodynamic activity in regions of the brain devoted to the processing of the affective-motivational aspects of pain and that it could extend to the activation of somatosensory areas, usually associated with processing of pain of physical nature, regardless the target of the social exclusion.

METHODS

Participants

A total of 23 female participants took part in the fMRI experiment. Female participants of the same age range were recruited to act as confederates in the experiment. Confederates were previously informed about the study and instructed to act as real participants, outside the scanner room. The mean age of the participants was 22.4 years (s.d. = 2.0, range = 20–28). All participants gave informed consent and the study was approved by the Ethics Committee of 'Santa Maria della Misericordia', Udine, Italy. Instructions about the experiment were provided to the participant and the confederate simultaneously to ensure that the participant believed that the confederate would also partake in the experiment. General empathic traits and alexithymic traits were measured with self-report questionnaires (the Interpersonal Reactivity Index; Davis, 1980; and the Bermond-Vorst Alexithymia Questionnaire; Vorst and Bermond, 2001).

fMRI design

The study consisted of two sessions entailing two runs each, performed on the same day. In one session, participants performed the physical pain task and in the other session, the social pain task. Both sessions included a 'self' and 'other' condition. The order of the two sessions was counterbalanced across participants. Therefore, the tasks were organized in a 2 × 2 × 2 within-subject factorial design, with the factors TARGET (self and other), TYPE of pain (physical and social) and INTENSITY of pain (pain and no-pain). In order to increase the ecological validity of the empathy sessions, participants were paired with a real person (confederate) as the target of the 'other' condition (see Singer et al., 2004).

Physical pain task

Stimulus set and apparatus

Electrical pain stimuli were delivered by a bipolar concentric surface electrode (stimulation area: 20 mm^2), which depolarizes predominantly Aδ-fibers, applied on the back of the participants' left hand. We delivered a 100-Hz train of electrical pulses of 2 ms pulse duration (square pulse waveform) for 1s via a direct current stimulator (Digitimer Electronics, model DS7, Hertfordshire, UK). Current amplitude was delivered in a range from 0.1 to 2.0mA, with steps of 0.1 mA.

Experimental paradigm

The experimental paradigm (based on Singer et al., 2004) consisted of two parts: in the first, participant's and confederate's pain thresholds were determined and in the second, the participant entered the scanner and the actual experiment took place. During the pain thresholds determination, participant and confederate had to judge the painfulness of each received stimulus, using a 10-point intensity ratings scale (0 = 'don't feel anything', 1 = 'can feel something but not painful', 2 = 'mildly painful', 8 = 'maximum tolerable pain', 10 = 'worst imaginable pain'). The intensities of the stimulations that the participant and confederate rated as 1 and 8 were noted and then used as stimuli for the 'no-pain' and 'pain' conditions, respectively.

During the fMRI experiment, visual stimuli were presented via goggles connected to the workstation in the MRI console room. Visual stimuli consisted of colored arrows pointing either to participant's hand or away from it. The color of the arrow was an indicator of the target and intensity of the stimulation: dark blue and light blue for, respectively, painful stimulation (self pain) and non-painful stimulation (self no-pain), delivered to the participant in the scanner, while dark pink and light pink for, respectively, painful stimulation (other pain) and non-painful stimulation (other no-pain), delivered to the confederate in the MRI console room. In reality, the confederate did not receive any stimulation.

Each stimulation trial started with a fixation cross in the middle of the screen. Then the arrow appeared and stayed on the screen for 2500 ms, before a circle of the same color appeared (1000 ms), representing the actual delivery of the stimulus. At the end of each stimulus, the participant was asked to rate the valence of emotions felt on a Likert-type rating scale with nine discrete values, from −4 = 'very negative' over 0 to +4 = 'very positive' (4000 ms). The response was given by moving an asterisk from a random

initial position toward the chosen position using the left and right keys on a response pad that the participant held in her right hand (**Figure 1**).

The session was divided in two separate runs of 40 randomized stimulations each (10 self pain, 10 self no-pain, 10 other pain and 10 other no-pain).

Social pain task

The social pain task was designed on the basis of the well-known Cyberball task (Williams et al., 2000), but using records of real people playing the game instead of animated cartoons and adopting the same manipulation of Singer et al. (2004) for the empathy condition. In particular, by replacing cartoons with real people and using a real confederate for the empathy part, we aimed to make the task more ecological and realistic. Videos were recorded using a Digital Video Camcorder (Canon Legria FS406, Tokyo, Japan) and then edited with Final Cut X software (Apple, Cupertino, CA, USA) in order to create black and white silhouettes.

Participants were told that they and the confederate, with whom they were paired, would have been alternatively connected via computer network to other participants controlling the decisions of the other two players visible in the videos, located in adjacent rooms of the building. Therefore, neither the participants nor the confederate met the other players. During the game, the participant was given the opportunity to decide to whom to throw the ball every time she was in possession of it by pressing either the left or the right keys on the pad that she held in her right hand.

The session consisted of two runs: in the first one, the participant herself was engaged in the game; in the second one, she watched the game played by the confederate seated in the MRI console room (while in reality the decisions of the confederate were computer controlled). In both runs, 10 blocks with 12 passes each were performed. The blocks were equally assigned to two conditions: 'social inclusion' and 'social exclusion'. The five blocks that we regarded as 'social inclusion' were the blocks in which the player, either the participant or the confederate, received at least one-third of the total passes (four passes); the remaining five, regarded as 'social exclusion', were the blocks in which the player received less than one-third of the total passes (**Figure 2**). The order of the blocks was fixed, with the first three and the last two blocks belonging to the inclusion condition. The decision to add inclusion blocks at the end of the session (differently from previous studies) was to minimize temporal order effects.

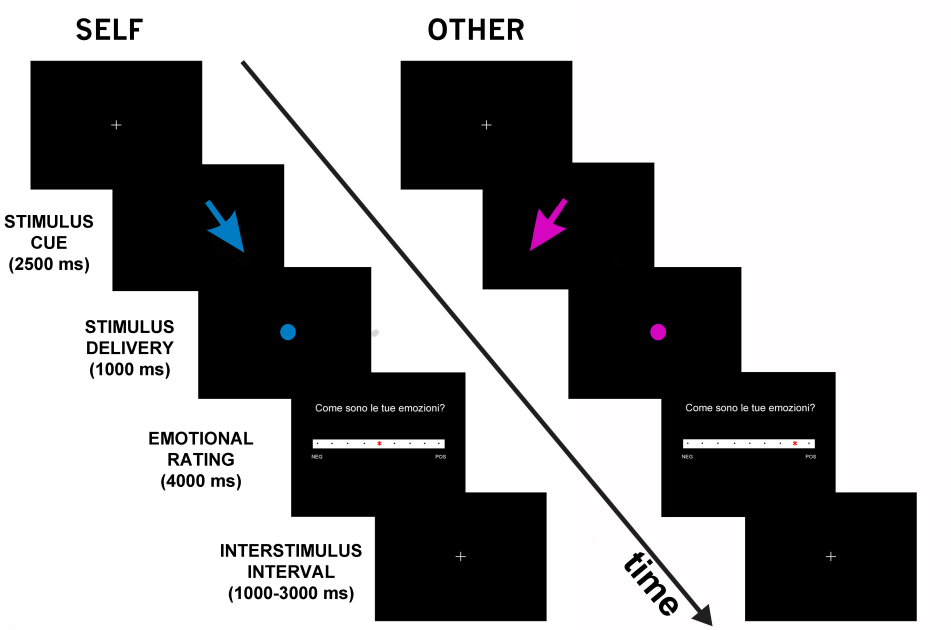

Figure 1 fMRI design for the physical pain task. In each trial, participants were first presented with colored arrows as cues indicating the target, either the participant (self) or the confederate (other) and the intensity (painful or non-painful) of the incoming stimulation. Specifically, dark colors indicated a painful stimulus, whereas light colors were paired with non-painful stimuli (in the figure only dark-colored cues are shown). The actual delivery of the stimulus was signaled by a dot of the same color of the arrow, appearing after 2500 ms. Participants judged their own emotion on a 9-points Likert scale, displayed for 4000 ms, immediately after the stimulation period (1000 ms). Interstimulus interval was randomly jittered (1000–3000 ms).

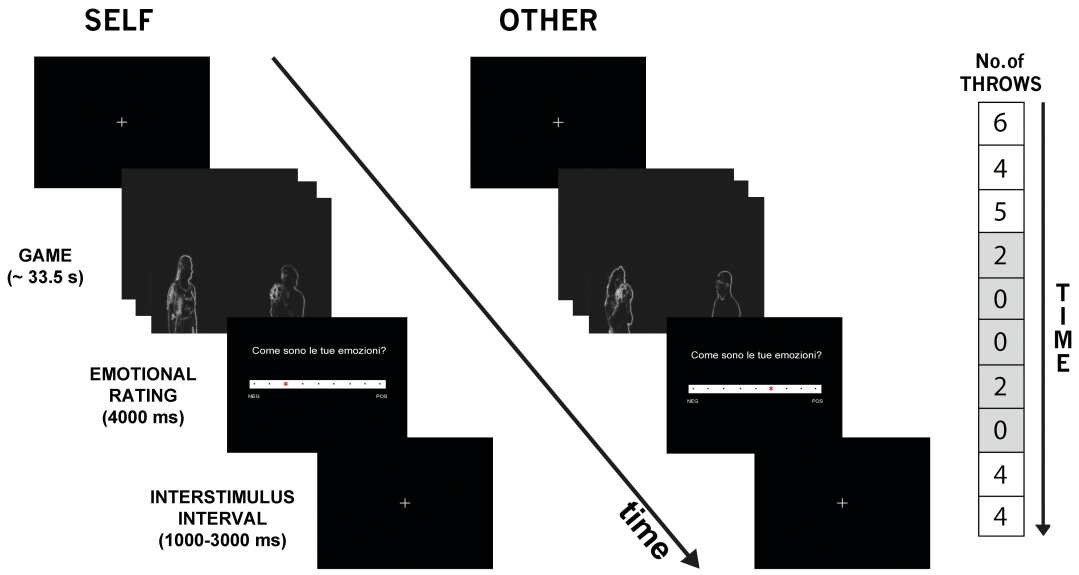

Figure 2 fMRI design for the social pain task. During each trial, participants could receive (or observe receiving for the 'other' condition) the ball from the other two players and decide to whom to throw the ball by pressing the left or the right key on the pad. Each round ended after 12 throws of the ball. Immediately after, they were asked to judge their own emotion on a 9-points Likert scale, displayed for 4000 ms. Interstimulus interval was randomly jittered (1000–3000 ms). On the right, the number of passes received by the player (either the participant or the confederate) in each of the 10 rounds is indicated. Inclusion rounds are depicted in white, exclusion rounds in gray.

Each block lasted an average duration of 33.5 s (range 30–40 s). At the end of each block, the participant was asked to rate the valence of the emotion felt during the game on a Likert-type rating scale with nine discrete values, from −4 = 'very negative' over 0 to +4 = 'very positive' (4000 ms). The response was given using the same keys used for throwing the ball.

At the end of the scanning session, participants were informally asked about the credibility of the entire experiment and debriefed about the deception involved in the Cyberball game. None of them reported to have been suspicious about the setup of the experiment.

fMRI acquisition and pre-processing

A 3 Tesla Philips Achieva whole-body MR Scanner at the Hospital 'Santa Maria della Misericordia' (Udine, Italy), equipped with an 8- channel head coil, was used for MRI scanning. Structural images were acquired as 180 T1-weighted transverse images (0.75 mm slice thickness). Functional images were acquired using a T2*-weighted echo-planar imaging (EPI) sequence with 33 transverse slices covering the whole brain (slice thickness 3.2 mm; interslice gap 0.3 mm; TR/ TE = 2000/35 ms; flip angle = 90°, field of view = 230 × 230 mm^2; matrix size = 128 × 128, SENSE factor 2).

Data were analyzed with SPM8 (Wellcome Department of Imaging Neuroscience, London, UK). All functional volumes were realigned to the first volume, segmented in gray matter, white matter and cerebrospinal fluid tissues, spatially normalized to the standard EPI template, and smoothed using a Gaussian kernel with full width at half maximum (FWHM) of 10 mm^3 (6 mm smoothing at first, 8 mm at second level). Following pre-processing, statistical analysis was carried out using a general linear model approach. High-pass temporal filtering with a cut-off of 128 s was used to remove low-frequency drifts. Regressors of interest were convolved with the canonical hemodynamic response function. The Anatomy Toolbox version 1.6 (Eickhoff et al., 2005) was used for anatomical and cytoarchitectonic interpretation. Whole-brain analyses were thresholded at $P < 0.05$, FWE corrected at the cluster level.

fMRI analysis

Physical pain

In the first-level analysis data were analyzed, separately for each subject. Two separate regressors (stimulation period and rating) were defined for each condition ('self pain', 'self no-pain', 'other pain' and 'other no-pain') for a total of eight regressors for each run. Residual effects of head motion were corrected by including the six estimated motion parameters of each participant as regressors of no interest in the design matrix. Neural activation related to conditions of interest was determined by entering the parameter estimates for the stimulation period regressors into a flexible factorial design ANOVA model (as implemented in SPM8), for random effect inference at the group level (Penny and Holmes, 2004). Linear contrasts of the repeated measure ANOVA with two within-subjects factors: TARGET (self and other) and INTENSITY (pain and no-pain) were used to assess main effects and interactions. Conjunction analyses (Nichols et al., 2005) of the contrasts 'high vs. low pain' for the 'self' and 'other'-related conditions were used in order to identify brain regions commonly activated during the direct and the vicarious experience of physical pain.

Social pain

In the first-level analysis, data were analyzed separately for each subject. Two separate first-level regressors (interaction period and rating) were defined for each condition ('inclusion' and 'exclusion') for a total of four regressors for each of the two runs ('self' and 'other'). Residual effects of head motion were corrected by including the six estimated motion parameters of each participant as regressors of no interest in the design matrix for each of the two runs ('self' and 'other').

Neural activation related to conditions of interest (split up by intensity and target) was determined by entering the parameter estimates for the stimulation period regressors into a flexible factorial design, for random effect inference at the group level (Penny and Holmes, 2004). Linear contrasts of the repeated measure ANOVA with two within-subjects factors: TARGET (self and other) and INTENSITY (exclusion and inclusion) were used to assess main effects and interactions. Conjunction analyses (Nichols et al., 2005) of the contrasts exclusion vs. inclusion for the 'self' and 'other'-related conditions were used in order to identify brain regions commonly activated during the direct and the vicarious experience of social pain.

Physical and social pain

Finally, in order to investigate neural responses shared by the two kinds of pain, the overall contrast images resulting from the first- level analyses of the two tasks were entered in a new flexible factorial design ANOVA with the factors: TARGET (self and other), INTENSITY (pain and no-pain) and TASK (physical and social). Conjunction analyses (Nichols et al., 2005) of the contrasts exclusion vs. inclusion and pain vs. no-pain for the 'self' and 'other'-related conditions were used in order to identify brain regions commonly representing the direct and the vicarious experience of both types of pain.

RESULTS

Behavioral results

Physical pain task

Participants were stimulated with current intensities ranging from 0.1 to 2.0 mA (overall mean of non-painful stimulations: 0.3 (SD = 0.2); overall mean of painful stimulations: 0.9 (SD = 0.6)).

Emotional ratings given by the participants during the physical pain task were analyzed through a repeated measure ANOVA with two within-subject factors: TARGET (self and other) and INTENSITY (pain and no-pain) using SPSS 20 (IBM software).

The analysis showed that the task was able to induce clearly distinct emotions according to the different conditions (**Figure 3A**). In particular, participants judged the stimuli applied to their own hands as more unpleasant than the stimuli applied to the confederate (main effect of TARGET, $F_{(1,22)} = 9.806$, $P = 0.005$); furthermore, they rated the painful stimulations compared with the non-painful ones as more unpleasant (main effect of INTENSITY, $F_{(1,22)} = 36.661$, $P < 0.001$). A trend toward significance was observed for the interaction between TARGET and INTENSITY ($F_{(1,22)} = 4.027$, $P = 0.057$), indicating that painful trials generated more negative judgments in the 'self' condition compared with the other condition (paired-samples *t*-tests, $t = -3.255$, $df = 22$, $P = 0.004$), while ratings in the non-painful trials only showed a trend toward significance ($t = -2.013$, $df = 22$, $P = 0.057$) with the 'other' condition being judged as more positive.

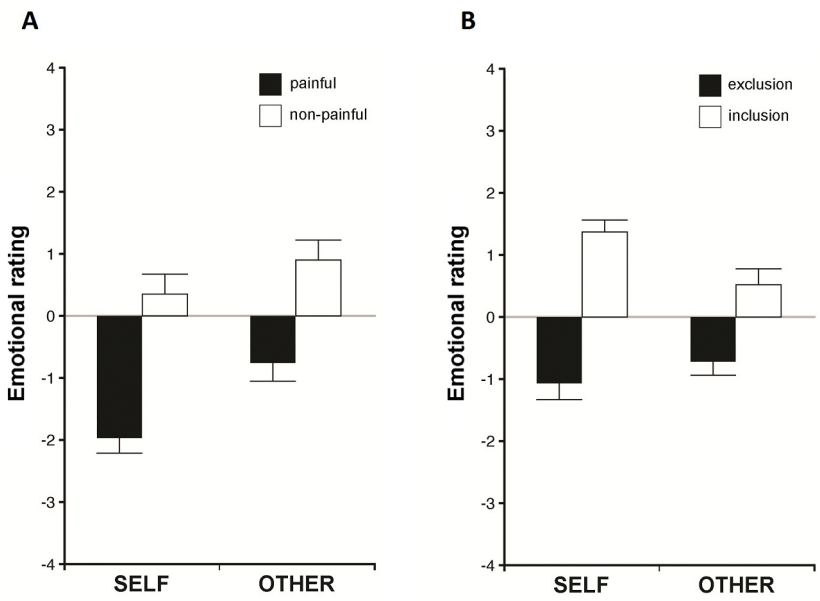

Figure 3 Emotional ratings for the physical pain (A) and social pain (B) tasks. Graphs represent means and standard errors.

Figure 4 Correlation between ratings (High – Low pain trials) for self and other conditions during the physical pain task. Note that the values are converted into positives.

Social pain task

Emotional ratings given by the participants during the social pain task were analyzed through a repeated measure ANOVA with two within- subjects factors: TARGET (self and other) and INTENSITY (exclusion and inclusion) (**Figure 3B**). The analysis showed that the task was effective in eliciting negative affect following the exclusion

from the game. In particular, participants rated more negatively the exclusion (painful) blocks compared with the inclusion (non-painful) ones (main effect of INTENSITY, $F_{(1,22)} = 50.990$, $P < 0.001$). Furthermore, an interaction between TARGET and INTENSITY was observed ($F_{(1,22)} = 18.353$, $P < 0.001$), resulting from inclusion blocks generating more positive judgments in the 'self' condition compared with the other condition (paired-samples *t*-tests, $t = -1.318$, df = 22, P = 0.007). No difference was found between ratings in the exclusion conditions ($t = 2.950$, df = 22, P = 0.201). Finally, no significant main effect of TARGET was observed ($F_{(1,22)} = 1.037$, P = 0.320).

An additional correlation was performed in order to investigate the relationship of the two variables: number of received passes and emotional ratings. The results show that the two variables are significantly correlated in both the 'self' condition ($r = 0.941$, $P < 0.001$) and the 'other' condition ($r = 0.959$, $P < 0.001$) (see **Figure 5**), confirming the association between exclusion from the game and negative affect for both first person and vicarious experience of social pain.

Notably, similarly to the physical pain task, participants judged the experience of being excluded (compared with being fairly treated in the game) and the experience of witnessing another person being excluded in a similar fashion (significant correlation between the difference between inclusion and exclusion ratings in the 'self' and in the 'other' condition, $r = 0.533$, $P = 0.009$, see **Figure 6**).

Physical and social pain tasks

Emotional ratings given by the participants during the two pain tasks were analyzed through a repeated measure ANOVA with three within- subjects factors: TARGET (self and other), INTENSITY (pain and no-pain) and TASK (physical and social).

On top of the main effects already reported in the previous sections, the analysis showed that the two tasks were comparable in eliciting negative affect, as indicated by the non-significant two-way interaction INTENSITY × TASK ($F_{(1,22)} = 0.267$, $P = 0.610$) and non-significant three-way interaction TARGET × INTENSITY × TASK ($F_{(1,22)} = 1.438$, $P = 0.243$), suggesting that the difference between painful and not painful trials and between exclusion and inclusion blocks was similar for both 'self' and the 'other' condition. Furthermore, correlational analysis between ratings given during the physical and social pain tasks for 'self' and 'other' conditions showed a significant correlation

between empathy for physical and social pain (r = 0.571, P = 0.004, see **Figure 7**). No significant correlation between the two types of pain for the self (r = 0.107, P = 0.623) was observed.

Figure 5 Correlation between emotional ratings and number of passes for self and other conditions during the social pain task.

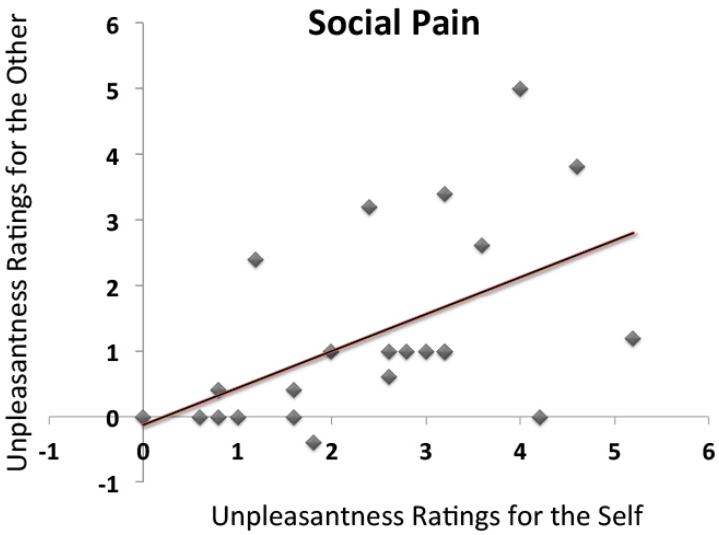

Figure 6 Correlation between ratings (Exclusion – Inclusion trials) for self and other conditions during the social pain task. Note that values are converted into positives.

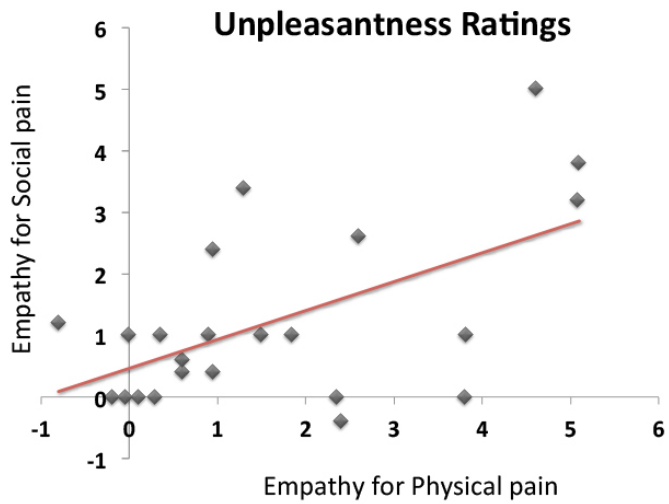

Figure 7 Correlation between ratings for the social and physical pain tasks during the 'other' condition. Note that values are converted into positives.

fMRI results

Physical pain task

Main effect of pain: self (pain > no-pain). Comparison of hemodynamic responses associated with painful vs. non-painful trials in the 'self' condition revealed increased activity in the regions classically associated with pain: anterior mid cingulate cortex (aMCC), posterior mid cingulate cortex (pMCC), bilateral anterior, mid and posterior insula (a, m, p -INS), bilateral postcentral gyrus (SI), thalamus and cerebellum. Other brain areas activated were: left mid frontal gyrus, right precentral gyrus, bilateral superior temporal gyrus, right superior temporal pole, left cuneus ($P < 0.05$, cluster-level corrected, see **Table 1** in Appendix I and **Figure 8**).

Conjunction: self ∩ other (pain > no-pain). In order to test shared activations between 'self' and 'other' for painful vs. non-painful trials, a conjunction analysis was performed. In line with previous findings, perigenual anterior cingulate cortex (pACC) and bilateral aINS were revealed, which are two key areas associated with pain shared between self and other (e.g. Lamm et al., 2011). In addition to these areas of the pain network, we observed significant clusters in right mid superior frontal gyrus, left superior frontal gyrus, left gyrus rectus, right inferior orbitofrontal gyrus, right mid temporal gyrus, right superior temporal pole and right mid temporal pole ($P < 0.05$,

cluster-level corrected, see **Table 2** in Appendix I and **Figure 9**). Note that the main effect of pain: other (pain > no-pain) is shown in **Figure 10** (**Table 3** in Appendix I).

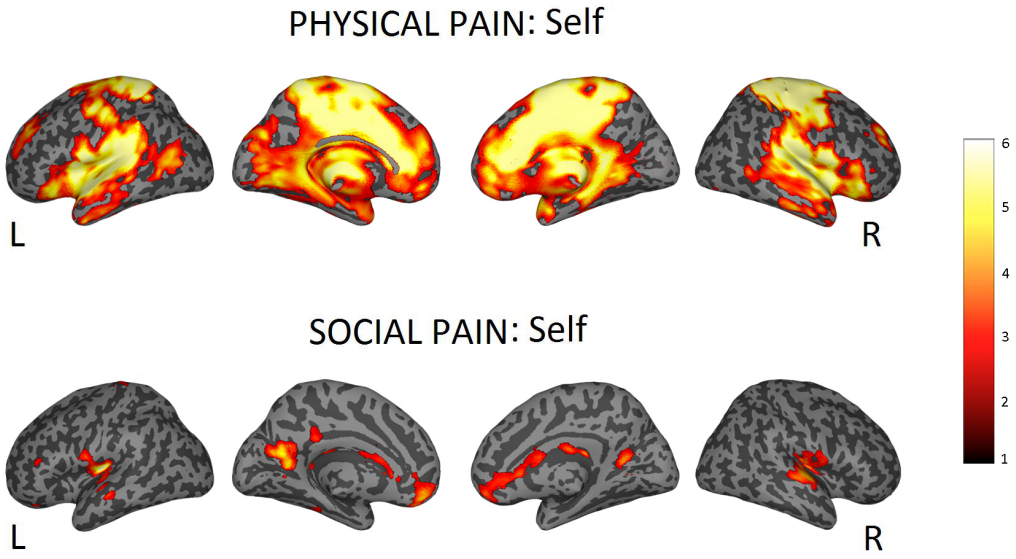

Figure 8 Top part: neural activations for the first person experience of physical pain (contrast: self (pain > no-pain)). Bottom part: neural activations for the first person experience of social exclusion (contrast: self (exclusion > inclusion)). Statistical maps are superimposed on a standard inflated surface (medial and lateral views are showed for each hemisphere). Maps are thresholded at $P < 0.005$ uncorrected, for illustrative purposes.

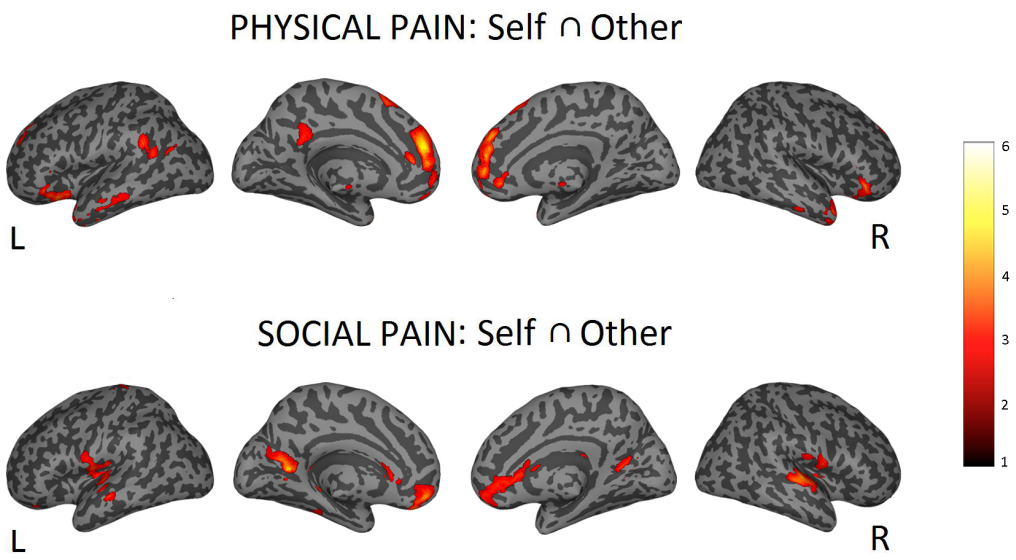

Figure 9 Top part: neural activations for empathy for physical pain (contrast: self ∩ other (pain>no-pain)). Bottom part: neural activations for empathy for social exclusion (contrast: Self ∩ Other (exclusion > inclusion)). Statistical maps are superimposed on a standard inflated surface (medial and lateral views are showed for each hemisphere). Maps are thresholded at $P < 0.005$ uncorrected, for illustrative purposes.

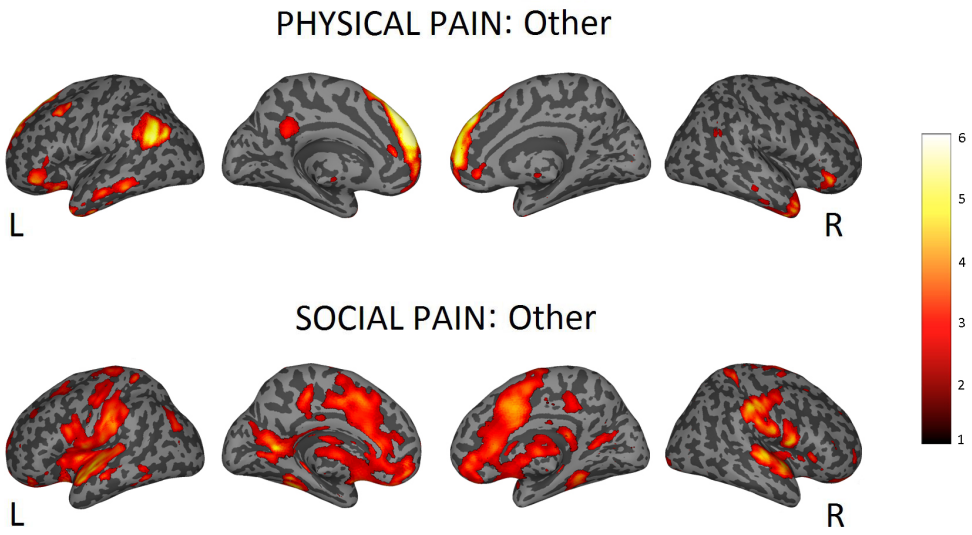

Figure 10 Top part: neural activations for empathy for physical pain (contrast: Other (Pain > No Pain)). Bottom part: neural activations for empathy for social exclusion (contrast: Other (Exclusion > Inclusion)). Statistical maps are superimposed on a standard inflated surface (medial and lateral views are showed for each hemisphere). Maps are thresholded at $p < 0.005$ uncorrected, for illustrative purposes.

Social pain task

Main effect of pain: self (exclusion > inclusion). Comparison of hemodynamic responses between exclusion vs. inclusion trials in the 'self' condition revealed enhanced activity in the following regions: left pINS extending to Rolandic Operculum (SII), right pINS, right subgenual anterior cingulate cortex (sACC), left mid orbitofrontal gyrus, right superior temporal gyrus, left mid temporal gyrus, left calcarine gyrus, caudate bilaterally ($P < 0.05$, cluster-level corrected, see **Table 4** in Appendix I and **Figure 8**).

Conjunction: self ∩ other (exclusion > inclusion). To test for shared brain networks between the direct and vicarious experience of social exclusion, a conjunction analysis was performed. Commonly activated areas belonging to the pain network were: right sACC, bilateral pINS and left Rolandic Operculum (SII). In addition, we observed left mid superior frontal gyrus, right medial orbitofrontal gyrus, bilateral gyrus rectus, bilateral superior temporal gyrus and left mid temporal gyrus ($P < 0.05$, cluster-level corrected, see **Table 6** and **Figure 9**). Note that the main effect of pain: other (exclusion > inclusion) is shown in **Figure 10** (**Table 5** in Appendix I).

Shared networks for physical and social pain

Conjunction: self (pain > no-pain) ∩ self (exclusion > inclusion). In order to test to which extent brain activity associated with physical and social pain is shared, a conjunction analysis was performed between areas recruited during the physical pain and the social exclusion task. Commonly activated areas of the pain network were right sACC, bilateral pINS and left Rolandic Operculum (SII). In addition, we observed left mid orbitofrontal gyrus, right superior temporal gyrus, left mid temporal gyrus, bilateral caudate ($P < 0.05$, cluster-level corrected, see **Table 7** in Appendix I and **Figure 11**).

Conjunction: self (pain > no-pain) ∩ self (exclusion > inclusion) ∩ other (pain > no-pain) ∩ other (exclusion > inclusion). The question about which brain areas commonly represent empathy for social and physical pain was assessed by an overall conjunction analysis. This revealed activation in right sACC and left mid orbitofrontal gyrus ($P < 0.001$, uncorrected, see **Table 8** and **Figure 11**).

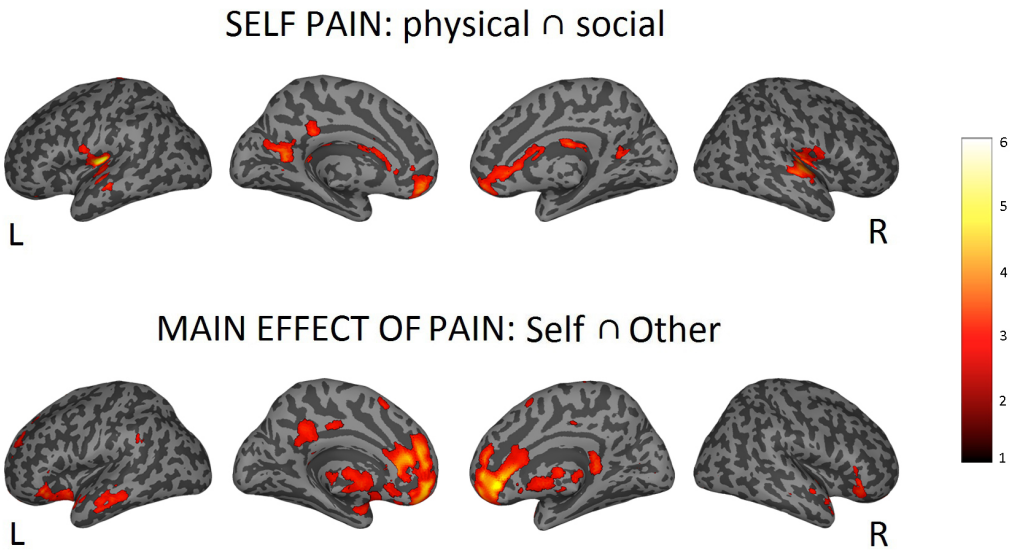

Figure 11 Top part: common neural activations for physical and social pain (contrast: self (pain > no-pain) ∩self (exclusion > inclusion)). Bottom part: common neural activations for empathy for physical and social pain (contrast: self (main effect pain > no-pain and exclusion > inclusion) ∩ other (main effect pain > no-pain and exclusion > inclusion)). Statistical maps are superimposed on a standard inflated surface (medial and lateral views are showed for each hemisphere). Maps are thresholded at $P < 0.005$ uncorrected, for illustrative purposes.

Difference between empathy for physical and social pain.

In order to test which brain areas were selectively engaged in empathy for physical and social pain, respectively, we formally compared the two conditions.

Other (pain > no-pain) > other (exclusion > inclusion). Higher activity in empathy for physical compared with social pain was observed in left mid superior frontal gyrus, right superior frontal gyrus, left inferior temporal gyrus, left angular gyrus and left temporo-parietal junction ($P < 0.05$, cluster-level corrected, see **Table 9** and **Figure 12**).

Other (exclusion>inclusion)>other (pain>no-pain). Higher activity during empathy for social compared with physical pain was observed in several regions, among them: left pMCC, left mINS, bilateral Rolandic Operculum, right supramarginal gyrus, bilateral postcentral gyrus, right superior temporal gyrus, left inferior parietal gyrus, left precuneus, bilateral fusiform gyrus, left mid occipital gyrus, right lingual gyrus, left calcarine gyrus and cerebellum ($P < 0.05$, cluster-level corrected, see **Table 10** and **Figure 12**).

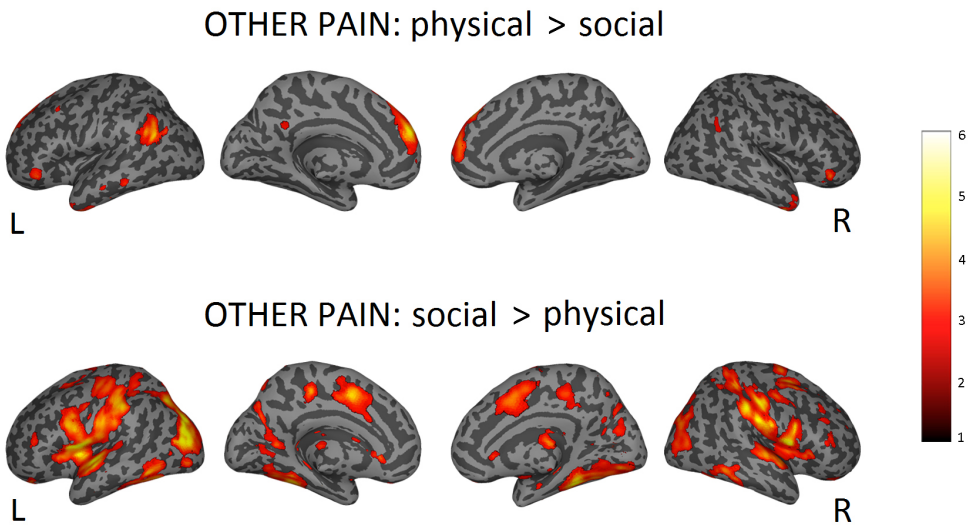

Figure 11 Top part: brain areas more active during the witnessing of the other person suffering from physical pain than from social pain (contrast: other (pain > no-pain) > other (exclusion > inclusion)). Bottom part: brain areas more active during the witnessing of the other person suffering from social pain than from physical pain (contrast: other (exclusion > inclusion) > other (pain > no-pain)). Statistical maps are superimposed on a standard inflated surface (medial and lateral views are showed for each hemisphere). Maps are thresholded at $P < 0.005$ uncorrected, for illustrative purposes.

DISCUSSION

The question to which extent physical and social pain rely on similar neural mechanisms is of growing interest in social neuroscience. In order to address the common and distinct neural substrates of social and physical pain, it needs to be considered whether the subjective experiences of physical and social pain are comparable. Previous studies investigating the neural correlates of first-person experiences of social pain have either used paradigms such as the exclusion from a virtual ball-tossing game (Eisenberger et al., 2003; Masten et al., 2012), or strong experiences of social loss like bereavement and romantic rejection (Kersting et al., 2009; Fisher et al., 2010). While the former studies revealed activation in the affective-motivational component of the pain network (aMCC, pACC and aINS), the latter also observed the involvement of somatosensory areas (pINS, PAG and thalamus, see Eisenberger, 2012, for a review). These inconsistencies might stem from a different degree of emotional involvement and unpleasantness triggered by the different scenarios. Hence, it might be that only bereavement and romantic rejection are powerful enough to elicit feelings of distress that can activate areas related to painful physical experiences.

Apart from differences in emotion involvement, a further complication when trying to identify the shared neural substrates of physical and social pain stems from the fact that these two types of pain have so far mainly been investigated in independent samples. However, evidence that social pain shares activation with the sensory-discriminative part of physical pain has recently been strengthened by Kross et al. (2011). Using a within-subject design, these authors observed that the neural activity related to two tasks involving different types of pain (physical and social) overlapped not only in the part of the pain network coding for the affective-motivational component (i.e. aMCC and aINS), but also in areas associated with the sensory-discriminative one (dpINS and SII). The authors concluded that when social pain is powerfully elicited, in this case by romantic rejection, it is capable of activating areas that so far were linked only to painful physical experiences.

However, as these findings differ from what has been reported in the social rejection literature so far (Eisenberger et al., 2003; Krill and Platek, 2009; Dewall et al., 2010; Masten et al., 2012), the involvement of the somatosensory cortex during social rejection by Kross et al. might relate to the intensity of the social pain experience (and

not only to the fact that their within-subject design might have been more sensitive). Recalling the experience of being subjected to the rejection of the partner is a very particular event and certainly more powerful than being excluded from a virtual game. The question whether everyday experiences of social exclusion activate areas associated with the somatosensory component of physical pain as well therefore remained unclear, so far.

Our study, however, using a within-subject design as well, shows that a modified version of the Cyberball social exclusion game reveals similar findings as during romantic rejection in the involvement of the somatosensory component of the experience. Cyberball is a successfully used approximation of real-life experiences of social exclusion and causes negative affect, as shown by behavioral findings and the consistent recruitment of affective areas such as aMCC, p- and s- ACC and aINS in previous research (Eisenberger et al., 2003; Krill and Platek, 2009; Dewall et al., 2010; Masten et al., 2012). Nevertheless, the strength of the unpleasant experience might be dampened by its computer-like appearance. The first aim of the present study was therefore to test a new and more ecological paradigm for investigating social pain, in order to elicit an aversive emotional response comparable to the one elicited by a physical threat.

The paradigm used video clips of people rather than cartoon manikins, as in Cyberball. It was indeed able to induce aversive feelings during exclusion trials of comparable size to the unpleasantness induced by painful physical stimulation, as indicated by the similar difference between high and low painful stimulation ratings for both types of pain. At the neural level, the first-person experience of social exclusion resulted in increased activity in the sACC, a region that has been found in other Cyberball studies (Masten et al., 2009; Bolling et al., 2011; Bolling et al., 2012; Moor et al., 2012) as part of a pool of areas (aMCC and pACC) involved in experiencing rejection (Eisenberger, 2012; Premkumar, 2012) and that has been associated to self-reported distress in response to social exclusion (Masten et al., 2009; Onoda et al., 2009), although this correlation was not observed in the present study.

sACC has been generally implicated in the processing of sadness (Mayberg et al., 1999; Phan et al., 2002) and negative affect (Drevets et al., 2008; Shackman et al., 2011).

Interestingly, in the specific case of the Cyberball task, sACC has been mainly observed in studies targeting adolescents (Masten et al., 2009; Masten et al., 2011a; Moor et al., 2012) or in paradigms where the excluding players on the screen were represented with

photos of real people (Bolling et al., 2011, 2012), leading to the question of the specific role of this structure in the processing of pain of a social nature.

Besides sACC, the first-hand experience of social exclusion resulted in increased activity also in regions coding for its somatosensory representation, such as pINS and SII. It is crucial to note the use of a within subject design allowed us to assess whether the overlap between the first-hand experience of physical and social pain reflects the recruitment of similar neural processes. This was the case, as shown by the conjunction analysis, which revealed that largely overlapping areas in the somatosensory areas were activated by the two types of pain.

Recent studies addressing the functional organization of the insular cortex have shown that this region can be divided in two or three subdivisions (anterior and mid-posterior, or anterior, mid and posterior, respectively), each associated with different functions (Mutschler et al., 2009; Kurth et al., 2010; Kelly et al., 2012). Specifically, the anterior insula has been mainly linked to emotional-cognitive processes, and the mid-posterior insula to sensorimotor processes, involving the coding of the intensity and the localization of pain, as well as primary interoceptive bodily representation (Craig, 2009).

Therefore, one possible interpretation of this pattern of results is that the increased ecological validity of the present version of the Cyberball task is associated to a more intense experience of social exclusion. The negative emotional experience of being excluded by participants represented on the screen as real people, with human motions and gestures, might have exacerbated the painful consequences of the social exclusion beyond the affective domain to the extent of being perceived as physically painful. However, a rigorous comparison between different versions of the Cyberball task is still lacking. Further studies are needed to clarify the impact of the presentation's modality on perceived negative affect and intensity of the emotion felt.

It is interesting to note, though, that our paradigm did not show the classical affective regions observed in most of the social exclusion studies, such as aINS and pACC/aMCC (Eisenberger, 2012). These regions have been associated not only with painful or aversive events, but in general with the processing of emotional stimuli and cognitive control (Kelly et al., 2012; Shackmann et al., 2011). One possible explanation could therefore be that similar activations during inclusion and exclusion trials alike prevented us from observing the classical affective network when formally comparing them. Indeed, that interpretation was confirmed by our data: in the 'self' condition,

inclusion trials showed similar activation strength as exclusion trials in both aINS and aMCC (see **Figure 1** in **Appendix I).** It is also possible that the order of the exclusion and inclusion blocks adopted in the present study could have played a role. Differently from the majority of previously published studies using the Cyberball paradigm, we decided to minimize temporal order effects by splitting the inclusion blocks in two parts, before and after the exclusion blocks, thus avoiding exclusion blocks being always at the end. Indeed, a repeated measure ANOVA on the emotional ratings of the inclusions trials, with the within factors: TIME (pre-exclusion and post-exclusion) and TARGET (self and other) show that ratings became less positive during post-exclusion trials (main effect of TIME: $F_{(1,22)} = 8.587$, $P = 0.008$) for both 'self' and 'other' conditions (TARGET × TIME: $F_{(1,22)} = 0.725$, $P = 0.404$). The result suggests that exclusion trials or habituation/fatigue could have dampened positive feelings associated with the re-inclusion in the game. Interestingly, neurophysiological data speak for the first hypothesis. In particular, if the last two blocks are perceived more negatively because of the preceding exclusion, we expect to observe increased activation in areas coding for negative affect (such as aMCC and aINS) in the contrast post-exclusion vs. pre-exclusion. This in turn would explain why we failed to observe these areas when contrasting exclusion vs. inclusion. A post hoc analysis indeed revealed that by comparing the last two blocks with the first three blocks of inclusion, no significant increased activation was observed in any of the pain-network regions during the post-exclusion trials, both for 'self' and 'other' conditions. On the contrary, during pre-exclusion trials, increased activation was found in the right pINS (44 −14 2) during the 'self' condition and in the aMCC (−6 14 28) and in the aINS (34 26 14) ($P < 0.05$, cluster-level corrected) for the 'other' condition (see **Figure 2** in Appendix 1). The data therefore suggest that sequence order cannot explain why we did not observe the affective regions classically found in most of the social exclusion studies. Conversely, a possible explanation of this pattern of results is that inclusion shows a general decrease of activations with time, with general arousal effects mainly at the beginning. This interpretation would be in line with the proposed hypothesis of similar activation of the affective network for inclusion and exclusion blocks. However, given the low number of available trials, further clarification about the effect of temporal presentation of stimuli on perceived social exclusion is needed.

The second goal of our study was to address whether the vicarious experience of social pain 'equally hurts'. This was achieved by comparing neural and behavioral responses

when being socially excluded oneself, and when witnessing the exclusion of another person. Our results show that empathy for another person undergoing social discrimination elicits an aversive response that is subserved by the same somatosensory areas that are also involved in the first-hand experience of social exclusion.

According to the few previous neuroscientific studies on empathy for social exclusion, witnessing another person suffering from pain of a social nature generally results in the activation of what has been referred to as the 'mentalizing network' (Mitchell et al., 2005; Amodio and Frith, 2006; Frith and Frith, 2006). In addition, the affective-motivational component associated with pain (i.e. aMCC, pACC and aINS) is activated only if the target of the social exclusion is a person affectively close to the observer (Meyer et al., 2012). Here, we were able to show that the first-person and vicarious experience of social exclusion not only overlaps in areas belonging to the 'mentalizing' network (like the vmPFC), but also in areas processing negative affect (sACC) as well as, more interestingly, the sensory-discriminative component of the painful experience, such as SII and pINS. These findings suggest that some experiences of social exclusion can trigger the same neural reaction for both self- and other-related experiences. This extends models of empathy proposing that this social skill relies on a partial sharing of the affective experiences of others, based on one's own emotional representations in similar experiences (Singer et al., 2004; Bastiaansen et al., 2009). We believe that along with the increased ecological value of our version of Cyberball, the presence of a real confederate as excluded player might have played a role in the emotional resonance process. A final intriguing question addressed in the present work relates to the relationship between empathy for physical and social pain. The conjunction analysis revealed common activation only in one region: the sACC. This area has not been classically associated with empathy for physical or social pain, but mainly with the processing of sadness (Mayberg et al., 1999; Phan et al., 2002) and negative emotions (Drevets et al., 2008; Shackman et al., 2011). Nevertheless, the finding reinforces previous evidence suggesting that the cingulate cortex, including its more rostral portions, plays a pivotal role in the processing of vicarious negative affect. For instance, while recent meta-analyses of empathy mainly stressed the role of medial cingulate cortex, they also indicate engagement of more rostral and subgenual cingulate areas in specific contrasts requiring cognitive skills such as overt evaluation of other emotions (Fan et al., 2011; Lamm et al., 2011; Shackman et al., 2011; Torta and Cauda, 2011). The idea of a common underlying mechanism for empathic responses to any type of

pain receives additional supported by our finding of a significant correlation between emotional ratings given by participants for vicarious experiences of both types of pain. In line with previous neuroscientific findings (Singer et al., 2004; Jackson et al., 2005; Lamm et al., 2011; Fan et al., 2011), our study also showed that witnessing another person suffering from physical pain reactivates areas restricted to the affective part of the pain network (aINS and pACC, in a portion slightly more anterior than the one classically observed though), while the sensorimotor component is not engaged. Conversely, empathy for pain of a social nature activated a more posterior portion of insular cortex and SII. This difference could be related to the different type of paradigm used to induce empathic responses. In particular, while an abstract cue-based paradigm (adapted from Singer et al., 2004) was used to indicate the painfulness and the target of stimulation, during the physical pain task, the social pain task involved the direct witnessing of the other's exclusion. It has recently been argued that cue-based paradigms engage top-down processes for the representation and coding of other's pain, rather than bottom-up sensory-based processes engaged by explicit depictions of painful situations and stimulations (picture-based), or their ensuing bodily expressions (Keysers et al., 2010; Lamm et al., 2011). In fact, when the somatic cause of the pain of the target is attended by the observer (for instance, seeing others' hands painfully stimulated), regions of neural overlap between this experience and the first-person experience are found also in the somatosensory cortices (see Keysers et al., 2010 for a review). The difference between empathy for physical and social pain with respect to somatosensory sharing could therefore be explained with the different way of triggering the empathic responses in the two tasks we used. While in the former, empathy is instantiated by semantic representations and abstract reasoning (top-down processes, mapped to TPJ and dMPFC), the latter used direct observations of the unpleasant event (bottom-up processes, mapped in primary visual and sensorimotor cortex and mid-posterior INS). Consequently, the more picture-based nature of the social pain task could have disclosed the somatosensory resonance with the target, in addition to the affective one. Further studies using comparable paradigms for investigating empathy for painful events are needed to clarify the actual differences between the different types of pain.

LIMITATIONS

The present study addresses important questions related to the neural substrates of physical and social pain and of the empathic responses for both the experiences. The within-subjects design was chosen in order to see the extent of neural overlap between all the conditions, and eventually it proved to convey interesting results.

On the other hand, the paradigm we use leads itself to the problem of spurious generalizations. In fact, it is possible that responses to the different types of pain are enhanced in a situation in which a combination of physical and social negative stimuli is delivered so closely in time.[3]

Similarly, empathic responses, especially in the social pain task, could have been possibly increased by people facing that same situation first, since in the present study participants always witnessed the other participant being excluded after experiencing exclusion at first hand. Further studies should address these problems, investigating the extent of vicarious responses without previous exposure to the same type of experience and separating in time the different types of pain.

Another limitation of the current study lies in the generalization of the results to the whole population. In fact, in order to increase statistical homogeneity, the present study investigated only female participants. Further research is needed to extend the validity of results to the male population.

---

[3] Interestingly that was the case: by comparing participants (labeled PS henceforth, N = 14) that underwent the physical pain task first, and participants (labeled SP henceforth, N = 9) that performed the social pain task first, we observed order effects. Specifically, we found higher activation for the social pain task in the PS group, in the sACC [4 12 −6], caudate [14 20 −6], right medial orbitofrontal gyrus [6 46 −10], right superior orbitofrontal gyrus [12 66 −16], right inferior orbitofrontal gyrus [28 34 −16], right insula [40 24 −8] ($P < 0.05$, cluster-level corrected). Interestingly, aMCC [16 24 28] was also found activated at threshold of $P < 0.001$, uncorrected. No evidence for activation differences was observed when comparing the physical pain task. These findings could be interpreted as a possible spillover effect of the unpleasant experience of physical pain to the unpleasantness of social exclusion. It is also possible that the observed difference between the two groups in the social pain task is not related to the nature of the preceding task (physical pain) but rather to the order of presentation of the task itself. Given the small sample size and the impossibility to disentangle these two hypotheses, further experiments targeting these issues are needed.

Study 2: Prosocial behavior[1,2]

INTRODUCTION

Contemporary human societies show the highest levels of complexity and social relationships, compared to any other animal species. Even if it is still a puzzle for many social scientists, such a complexity seems to be the driving force that has favored the evolution of a larger and more complex brain (Byrne and Bates, 2007; Dunbar and Shultz, 2007; Silk, 2007). During evolution, humans have developed neuronal circuits dedicated to mental abilities that are fundamental to tie social bonds and effective interactions. Specifically, empathy, mentalizing and the capacity to understand other's actions are considered the basis of social cognition, (see Frith and Singer, 2008; Singer, 2012). Furthermore, evolution has promoted moral systems as well as cooperative and caring behaviors that go beyond relatedness and genetic similarities (Fehr and Fischbacher, 2003; Boyd, 2006). It has been recently proposed that intergroup competition and reproductive leveling might have allowed the proliferation of a genetically transmitted predisposition to behave altruistically (Bowles, 2006), i.e. engaging in actions that increase the benefits of other individuals, even if at our own costs. Despite the importance of this social phenomenon, the understanding of its neurophysiological basis is far from being complete (Lieberman, 2012; Singer, 2012), and some questions are greatly unsolved, such as why altruistic actions are so differently engaged among individuals and which cognitive and neurophysiological mechanisms are predictive of such behaviors.

In social neuroscience, the investigation of prosociality, fairness and altruism has taken advantage mainly of socio-economic games and other paradigms in which participants were asked to decide monetary allocation between themselves and another person

[1] This research was published in a peer-reviewed journal: Zanon, M., Novembre, G., Zangrando, N., Chittaro, L., & Silani, G. (2014). Brain activity and prosocial behavior in a simulated life-threatening situation. *NeuroImage*.

[2] This research was partially funded by the Viennese Science and Technology Fund (WWTF, CS11-016).

(Rilling et al., 2002) or spontaneously donate a certain amount of their income (FeldmanHall et al., 2012a; Morishima et al., 2012; Waytz et al., 2012). However, altruistic behaviors do not always imply exclusively monetary losses in order to increase the welfare of another person, but also actions that could involve physical threat to the agent and, in the most extreme case, pose a risk to the agent's own life. Because of obvious experimental and ethical consideration, most of neuroscience studies investigating helping behaviors under physical threat have used scenarios with very limited ecological validity, such those described by a text or cartoon strips. As a result, it is difficult to transfer experimental findings to real-life contexts. FeldmanHall and collaborators have recently taken into account the effect of contextual information on participants' altruistic behavior (FeldmanHall et al., 2012a; FeldmanHall et al., 2012b). To investigate the gap between moral judgment and moral action, they observed that the amount of information available to the participants influences their choices in a 'Pain vs. Gain' paradigm. In particular, the more abstract the context, and the higher the need of mentalizing, the bigger is the gap between beliefs of acting altruistically and real behaviors. This study focused specifically on moral decisions, but demonstrated the difference between judgments and actions and that very limited scenarios may not accurately reflect social behaviours in everyday life. It therefore pinpointed the importance of ecologically valid and action-relevant experimental paradigms for testing complex behaviors such as moral cognition and prosocial behaviors (FeldmanHall et al., 2012b).

So far, only few studies have used real-life paradigms suitable for addressing the question of altruistic behavior under physical threat. An example is provided by Hein and colleagues who observed physiological and behavioral responses of participants who were given the possibility to prevent another person from suffering from physical pain, by 'sacrificing' themselves as the target of the painful stimulation. They showed that the strength of empathy-related skin conductance responses predicts later costly helping (Hein et al., 2011). Similarly, the authors provided evidence that activity in brain areas involved in empathy, such as the anterior insula, predicts the costly helping behavior later in time (Hein et al., 2010). Moreover, they observed that participants helped more frequently other participants considered as ingroup members, rather than outgroup members, and thus demonstrated that social context can influence prosocial decision-making.

In the present study, we aimed at extending the knowledge about the neurophysiology of prosocial decision making, by combining Virtual Reality (VR) with Independent Component Analysis (ICA) of fMRI data. In particular, we used VR to simulate a life-threatening situation, in which participants were faced with the decision whether to save another participant, risking their own life. The employed methodology allowed us to avoid two main shortcomings in social neuroscience: on one hand, we were able to provide a contextually rich environment that the experimenter can control, without the obvious practical and ethical constraints of the classical experimental paradigms (Bohil et al., 2011); on the other hand, we were able to decode brain activity during a flowing experience, when no a priori models of signal changes are available (McKeown et al., 1998; Spiers and Maguire, 2007; Bressler and Menon, 2010; Beckmann, 2012).

Since the first studies that applied ICA as a model-free approach to fMRI data, it has been demonstrated that segregated patterns of neuronal activity can be consistently identified and that these intrinsic connectivity networks (ICNs) are present both at rest or during task performance (Damoiseaux et al., 2006; Bressler and Menon, 2010; Beckmann, 2012; Arbabshirani et al., 2013). Typically, ICNs include primary sensory and motor cortices, the default-mode network and attentive networks. It has been suggested that they represent functional networks, spatially segregated by the fact that they are differentially recruited according to the type of ongoing mental process (Cole et al., 2010).

By comparing neuronal activity between participants who showed a prosocial or a selfish behavior, we aimed at identifying the cognitive processes involved in social decision during a life-threatening situation. We hypothesized that the main differences among the groups would be observed in the salience network (Seeley et al., 2007; Bressler and Menon, 2010) and in the anterior part of the default-mode network (Harrison et al., 2008a; Uddin et al., 2009). The former comprises the anterior insula and the anterior cingulate cortex, two cortical areas involved in social cognition, empathy and prosocial behavior (Bernhardt and Singer, 2012), the later is constituted by the medial prefrontal cortex, a key brain region for social cognition (Mitchell et al., 2005b; Bzdok et al., 2013).

METHODS

Participants

Forty-three healthy young adults (30 women, 13 men, M_{age}: 22,8, age range: 21-30 years, all right-handed) participated in the study and received a monetary compensation for their participation. All participants reported no neurological diseases and no history of head injury, and their visual capacity was normal or corrected to normal by MRI scanner compatible goggles. The study was approved by the ethics committee of the hospital 'Santa Maria della Misericordia' (Udine, Italy), where the MRI scans were performed. Before starting the experiment, exhaustive information about the procedure was provided and participants gave informed consent. Outside the scanner, before and after the experiment, the participants were asked for a self-reported evaluation on the dimensions of tension, sadness and anxiety, by means of a Visual Analog Scale (VAS). Specifically, the opposite ends of the three scales were respectively tagged as 'relaxed' and 'tense', 'happy' and 'sad', 'calm' and 'anxious' (in Italian, the three scales were respectively tagged as 'rilassato' and 'nervoso', 'felice' and 'triste', 'tranquillo' and 'ansioso'); the midpoint of each scale was also indicated. Furthermore, at the end of the experiment, general empathic tendency and alexithymic traits were measured respectively with the Interpersonal Reactivity Index (IRI) (Davis, 1980) and the Bermond-Vorst Alexithymia Questionnaire (BVAQ-B) (Vorst and Bermond, 2001). Finally, sense of presence experienced in the virtual environment was evaluated with the Igroup Presence Questionnaire (IPQ) (Schubert et al., 2001), freely available at http://www.igroup.org/pq/ipq/index.php. The IPQ is a 14-item self-report scale, subdivided in 3 subscales and a general item related to 'the sense of being there' (presence). Subscales are aimed to evaluate three independent dimensions of the VR experience, i.e. spatial presence (5 items), involvement (4 items) and experienced realism (4 items). All IPQ items are statements and respondents have to rate their degree of agreement on a 7-point Likert scale, ranging from -3 to +3.

Procedures and measures

Participants' behavior during a life-threatening situation was evaluated by using a computer-based environment developed by the Human-Computer Interaction

Laboratory (HCI Lab), at the Department of Mathematics and Computer Science (University of Udine, Italy). In particular, an emergency evacuation experience of a building on fire was simulated in VR. The virtual experience was implemented using the C# programming language and NeoAxis (http://www.neoaxisgroup.com), a game engine based on the Ogre rendering engine (http://www.ogre3d.org). Participants were told to behave in the virtual environment as they would in a real-world situation and thus to evacuate the building as quickly as possible, by following the clearly visible exit signs, which reproduced accurately the familiar signs that are legally mandatory for public buildings in the participants' country (see **Figure 1C**). To increase sense of presence in the simulated experience, the scenario was experienced from a first-person perspective (Vogeley and Fink, 2003; Vogeley et al., 2004; Slater et al., 2010), using fMRI-compatible goggles and earphones. Participants could move and act in the virtual environment by pressing four buttons on two fMRI-compatible response pads: index, middle and annular fingers of the right hand were used to move respectively leftward, forward and rightward, whereas index finger of the left hand was used to interact with objects in the virtual environment. Indeed, participants knew that a message appear on the lower part of the screen, whenever it was possible to perform an action on a virtual object, e.g. opening a door in front of them.

Before starting the virtual experience, participants were familiarized with buttons usage by navigating a small virtual building (**Figure 1A**) and interacting with objects in it. For instance, when a participant approached a closed door, the word 'open' ('apri' in Italian) was displayed in the lower part of the screen and (s)he could decide to open the door by pressing the button on the left pad. At the end of this familiarization phase, participants were asked to lift and move away three boxes placed in an empty room of the environment. When approaching any of the three objects, the word 'push' ('spingi' in Italian) appeared on the screen (**Figure 1A**). To simulate the effort needed for successfully moving the box, the participant had to repetitively press the button on the left pad, until the object moved (41 button presses were required to move away the object). The time to successfully move each of the three objects (MovingTime) was recorded to measure variability in the speed of button presses across participants. The familiarization phase ended when the participant moved all three boxes. The participant was then virtually placed in a meeting room (**Figure 1B)** of a large building, together with three virtual humans; (s)he was told that the virtual humans were avatars controlled by other human participants, who were going to perform the same task from computers

located in another building (Department of Mathematics and Computer Science). In fact, the movements of the virtual humans were pre-programmed and controlled by the computer application. The participant was free to explore the meeting room for about a minute and observe the behaviors of the other virtual humans. If (s)he approached the virtual humans, they did not engage in social interaction but continued to move in the environment or stare at objects or from windows. The task started when a voice message on the public address system and a subsequent emergency bell alerted the participant that a fire had broken out in the building and all people had to evacuate it immediately by following the emergency signs (see **Figure 1C**). Throughout the simulation, visual and auditory cues were delivered to provide aversive feedback and to increase the feeling of danger and unpleasant emotions. In particular, the emergency bell and the speaker voice were repeated and the participant ran into smoke and fire along the way. Furthermore, the participant heard the sound of her/his own avatar coughing due to smoke inhalation and the visual field was reduced when (s)he was in danger, to simulate tunnel vision phenomena that occur in high stress conditions. Finally, participants were warned about the risk to their life by a bar indicating their remaining 'life energy' (see **Figure 1C**). Using aversive visual and auditory feedback similar to that summarized above was found to be effective in creating an experience of risk and danger in VR (Chittaro and Zangrando, 2010).

Toward the end of the path to exit the building, participants unexpectedly encountered an injured male virtual human previously seen in the meeting room but now lying on the floor, trapped under a heavy cabinet and asking for help (see **Figure 1C**). Each participant was thus faced with the dilemma of either exiting the building without stopping or spending time at the possible cost of his/her own life to help the trapped virtual human, by moving away the heavy. The amount of effort to move away the cabinet and free the virtual human was set to 150 button presses. When the participant engaged in the attempt to move the cabinet, two stimuli emphasized the presence of danger: (i) a flashing red aura in the peripheral visual field, and (ii) heartbeat sound at a progressively increasing frequency, played through the headphones. Note that from the beginning of the evacuation, the energy bar decreased at the same rate for each participant, thus they all had the same very low amount of 'life energy' left when they encountered the trapped virtual human. Furthermore, if a participant stopped to rescue the virtual human, the bar kept decreasing, although the decrease was controlled in such a way that the participant could not “die” in the virtual experience.

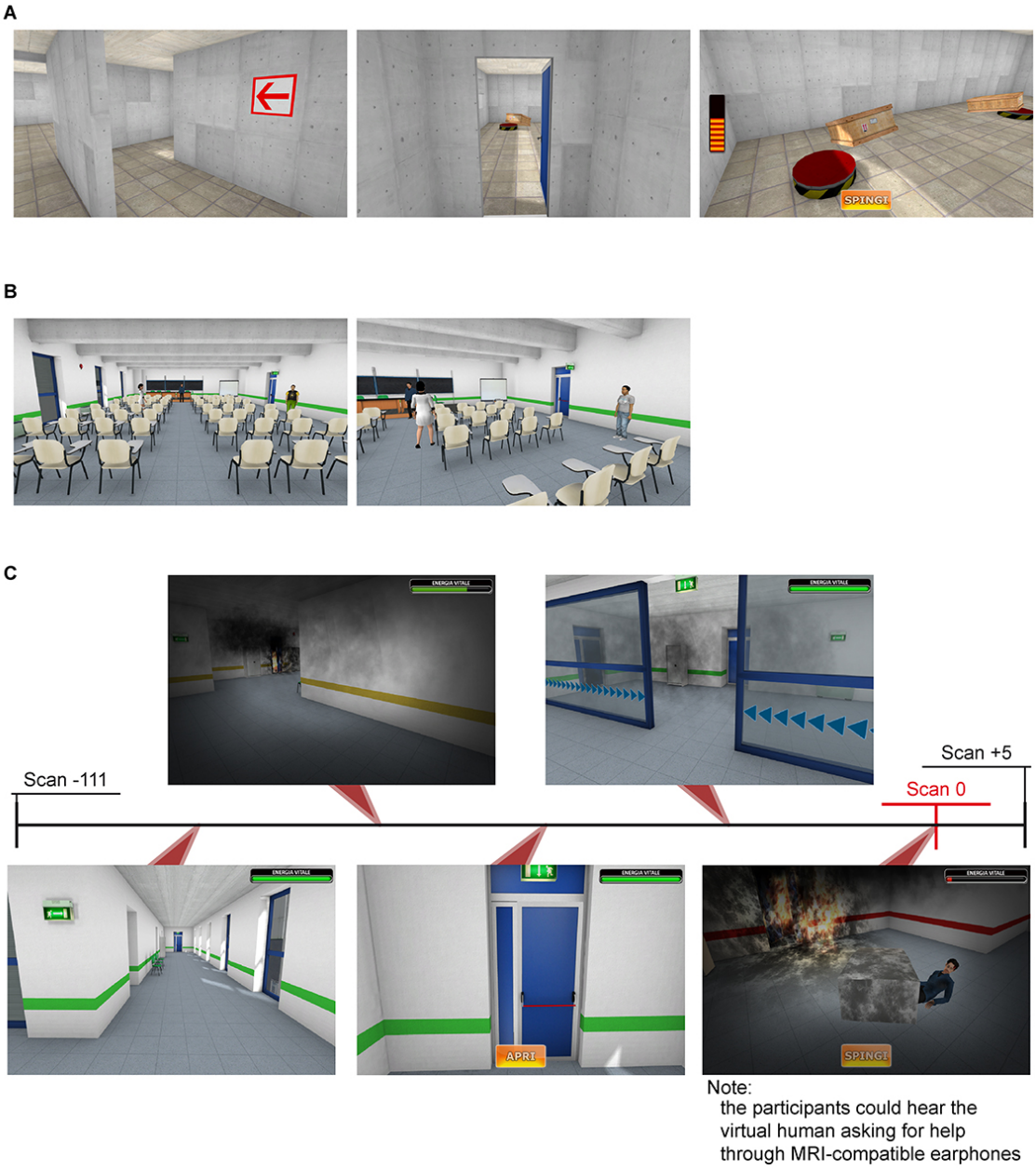

Figure 1 The virtual experience. (A) Screenshots of the initial familiarization phase session in which participants learn how to move, open doors (middle screenshot) and lift objects (right screenshot). (B) Screenshots of the meeting room populated by other virtual humans (the participants were told that these virtual humans were controlled by volunteers participating to the same experiment). (C) Representative screenshots and timeline of the task. The danger of the situation was emphasized by visual cues, such as smoke in the corridors, reduced visibility and sounds such as coughs. The encounter with the virtual human trapped by the heavy cabinet is shown in the bottom right of the picture. In each screenshot, the 'life energy' bar, which informs participants about the amount of life left, is visible in the upper right corner of the screenshot itself. The black horizontal line depicts the fMRI scans considered for the gICA (volume 0: encounter with the virtual human; volume −111: number of scans for the fastest participant in reaching the virtual human; volume +5: number of scans for the fastest participant in completing the task).

The time taken by participants to reach the virtual human from the beginning of the evacuation (EncounterTime) was recorded and participants' behavior was evaluated by observing their actions towards the trapped virtual human. In particular, participants can be divided in three groups: (i) those who stopped and successfully helped the virtual human (SuccessfulHelp (SH) group), (ii) those who stopped and started helping, but then left before moving the cabinet away completely, without freeing the virtual human (UnSuccessfulHelp (UnSH) group), (iii) those who passed by without stopping (NoHelp (NoH) group). The emergency experience ended when participants moved away from the point of encounter with the virtual human and approached the emergency exit, with the scene fading away automatically.

At the end of the experiment, participants were informally debriefed about their experience in the virtual environment, in particular about the fact that the virtual humans were controlled by the computer application. None of them openly reported to have been suspicious about the experimental procedure.

Image acquisition and preprocessing

Blood-oxygen-level-dependent (BOLD) functional images were obtained while the task was performed. A 3-Tesla Philips Achieva whole-body MR Scanner, equipped with an 8-channel head coil, was used for MRI scanning. Structural images were acquired as 180 T1–weighted transverse images (0.75 mm slice thickness). Functional images were acquired using a T2*-weighted echo-planar imaging (EPI) sequence with 33 transverse slices covering the whole brain (slice thickness 3.2 mm; interslice gap 0.3 mm; TR/TE=2000/35ms; flip angle=90°, field of view=230x230 mm^2; matrix size=128×128, SENSE factor 2). Volume acquisition started synchronously with the beginning of the task (first emergency bell) and continued until the participant completed the evacuation. Three 'dummy' scans were acquired and discarded for the subsequent analysis. Given the self-paced duration of the virtual experience, a different number of volumes was obtained for each participant (M = 159, SD = 36). Statistical parametric mapping software (SPM8, http://www.fil.ion.ucl.ac.uk/spm/software/spm8/) was used for the pre-processing of the fMRI data. Data were corrected for head movement artifacts by rigid-body volume realignment, spatially normalized into the standard Montreal Neurological Institute (MNI) space, and spatially smoothed with 8x8x8 mm^3 full width at half-maximum (FWHM) Gaussian kernel.

Group spatial ICA for fMRI data

To avoid possible confounds due to different sample sizes, gICA as well as the statistical tests on independent components (ICs), behavioral measures and questionnaires were performed considering only the two groups with comparable numbers of participants, precisely the SH and NoH groups (see paragraph "Behavioral results").

Datasets of equal length were considered for each participant. The volume that corresponded to the encounter with the trapped virtual human was considered as volume 0. This was specifically chosen because the present study focused on brain processes related to this event. Then, considering the number of volumes acquired for the fastest participant reaching the virtual human and the fastest one completing the whole virtual experience, 111 volumes before and 5 volumes after volume 0 were selected and further analyzed (see **Figure 1C**).

Group spatial ICA (Calhoun et al., 2009) was used to decompose the data into components using the Group ICA for fMRI Toolbox (GIFT - http://mialab.mrn.org/software/gift/), developed by Calhoun and colleagues (2001b). According to this method, gICA was basically performed in three steps: i) dimensionality of the data was reduced for each participants and then datasets were temporally concatenated, ii) the independent sources were extracted using the Infomax algorithm (Bell and Sejnowski, 1995), iii) datasets were back-reconstructed, in order to produce subjects-specific IC maps and time courses. The dimensionality for the set of 35 fMRI acquisitions was estimated by using the minimum description length (MDL) criteria, modified to account for spatial correlation (Li et al., 2007) and then reduced by applying a 2-steps Principal Component Analysis (PCA) before temporal concatenation and gICA. At the end, 26 spatially-independent IC maps and the respective time courses were created for each participants, after gICA and back-reconstruction. Each resulting group IC map was thresholded performing a voxel-wise one-sample Student's *t*-test (Calhoun et al., 2001a). Specifically, for each IC, back-reconstructed single-participant spatial maps entered the test and the resulting t-map was thresholded at $p < 0.05$, corrected for multiple comparisons according to the family-wise error approach (FWE-corrected). Finally, each of the 26 components was visually inspected and compared with components previously described in the literature (see for example Calhoun et al.,

2008; Smith et al., 2009; Cole et al., 2010; Laird et al., 2011; Beckmann, 2012; Shirer et al., 2012). Nine ICs were selected as biologically meaningful, non-artifactual networks.
To better investigate differences among ICs of the SH and NoH groups, a single gICA was performed for each group separately, using the GIFT toolbox (Celone et al., 2006; Harrison et al., 2008a; Harrison et al., 2008b). This approach was meant to reduce the bias in extracting components from groups with different sample sizes (see paragraph "Behavioral results"). Furthermore, to prevent from splitting components in different sub-systems in the single-group gICA, the number of ICs to be extracted was set to be 26, equal to that of the previous analysis. Finally, the components from each groups with the highest spatial correlation (Pearson's r range = 0.40 to 0.96) to the spatial maps of the previously identified nine components were selected. In other words, the nine ICs identified using fMRI data from all the participants were used as templates for choosing and matching the components extracted performing gICA for each group separately.
Differences in IC maps between the SH and NoH groups were assessed by means of independent two-sample Student's t-tests. All results were thresholded at $p < 0.05$ (voxel-wise FWE-corrected).

Statistical analyses of behavioral data and questionnaires

Differences in MovingTime and EncounterTime between SH and NoH participants were analyzed with independent two-sample Student's t-tests. Four separate multivariate analysis of variance (MANOVA), with GROUP ('SH' and 'NoH') as between-subjects factor, were performed to analyze the IRI scores for each of the four subscales (Fantasy, Empathic Concern, Perspective Taking, and Personal Distress), the BVAQ-B scores for the five subscales (Verbalizing, Fantasizing, Identifying, Emotionalizing and Analyzing), the IPQ scores and the self-reported evaluation of tension, sadness and anxiety. In the latter case, the ratings at the beginning of the experiment ($tension_{pre}$, $sadness_{pre}$, $anxiety_{pre}$) and the difference between post- and pre-scanning ratings ($tension_{diff}$, $sadness_{diff}$ and $anxiety_{diff}$) entered the MANOVA as dependent variables.
The level of significance was set at $p < 0.05$ and all the analyses were carried out by using SPSS for Windows, version 21.0 (SSPS Inc, Chicago, Illinois, USA).

RESULTS

Behavioral results

The present study aimed to investigate the prosocial or selfish moral choices made by healthy participants in a simulated life-threatening situation. According to their behavior after encountering the virtual human trapped under the cabinet, participants were subdivided in three groups: 16 out of 43 participants saved the trapped virtual human (SH group), 19 passed by without helping (NoH group), whereas the remaining 8 participants stopped to help, but then left prematurely without freeing the virtual human (UnSH group). Given that the sample sizes of the three groups were not consistent (with the SH and NoH groups of similar sizes, but substantially different from the UnSH group) and that these differences could have possibly affected the statistical power of the planned tests, data from the UnSH group were discarded and not analyzed further.

Figure 2A shows a graphical representation of the total number of participants in each group and the number of females and males in each of them. In particular, the female to male ratios were similar in the SH group and the NoH group (respectively 11:5 and 12:7) and a chi-squared test did not show any significant differences between the two groups (Pearson's $\chi^2 = 1.21$, $p = 0.728$).

Participants in the two groups of interest showed no significant differences in interacting with objects in the virtual environment. Mean values of the variable recorded during the familiarization phase (MovingTime; **Figure 2B**) were similar between the two groups (SH: $M = 11.6$, $SD = 7.7$; NoH: $M = 13.2$, $SD = 12.9$) and independent two-sample *t*-test showed no significant differences ($t_{33} = -0.435$, $p = 0.666$). The mean time participants spent to reach the virtual human (EncounterTime; **Figure 2C**) was also similar in the two groups. Specifically, the SH group encountered the virtual human 282.7 ($SD = 42.0$) seconds after the beginning of the evacuation, and the NoH group after 284.1 ($SD = 93.1$) seconds. Independent two-sample *t*-test on EncounterTime showed no significant differences ($t_{33} = -0.053$, $p = 0.958$)

The statistical analyses on the self-reported questionnaires showed no significant differences between the SH and NoH groups. Bar graphs representing the mean scores for each questionnaire and the three negative emotional scales are reported in **Figure 3**, whereas numerical values and results of the multivariate tests are reported in **Tables 1-5** in Appendix II.

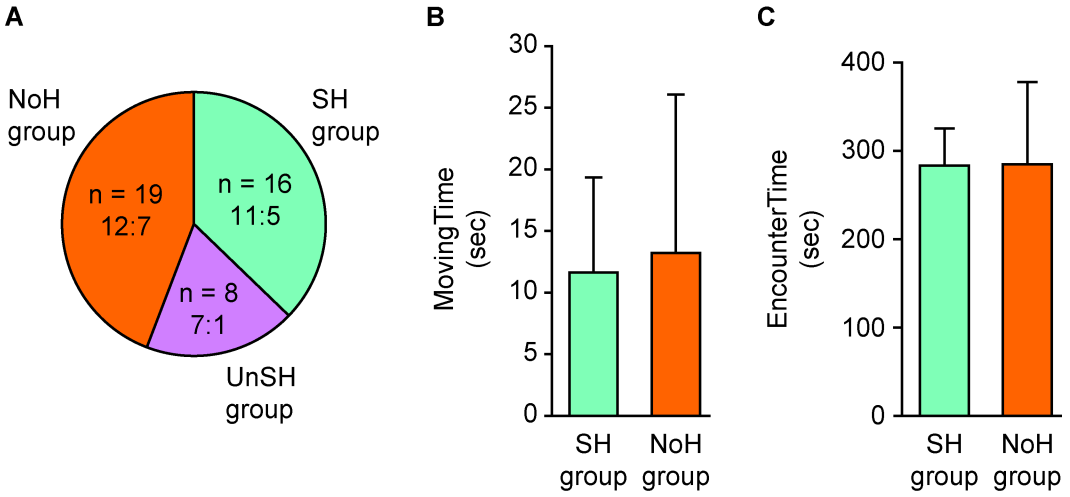

Figure 2 Behavioral data. (A) Distribution of the behavioral responses in the overall group. According to their behavior, participants were classified in: NoH group, those who passed by the virtual human without helping; SH group, those who stopped and successfully helped the trapped virtual human; and UnSH group, those who started helping, but abandoned the virtual human before freeing it. The ratio indicates female to male participants. (B) Means and standard deviations of the MovingTime variable for the two groups with similar sample size. (C) Means and standard deviations of the EncounterTime variable for the two groups with similar sample size.

ICA results

The spatial map and the time course of each of the 26 independent components (IC) found by the group independent component analysis (gICA) were visually inspected and compared with maps and time courses of ICs already published in the literature (see for example, Calhoun et al., 2008; Cole et al., 2010). Seventeen of these components were discarded because they did not include clearly identifiable neuronal sources or they accounted for non brain-derived sources of signal, such as maps that showed head movements artifacts or ventricle regions. The remaining 9 components were investigated both for similarities and differences across the three groups of participants.

IC1 - Component 1 included the left and right primary sensorimotor areas located laterally in the precentral and post central gyri and medially in the paracentral lobule, with peaks of maxima IC weight at [34 -30 58] and [28 -42 62] in the lateral sides and at [8 -36 64] in the medial wall (**Figure 4A**). The latter comprised also the supplementary motor cortex [0 -6 56], whereas a second significant cluster was found in the cerebellum [-4 -56 -2]. The complete list of brain areas included in the IC1 is reported in **Table 6** in Appendix II.

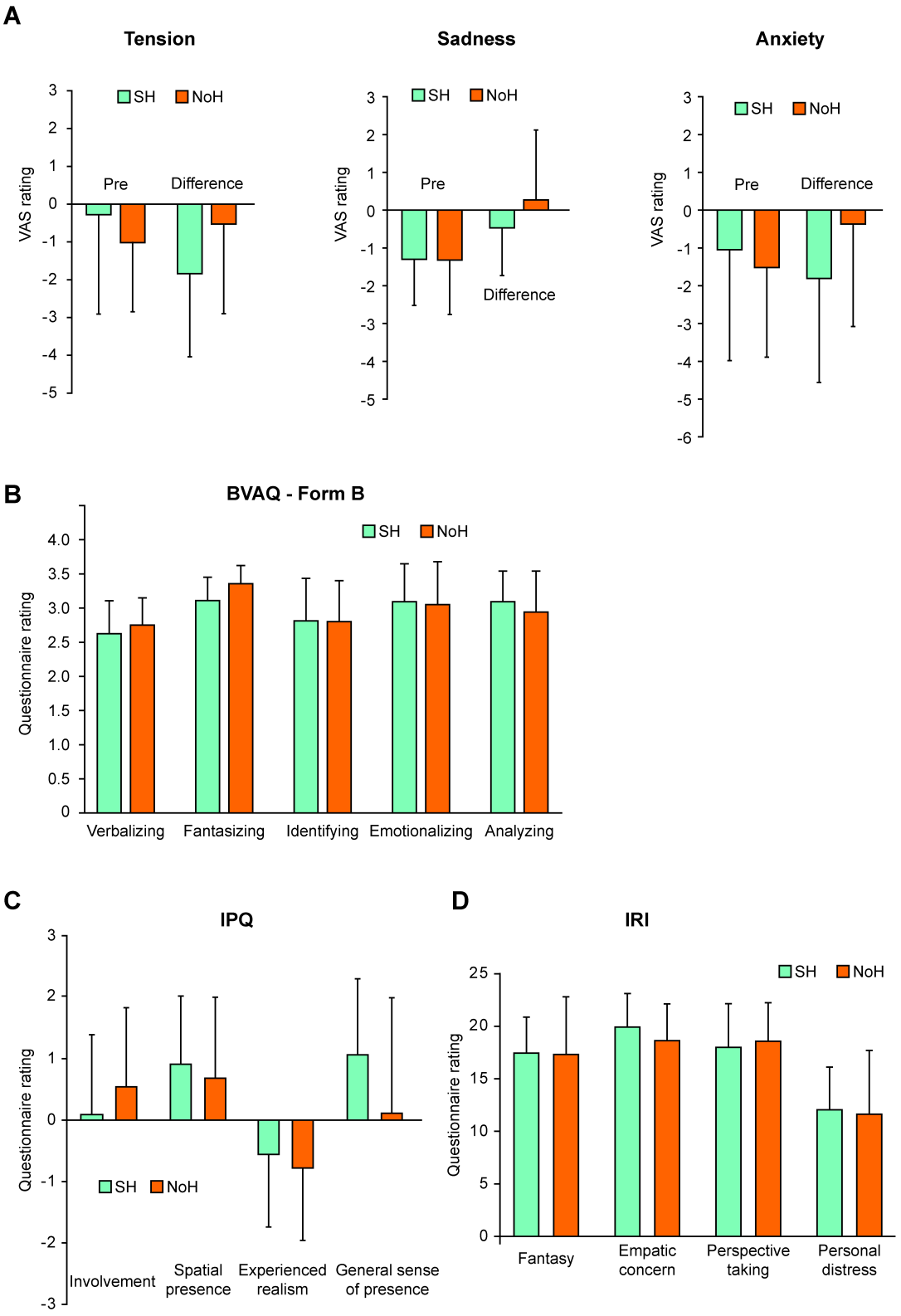

Figure 3 Results of behavioral surveys and questionnaires. Mean groups' scores for the three scales evaluating the emotional state (Tension, Sadness, and Anxiety - A) of the participants, the Bermond-Vorst Alexithymia Questionnaire, form B (BVAQ-B - B), the Igroup Presence Questionnaire (IPQ - C), and the Interpersonal Reactivity Index (IRI - D). Error bars represent standard deviations.

IC2 - The results showed a significant cluster (**Figure 4B**) comprising voxels in the left inferior, middle and superior frontal gyri (respectively at [-4 8 30], [-22 10 52] and [-22 52 8]), in the left precentral gyrus ([-36 0 54]) and the supplementary motor cortex ([-2 20 56]). Furthermore, this component included also the bilateral parietal lobules (main peaks at [-36 -58 50] and [32 -50 44]). Finally, a cluster of significant voxels was also observed in the right frontal cortex, in particular in the precentral and the inferior frontal gyri (respectively at [50 6 28] and [34 6 30]). This cluster was less extended than the one in the left hemisphere; it comprised 3133 significant voxels, whereas the contralateral one included 13545 voxels. The complete list of brain areas included in the IC2 is reported in **Table 7** in Appendix II.

IC3 - IC3 comprised a fronto-parietal network lateralized in the right hemisphere (**Figure 4C**). In particular, the two main clusters included in this IC were centered in the right superior frontal gyrus and in the inferior parietal lobule, respectively at [18 30 46] and [42 -56 44]. The complete list of brain areas included in the IC3 is reported in **Table 8** in Appendix II.

IC4 – A cluster of voxels was found to be significant in the temporal lobes (**Figure 4D**). The brain structures comprised the bilateral rolandic operculum ([-60 0 10] and [62 0 12]) and the bilateral middle and superior temporal gyri (respectively at [-56 -28 4] and [66 -14 -10], and at [-60 4 -8] and [62 -16 4]). It is worth noting that this component extended in much of the superior and middle temporal lobe and its temporal dynamic was strictly related with the encounter with the trapped virtual human (see **Figure 4D**). The complete list of brain areas included in the IC4 is reported in **Table 9** in Appendix II.

IC5 and IC6 - Two independent components accounted for the functional connectivity of the BOLD signal in visual areas and the visual-processing cortical regions (**Figure 4E** and **Figure 4F**). The magnitude of IC5 peaked at [8 -90 4] in the right calcarine cortex (**Figure 4E**, but it also comprised the left primary visual cortex (peak at [-6 -94 6]). The activity of extrastriate visual areas was segregated in a second component (IC6; **Figure 4F**); in particular, significant voxels were observed bilaterally in the fusiform gyrus ([-30 -62 -16] and [34 -56 -12]), and in the middle and inferior occipital gyri (respectively at [-32 -92 8] and [36 -84 6], and at [-48 -66 12] and [42 -68 10]).

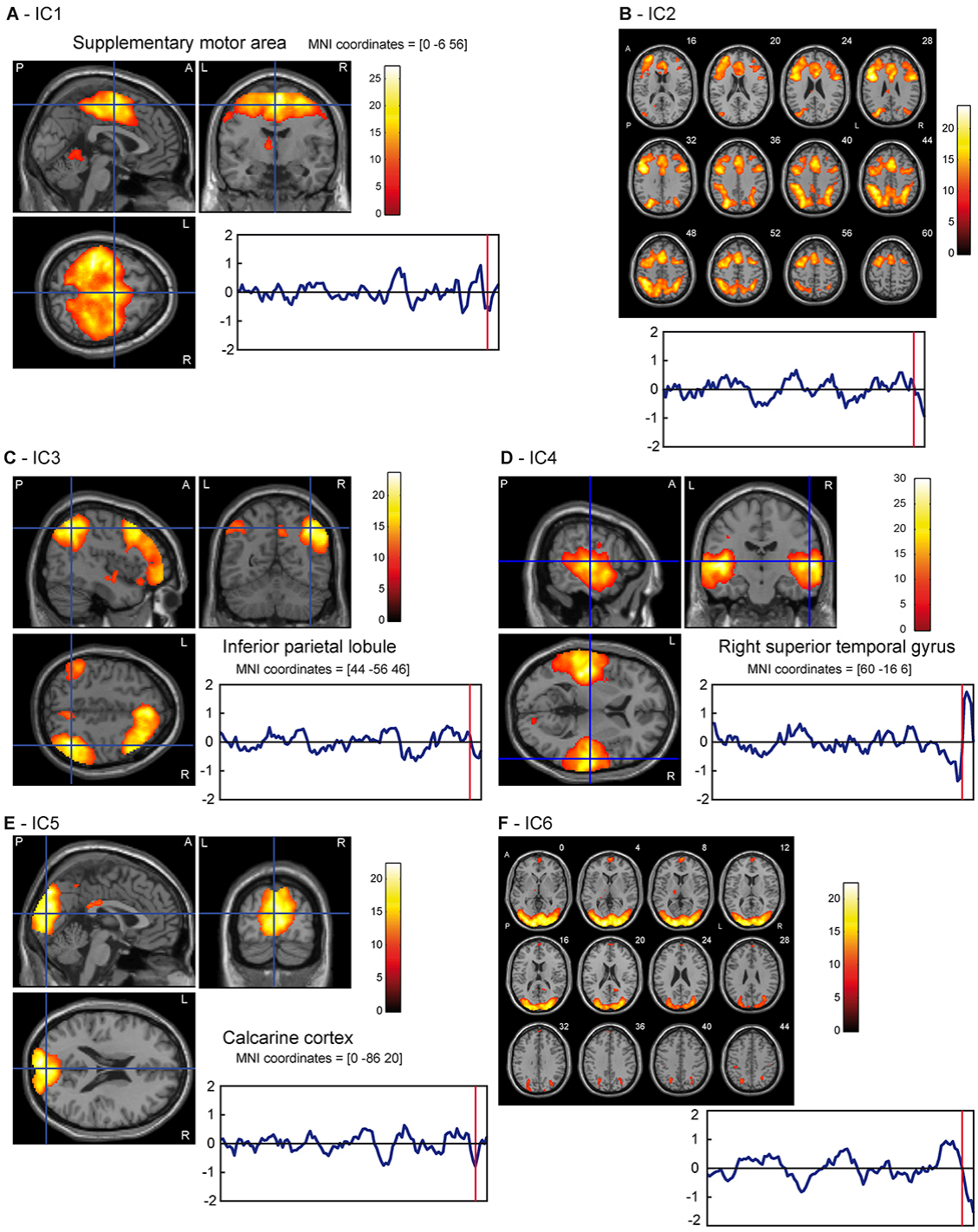

Figure 4 Functional connectivity data. The functionally relevant independent components (ICs) resulting from the gICA conducted on the datasets of the two groups are shown; these inde- pendent components did not show significant group differences. According to the existing literature, they were labeled as: (A) the somatosensory network, (B) the visuospatial network, (C) the right executive control network, (D) the auditory network, and two networks comprising respectively (E) the primary visual areas and (F) the higher-order extrastriate visual areas. Thresholded statistical maps and time courses are depicted for each IC. Statistical maps were thresholded at p b 0.05, corrected for family-wise error; the color bars represent t values. MNI coordinates (in mm) refer to the crosshair. A = anterior; L = left; P = posterior; R = right.

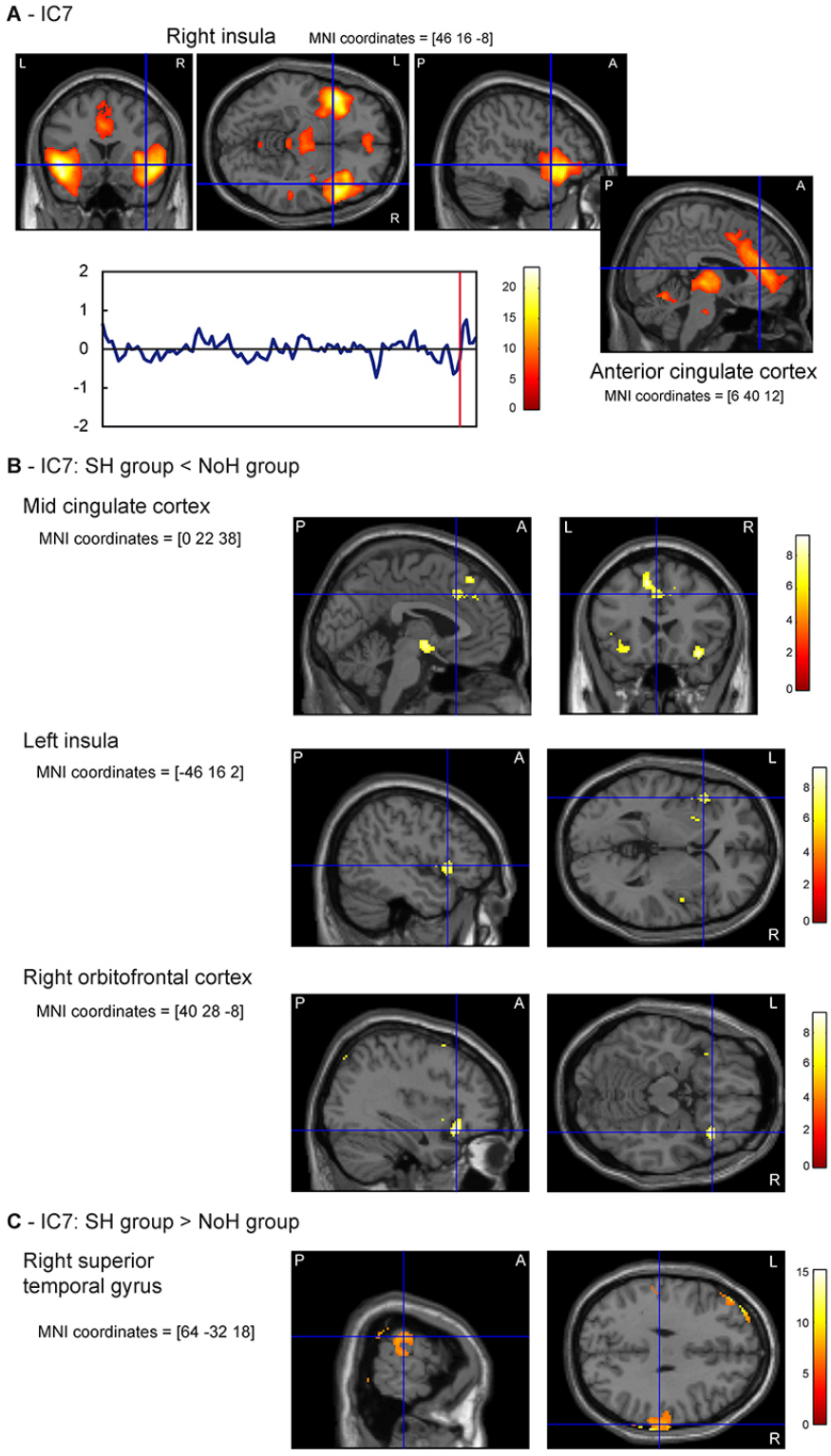

Figure 5 Salience network. (A) The spatial map and the time course of the independent component commonly observed in the two groups of interest that includes the insula and the cin- gulate cortex. Some nodes of this network show significant differences between the participants who saved the virtual human (SH group) and those who did not (NoH group). Specifically, functional connectivity in the first group was decreased in the cingulate cortex, the left insula and the right orbitofrontal cortex (B), whereas increased in the right superior temporal gyrus (C). Statistical maps were thresholded at p b 0.05, corrected for family-wise error; the color bars represent t values. MNI coordinates (in mm) refer to the crosshair. A = anterior; L = left; P = posterior; R = right.

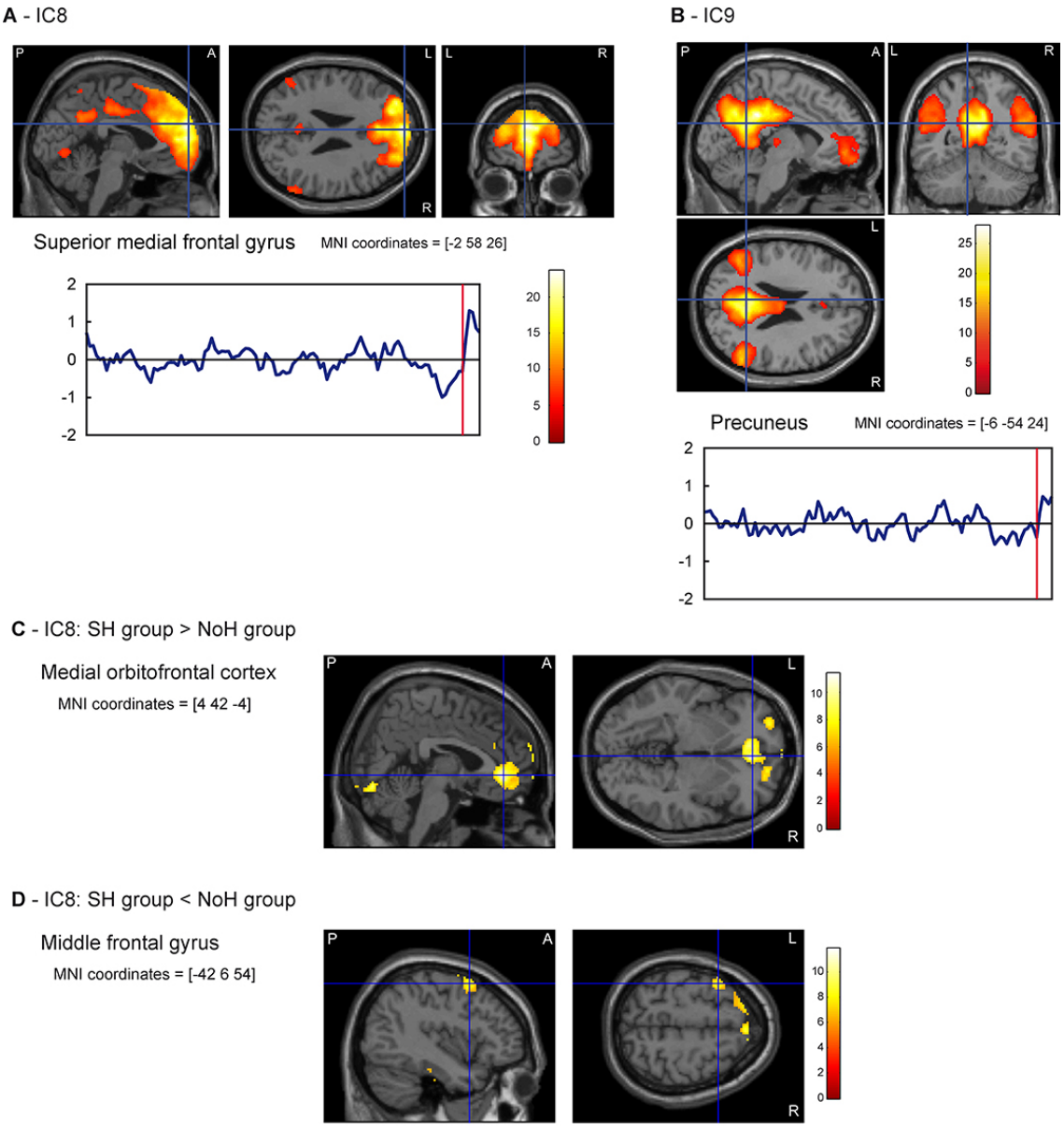

Figure 6 Default-mode network. The default-mode network was commonly observed in the two groups and segregated in two independent components. The first is anterior and comprises the medial prefrontal cortex (A), whereas the latter includes both the medial and lateral nodes of the posterior default-mode network (B). Significant differences between groups in the functional connectivity within this network are shown in panels (C) and (D). Statistical maps were thresholded at p b 0.05, corrected for family-wise error; the color bars represent t values. MNI coordinates (in mm) refer to the crosshair. A = anterior; L = left; P = posterior; R = right.

The complete lists of brain areas included in the IC5 and IC6 are reported in **Table 10** and **Table 11** in Appendix II.

IC7 – A single independent component (**Figure 5A**) included the bilateral anterior insula ([-42 10 -4] and [34 18 2]) and the anterior mid cingulate cortex ([-2 32 26] and

[4 40 12]), together with subcortical structures, like the thalamus ([-6 -16 0]) and the cerebellum ([10 -60 -16]). The complete list of brain areas included in the IC7 is reported in **Table 12** in Appendix II.

IC8 and IC9 - The neuronal sources that contributed to the default-mode network (DMN) were split in two components (**Figure 6A** and **Figure 6B**). On the one hand, IC8 accounted mainly for the activity in the frontal pole and comprised the bilateral superior medial frontal gyri ([-2 58 24] and [4 46 50]). Furthermore, it extended on the lateral surfaces of both hemispheres, including the superior frontal gyri ([-14 24 58] and [18 56 30]). A significant cluster was also observed caudally, in the posterior cingulate cortex/precuneus at [-2 -54 32]. Notably, the temporal dynamic of this component was strictly related with the encounter with the trapped virtual human (see **Figure 6A**).
On the other hand, IC9 comprised the sources in the posterior medial surfaces of the brain. The main cluster of this IC was centered in the posterior cingulate cortex and in the precuneus, respectively [-6 -42 32] and [-6 -54 22], although other clusters of significant voxels were also observed in the lateral surfaces, specifically in the left and right angular gyri at [-44 -60 30] and [56 -60 30], and in the superior medial frontal cortex (peak at [4 62 -2]). The complete lists of brain areas included in the IC8 and IC9 are reported in **Table 13** and **Table 14** in Appendix II, respectively.

Differences in network activity between groups

Differences between the two groups of participants were assessed by performing a separate independent two-sample Student's *t*-test for each component. Differences were found to be significant in two of the nine ICs previously described and therefore the differences among pairs of groups were further investigated in these networks.
The network comprising the bilateral insula and the cingulate cortex (IC7; **Figure 5B**) showed reduced IC weights in the SH group compared to the other group, mainly in the anterior mid cingulate cortex at [-8 36 20], but also in the anterior insula bilaterally (peaks at [-40 20 4] and [46 -4 4]). Conversely, the SH group showed higher activity in a right cluster of voxels encompassing the superior temporal, the postcentral and the supramarginal gyrus (mean peak of activation in [66 -30 28]; **Figure 5C**). The complete lists of significant voxels are reported in **Table 15** in Appendix II for the contrast SH

group < NoH group and in **Table 16** in Appendix II for the contrast SH group > NoH group.

Participants in the SH group also showed significant differences in IC8 when compared with the NoH group. Specifically, significant voxels were found in the medial orbito/prefrontal and anterior cingulate cortices, respectively at [4 42 -4] and [-6 40 -6], for the comparison SH group greater than the NoH group (**Figure 6C**), while a lateral cortical area was identified in the opposite comparison, SH group smaller than NoH group (peak in the left middle frontal gyrus at [-40 10 58]; **Figure 6D**). The complete lists of significant voxels are reported in **Table 17** in Appendix II for the contrast SH group > NoH group and in **Table 18 in Appendix II** for the contrast SH group < NoH group.

DISCUSSION

Studying the neural underpinnings of altruistic behavior in highly salient and ecologically valid environments is one of the major challenges of modern social cognitive neuroscience. In the present study, by combining a VR-based experimental methodology with 'model-free' analysis of fMRI data, we were able to detect patterns of functional connectivity associated with the flowing experience in a stressful situation requiring to engage in prosocial decision-making. More importantly, we were able to observe that prosocial behavior varies between participants and that this variability is predicted by differential connectivity in dedicated functional brain networks.

The overall VR experience was associated to functional brain networks previously identified in the literature during both resting state and active tasks (Calhoun et al., 2008; Bressler and Menon, 2010; Arbabshirani et al., 2013), as revealed by gICA. In particular, networks related to the processing of the basic features of sensory stimuli (visual and auditory) and to higher-order cognitive functions, such as the planning and execution of actions were detected. Indeed, on one hand, clusters of functional connected regions were found both in primary and secondary sensory areas, and in motor areas, whereas on the other hand, higher-order cognitive networks were also detected, such as the attentive fronto-parietal and the default-mode networks (Smith et al., 2009; Laird et al., 2011).

Interestingly, only two of the identified networks showed significant differences between the participants who succeeded in acting prosocially and those who did not. Specifically, differences in functional connectivity were observed in the network including the anterior insula (aINS) and anterior mid cingulate cortex (aMCC), with weaker connectivity of these areas in the group of participants who acted prosocially compared to those that failed, and increased activity in a cortical domain at the border between superior temporal and supramarginal gyri, in the right hemisphere. Furthermore, the prosocial group showed greater activity in a second functional network including the medial orbito/prefrontal and the anterior cingulate cortices.

It has been suggested that an automatic emotional response, evoked by the observation of another individual's suffering, could drive the decision of helping the person in need and therefore acting prosocially. In other words, empathic processes motivate the costly aiding behavior and the empathy-altruism hypothesis was proposed as a reference framework to study this distinguishing human behavior (Batson et al., 1991; Singer and Lamm, 2009; Hein et al., 2010). Hein and colleagues (2011), for example, reported that the autonomic emotional response (evaluated by skin conductance) in participants who witnessed other participants suffering predicted their willingness to share the other's pain. The empathy-altruism hypothesis has led neuroscientists to investigate the role of empathy-related cortical regions, such as aINS and aMCC, in prosocial behavior and the possibility that the activity in these brain structures might predict the tendency to act with the intention to help others (Lamm and Singer, 2010). Although several findings have linked altruism with the brain network underlying our capacity to understand and share others' emotional states (Hein et al., 2010; Masten et al., 2011b; Morishima et al., 2012; Rameson et al., 2012; Waytz et al., 2012), some authors have pinpointed the role of factors other than empathic processes as motivators of prosocial behavior (Fahrenfort et al., 2012). This stems from the findings that in some cases the link between empathy and prosocial behaviors was inconsistent. Singer and collaborators (2008), for example, failed to show an association between activity of empathic-relevant regions and prosocial tendencies. In that study, the volunteers interacted in an economic game and subsequently were subdivided in two groups (prosocial and selfish) according to their tendency to cooperate. The authors found that the prosocial group did not show higher BOLD signal in aINS or aMCC compared to the selfish group when witnessing another person suffering. Interestingly, as the authors pointed out, other causes like the willingness to avoid negative social consequences may motivate the desire to increase

the wellbeing of others and therefore may explain the lack of a relation between empathic brain responses and altruistic tendencies. In other words, factors that may prompt to avoid helping should be also considered, in addition to processes that lead toward prosocial behaviors. In this sense, contextual factors and self-referenced emotional state could be relevant for determining the other-oriented choices. For example, the situation in which a person is seeking for help could be perceived as a threat to the self and the high personal distress may evoke an egoistic motivation that leads to reduce one's own aversive arousal by escaping without helping (Batson et al., 1987). Therefore, two opposite processes could operate in social decision-making (Paciello et al., 2013): one might be initiated by empathic response and lead to altruistic decisions, the other might be related to the evaluation of the situation as excessively costly and stressful, thus resulting in selfish behaviors.

The results of our study can be discussed in the light of this hypothesis. In particular, the simulated dangerous situation was possibly perceived as a stressful event for the participant, resulting in the decision not to risk personal damage and therefore act selfishly. The higher degree of functional connectivity within and between aINS and aMCC in the group that did not help the virtual human in comparison to the group that did could therefore reflect the higher level of personal distress in those participants who decided to escape. Note that the temporal dynamic of this network was not strictly related to the encounter with the trapped virtual human, but instead showed a constant activity throughout the entire virtual experience. This further suggests that the activity in the aINS and aMCC during the task execution reflected the processing of the high level of risk and threat to the self, leading to a self-centered behavioral response. This hypothesis is supported by evidence showing that aINS is involved in monitoring the risk and evaluating the error in risk prediction (Preuschoff et al., 2008; Singer et al., 2009) and that the cingulate cortex is involved in autonomic arousal responses that accompany and perhaps guide cognition and behavior (Critchley, 2004). The activity of aINS and aMCC has been associated not only to the representation of internal bodily states and interoception (Craig, 2003), but also to the processing of the salience inherently embedded in any internal and external stimulus (Laird et al., 2011; Legrain et al., 2011; Mouraux et al., 2011). Indeed, the intrinsic connectivity network comprising these two cortical areas has been referred to as 'salience network' (Seeley et al., 2007). The functional connectivity within the salience network has been shown to correlate with anxiety state, rated by participants who were about to begin a task-free fMRI scan

(Seeley et al., 2007). Interestingly, in our study the participants who behaved prosocially were those who reported the higher (although not statistically significant) reduction in the anxiety level at the end of the experiment (see **Figure 1A** in Appendix II). It has also been demonstrated that this network acts as a top-down control system whose activity is relatively stable across tasks and therefore it is supposed to provide a 'set-maintenance' and monitoring signal (Dosenbach et al., 2008). Finally, Markett and colleagues (2013) found a positive correlation between the activity of the network encompassing the aINS and aMCC and self-reported scores of harm avoidance, suggesting a relationship between the functional connectivity in this network and a trait of personality (namely the anxiety trait).

The second network found to be functionally different between the two groups of interest, with greater degree of connectivity in the prosocial group, included the medial orbitofrontal and anterior cingulate cortices. In the neuroscience literature, activity in the mPFC has been associated with the human ability of taking the perspective of other individuals (Decety and Sommerville, 2003; Jackson et al., 2006) and inferring their mental state (Mitchell et al., 2005b; Bzdok et al., 2013). Moreover, neuroimaging and brain lesion studies have linked these structures (in particular the orbitofrontal portion) with moral cognition and moral decision-making (Anderson et al., 1999; Greene et al., 2001; Koenigs et al., 2007). To behave prosocially, the other individual has to be recognized as an entity capable of conscious experience, action and with specific mental and emotional states. Therefore, it has been hypothesized that the human ability of inferring mental disposition is fundamental for altruistic behavior. According with this hypothesis, several studies have demonstrated the involvement of the medial prefrontal cortex in altruistic decision (Waytz et al., 2012), with a positive correlation between the activity in this area and the preference of prosocial choices (Rilling et al., 2002; Moll et al., 2006; Mathur et al., 2010).

Our results support the hypothesis that a greater activity in mPFC leads to behave prosocially. Interestingly, the temporal dynamic of this network was strictly related with the encounter with the trapped virtual human, unlike what was observed for the salience network. Therefore, the mPFC seems to underlie cognitive functions that are initiated by an external socially-relevant stimulus, such as taking the perspective of the other person or the evaluation of the different moral choices.

A second hypothesis may be put forward to explain the significant findings in the mPFC. Indeed, the way participants behaved in VR could have been affected by

concerns about good reputation (and not concerns about the welfare of the virtual human) and they could have behaved altruistically in order to increase it. Consequently, it is possible that the social information elaborated by the mPFC in this case might be that needed for a third-person perspective taking and for elaborating how the experimenter would judge the participant on the basis of her or his decision regarding the virtual human. Evidence supporting this role of the mPFC has demonstrated that this region, in particular its most anterior part, is active when a person has to think how oneself is represented by another one (Amodio and Frith, 2006; Frith and Singer, 2008; Izuma et al., 2010). Although our data do not allow us to definitely endorse one hypothesis over the other, they still support the idea that mPFC has a pivotal role in social cognition and in processing information relevant for social goals and behaviors which can affect other individuals (Amodio and Frith, 2006; Denny et al., 2012; Bzdok et al., 2013).

Together, the results observed in the mPFC and in the salient network lead to speculate an interplay between these two networks in the context of our experiment and that their interaction is likely to determine the behavioral response of participants in the threatening situation simulated during the virtual experience. The activity of mPFC prompts to helping behavior; conversely, the aINS and aMCC seem to be responsible for the evaluation of risk during the entire task and the prevailing self-oriented choice.

It is worth noting that another network showed an activity timecourse that peaked after the encounter with the virtual human. This network comprised the superior temporal gyrus (STG) bilaterally. Investigations in animals and humans have related the role of the superior temporal cortex to social perception, in particular the processing of those sensory stimuli components that are important for social interaction or analysis of the intentions of other individuals (Allison et al., 2000; Hein and Knight, 2008; Strobel et al., 2008). Indeed, the observation of significant activity in STG (similarly engaged by all the participants) in concomitance with the encounter with the trapped virtual human suggests that the event was a highly relevant and novel social stimulus, whose processing would end with the participant's decision of risking or not his/her own life in the virtual experience to save the virtual human.

Finally, the temporoparietal junction (TPJ) was observed to be statistically more active in the prosocial group than in the other group. This area has been shown to be involved in social cognitive processes, such as mentalizing, self/other distinction, and more generally other-oriented behavior (Decety and Sommerville, 2003; Jackson et al., 2006;

Decety and Lamm, 2007). Recently, Morishima and colleagues (2012) have demonstrated a close relationship between the right TPJ and the tendency to behave altruistically. In our study, the observation of the different engagement of this area between groups suggests its role in a general predisposition to act altruistically and thus facilitating the decision to help the trapped virtual human.

Although we cannot draw definitive conclusions about the involvement of brain networks such as the salience network and mPFC in driving prosocial behaviors, we provided a first example of how a more ecologic setting can be implemented to investigate complex social decision-making in humans. Notably, our study might inspire new hypotheses or experimental protocols based on different neurophysiological techniques, which will substantially help to disentangle the causal relations between the social context here investigated and the underlying neurobiological substrates. For instance, modified versions of our VR paradigm could be implemented to investigate how prosocial attitudes depend on specific features of both the agent and the person in need (i.e., age, gender, etc.). Some insights about the effect of gender in the present experimental context could be drawn from the observation that participants of both genders engaged in similar helping behaviors, although the current study was not aimed to address this issue systematically. In the past, several studies have focused on the role played by gender, age or group membership on the tendency to behave prosocially (Eisenberg and Lennon, 1983; Eisenberg and Miller, 1987; Eagly and Becker, 2005; Eagly, 2009; Hein et al., 2010; Mathur et al., 2010) suggesting that gender and age have an effect on mental processes that are crucial for eliciting helping behaviors, such as the empathic response or the capacity to detect pain-related cues in facial expressions (Eisenberg and Lennon, 1983; Cole et al., 2010; Riva et al., 2011; Groen et al., 2013; Michalska et al., 2013). Although these studies have provided insights about prosocial behaviors, new paradigms like the one presented in the current study will allow researchers to better clarify the complex mental processes and the neurobiological basis underlying prosocial decisions.

LIMITATIONS

Although our study stands for its novelty in applying the ICA approach on fMRI data acquired in a virtual environment, particularly in the field of social neuroscience, it has some limitations that should be kept in mind when discussing its neurophysiological findings.

Firstly, it should be considered that ICA does not allow one to easily draw inference at a group level (Calhoun et al., 2009) and different approaches have been proposed to tackle the issue, each one with its own advantages and drawbacks (Calhoun et al., 2009; Cole et al., 2010). Secondly, a common issue these methods try to deal with is how to separate biological meaningful components from those that account for artifacts (i.e., head movements, high-frequency noise). In the present study, only 9 out of 26 components were selected and considered in the statistical analysis. Although the final number of selected ICs was comparable with that of previously published studies investigating functional networks either at rest or during tasks (Chen et al., 2008; Harrison et al., 2008b; Cole et al., 2010; Laird et al., 2011; Shirer et al., 2012), it might be possible that our approach was too conservative and thus some neuronal-related components were missed.

Finally, an issue related to our VR-based paradigm is to what extent the participants perceived the virtual environment as a real-world situation or as an artificial videogame-like experience. Although we sought to create a vivid VR setting close to a real experience (as indicated by positive ratings for both the "spatial presence" and the "general sense of presence" subscales; see **Figure 1** in Appendix II) and all participants were expressly instructed to behave as naturally as possible, it should be noticed that they also reported low mean ratings for the IPQ "Experienced realism" subscale (see **Figure 1C** in Appendix II). This may raise some questions about what mental processes are responsible for prosocial behavior when the participants encountered the trapped virtual human. For example, participants' behavior could be driven by reputation concerns as well as by a real understanding of the affective and mental state of an individual in danger.

Study 3: Role of the opioid system[1]

INTRODUCTION

Whereas research in the last years has shed light on the neural mechanisms underlying empathic brain responses in the normal adult population (see Bernhardt and Singer, 2012, for a review), little is known about the neurochemical ones and how they are related to the perceptual and motivational aspects of empathy.

The opioid system is a prime candidate for the modulation of empathic responses, as it also plays a key role in the regulation of aversive experiences experienced by the self, including pain.

Indeed, substantial evidence implicates the endogenous opioid system in the mediation of placebo effects under conditions of expectation of analgesia (Benedetti et al., 2005; Zubieta et al., 2005). During both clinical and experimentally induced pain, placebo–induced expectation of analgesia has been associated with reductions in pain ratings. The reductions were reversed by either the open or hidden administration of opioid receptors antagonists (e.g., naloxone), indicating that they were mediated by pain-suppressive endogenous opioid neurotransmission (Gracely et al., 1983; Grevert et al., 1983; Levine and Gordon, 1984; Benedetti, 1996; Amanzio and Benedetti, 1999). Non-opioid mechanisms have also been described, particularly in the context of preconditioning with non-opioid agents (Amanzio and Benedetti, 1999).

Recent functional neuroimaging studies have also identified a top-down mechanism at the core of placebo responses (see Colloca et al., 2013 for a review). In particular, the dorsolateral prefrontal cortex (DLPFC) seems to play a crucial role in initiating the placebo response following verbally-induced expectations, social learning or cues and contextual conditioning. DLPFC would coordinate the response of cortical and subcortical regions, like the most anterior part of the anterior cingulate cortex (rACC), hypothalamus, amygdalae and periaquedutal gray matter (PAG). Consequent alteration

[1] This research was partially funded by the Viennese Science and Technology Fund (WWTF, CS11-016).

of pain experience, mostly in the direction of reduction of pain responses, is accompanied by decreased activity in the pain-matrix, especially in the somatosensory cortex, insula and thalamus (Wager et al., 2004; Price et al., 2007; Eippert et al., 2009). Moreover, many pain-processing brain regions house a large part of the total amount of opiate receptors, especially μ-type (Fine and Portenoy, 2004).

Interestingly, opiate receptors are not uniquely present in pain-regulating areas like PAG and thalamus and in areas belonging to the sensory-discriminative component of the pain network (primary and secondary somatosensory cortices, frontal operculum, posterior insula). Instead, a high μ-opioid receptors density is found in areas like the anterior cingulate cortex and the anterior insula (see Baumgartner et al., 2006 for a quantitative analysis of μ-opioid receptors localization), usually considered as crucial nodes of the affective component of pain.

These findings, together with the increasing evidence that placebo acts through the opioid system by targeting brain structures such as rACC and aINS (Wager et al., 2007; Zubieta and Stohler, 2009) provide a unique, yet so far unexplored opportunity to investigate the functional specificity and the neurochemical mechanism of the neural networks underlying empathic responses.

The present study aimed at indirectly investigating the role of the opioidergic pain system in empathy for pain through the induction of placebo analgesia (known, as already mentioned, to enhance the endogenous opioid system).

Despite a systematic review on the proportion of success in placebo induction protocols is not available, it is a matter of fact that in both clinical trials and experimental conditions, the placebo response varies dramatically among individuals (Colloca et al., 2013). Current research is trying to understand which factors can predict the susceptibility to placebo effect. So far, predictability of placebo response has been associated to genetic profile, individual's brain anatomy, or personality traits like agreeableness and resilience (Hall et al., 2012; Stein et al., 2012; Pecina et al., 2013), but definitive evidence about brain related functional differences during placebo-induction is still lacking. Therefore, a second goal of our study was to characterize and understand possible neurophysiological differences between responders and non-responders. For this purpose, data of three groups were compared: the natural history (control) group who did not underwent the placebo manipulation; a group of responders, whose members behaviorally showed evidences of effectiveness of the placebo

induction; a group of non-responders who did not show significant changes in behavior compared to controls.

To this purpose, we took advantage of the physical pain paradigm used in Study 1 (based on Singer et al., 2004) in order to detect possible differences in the behavioral and neurophysiological responses between groups of participants with different recruitment of the endogenous opioid system. In order to maximize empathic brain responses, the experimental task was modified in three ways. First, since many studies report a modulation of empathic responses according to the perceived affective closeness of the target (e.g., Cheng et al., 2010 and Bernhardt and Singer, 2012 for a recent review), we paired participants with their romantic partner, instead of unknown confederates. Second, we scanned male participants paired with their female partner, hypothesizing that empathy for physical pain could strongly trigger protective behaviors (Glick and Fiske, 1997). Third, stimuli were made more salient and self-relevant by adding on the screen photos of participant's and partner's hands on every trial, since previous research has shown that empathy network enlarges when the somatosensory qualities of the stimuli are enhanced (see Keysers, 2010 for a review).

We hypothesize that the induction of the placebo analgesia in a group of responders would not only decrease their response to the first-hand exposure to physical pain (via the opioid system), but it would also alter the vicarious experience of the same kind of pain. Specifically, the perceived analgesia will be accompanied by a decreased brain activity in the first-hand experience of pain and in empathy for pain related-areas (aMCC/rACC, aINS), in comparison to the control group. On the psychological level this would translate into a reduction of negative affect and of reported unpleasantness both for self and other pain.

On the contrary, participants who will not benefit from placebo effect because of lower or missing susceptibility to our type of placebo induction (non-responders), will likely display equal or even increased negative affect in both the direct and empathic experience of pain in comparison to the control group, as a possible consequence of additive effect of violated expectancies of pain relief. On the neurophysiological level we expect to find equal or increased activity compared to controls and increased activity compared to responders in the affective component of the pain-network (e.g., aMCC, aINS) during both first-hand and vicarious experiences of physical pain.

METHODS

Participants

A total of 53 male participants took part in the fMRI experiment. Participants came to the lab with their romantic partner with whom they had been having a relationship for six months at least.

The mean age of the participants was 23.5 years (SD = 2.7, range = 19–30). All participants gave informed consent and the study was approved by the Ethics Committee of 'Santa Maria della Misericordia', Udine, Italy. Instructions about the experiment were provided to the participant and his partner simultaneously to ensure that the participant believed that his partner would also take part in the experiment. General empathic traits and alexithymic traits were measured with self-report questionnaires (the Interpersonal Reactivity Index; Davis, 1980; and the Bermond-Vorst Alexithymia Questionnaire; Vorst and Bermond, 2001).

Participants were initially randomly assigned to the two groups: the control group (N = 21) and the placebo group (N = 32). Participants in the latter group were informed that they had to take orally an analgesic drug just before starting the experiment.

According to the behavioral response given during the physical pain task, participants in the placebo group were assigned post-hoc to subgroups of responders (N = 16) and non-responders (N = 16) (see next section for a detailed explanation).

Assignment of placebo participants to subgroups

Placebo effect does not easily occur in every person and in every context. Instead, placebo response varies dramatically among individuals. According to individual differences in terms of psychological traits (e.g., anxiety, dispositional optimism, hypnotic suggestibility), genetic predisposition and brain anatomy, reactions to placebo treatment range from complete no response to full pain relief (Colloca et al., 2013).

We took this aspect in account in order to avoid including participants who did not respond to the placebo induction in the same group along with participants who showed hints of placebo effect. Therefore participants in the placebo group (N = 32) were arbitrarily divided in two subgroups of equal size (N = 16). The parameter we used to make this subdivision was the mean difference between emotional ratings the participants gave when they received non-painful and painful stimulations. The

rationale of this choice is the following: if placebo effect occurs, it should mainly act on 'pain' rather than 'no-pain', thus reducing both perceptually and emotionally the difference between the two conditions. Therefore participants were split in two groups based on the median value (Me = 1.49), with the 16 participants below the median (who presented the lower difference) assigned to the 'responders' group (range: -0.75 – 1.38), and the 16 participants above the median (who presented the higher difference) assigned to the 'non responders' group (range 1.60 – 4.65).

To formally test the reliability of such a categorization, we performed independent samples t-tests to compare the newly formed groups between them and with the control group. Comparisons showed that scores of the first group (M = 0.68, SE = 0.15) and of the second group (M = 2.70, SE = 0,36) were different (t_{30} = −7.571, P = 0.000). Moreover, scores of controls (M = 2.26, SE = 0.36) were statistically different from the first group (t_{35} = 3.672, P = 0.001), but not from the second group (t_{35} = −0.970, P = 0.339). Therefore we decided to label the two groups as 'responders' and 'non-responders', respectively.

fMRI design

This fMRI paradigm consisted of one session entailing two runs each. Both runs included a 'self' and 'other' condition. Therefore, the design was a 2 × 2 within-subject factorial design, with the factors TARGET (self and other) and INTENSITY of pain (pain and no-pain). In order to further increase the ecological validity of the empathy sessions, participants were paired with the partner as the target of the 'other' condition (replicating what was used in Singer et al., 2004).

Physical pain task

Stimulus set and apparatus

Electrical pain stimuli were delivered by a bipolar concentric surface electrode (stimulation area: 20 mm^2), which depolarizes predominantly Aδ-fibers, applied on the back of the participants' left hand. We delivered a 100-Hz train of electrical pulses of 2 ms pulse duration (square pulse waveform) for 1s via a direct current stimulator (Digitimer Electronics, model DS7, Hertfordshire, UK). Current amplitude was delivered in a range from 0.1 to 3.5 mA, with steps of 0.1 mA.

After electrodes were applied on participants' skin, photos of their hands were taken and included in the task, in order to increase the saliency of the stimulations and to provide the participant inside the scanner with a visual help when imagining his partner being stimulated.

Experimental paradigm

The experimental paradigm (based on Singer et al., 2004) was similar to that of Study 1, but with an additional manipulation for the participants in the placebo group. In particular, immediately after the assessment of participant's and his partner's pain thresholds, the analgesic placebo induction took place; after that, the participant entered the scanner and the actual experiment took place.

During the pain thresholds assessment, the participant and his partner had to judge the painfulness of each received stimulus, using a 10-point intensity ratings scale (0 = 'don't feel anything', 1 = 'can feel something but not painful', 2 = 'mildly painful', 8 = 'maximum tolerable pain', 10 = 'worst imaginable pain'). The intensities of the stimulations that the participant and his partner rated as 1 and 8 were noted and then used as stimuli for the 'no-pain' and 'pain' conditions, respectively.

At this point participants in the control group entered the scanner to perform the tasks. Participants in the placebo group, instead, were administered with an inert pill, with the expectation to take an analgesic drug. A real doctor wearing a white coat and identified by a personal badge entered the experimental room and administered the participant with the pill. The doctor explained to the participant that the drug was 'extremely effective in reducing pain sensation on both the physical and psychological level. Moreover, the participant was informed that the experiment would start 45 minutes after the administration, because according to its pharmacokinetic profile that was the time the drug needed to reach the peak-level in the bloodstream.

In line with the most used neuroimaging placebo paradigms (Atlas and Wager, 2014) verbal instructions were coupled with a conditioning phase in which covertly reduced pain intensities were delivered before the experiment started, in order to convince the participant of the real effectiveness of the drug and thereby enhance their expectations of future pain relief. Precisely, at time points of 15, 20, 25 and 30 minutes after the administration of the pill, we delivered two stimulations that the participant believed to correspond to the intensities he had previously indicated as 1 ('no pain') and '8'

(‘pain’), respectively. In fact, while the intensity of the lowest stimulation was never changed by the experimenter, the painful intensity was lowered every time until, the participant himself was rating the last stimulation received around a value of 4-5 on the scale. The entire procedure was justified to the participant as the standard procedure to check when the drug was circulating the bloodstream and consequently showing its first effects on pain perception.

The fMRI experiment started after the 45 minutes were elapsed. During this phase, visual stimuli were presented via goggles connected to the workstation in the MRI console room. Visual stimuli consisted of colored arrows pointing either to participant’s or his partner’s photo of the hand. The color of the arrow was an indicator of the target and intensity of the stimulation: dark blue and light blue for, respectively, painful stimulation (self pain) and non-painful stimulation (self no-pain), delivered to the participant in the scanner, while dark pink and light pink for, respectively, painful stimulation (other pain) and non-painful stimulation (other no-pain), delivered to the partner in the MRI console room. In reality, the partner did not receive any stimulation.

Each stimulation trial started with a fixation cross in the middle of the screen. Then the arrow appeared and stayed on the screen for 2500 ms, before a circle of the same color appeared (1000 ms), representing the actual delivery of the stimulus. During this phase, when a painful stimulation was delivered either to participant’s or his partner’s hand, a red frame flashed around the photo of the stimulated hand. At the end of each stimulus, the participant was asked to rate the valence of emotions felt on a Likert-type rating scale with nine discrete values, from −4 = ‘very negative’ over 0 to +4 = ‘very positive’ (4000 ms). The response was given by moving an asterisk from a random initial position toward the chosen position using the left and right keys on a response pad that the participant held in her right hand (**Figure 1**).

The session was divided in two separate runs of 40 randomized stimulations each (10 self pain, 10 self no-pain, 10 other pain and 10 other no-pain).

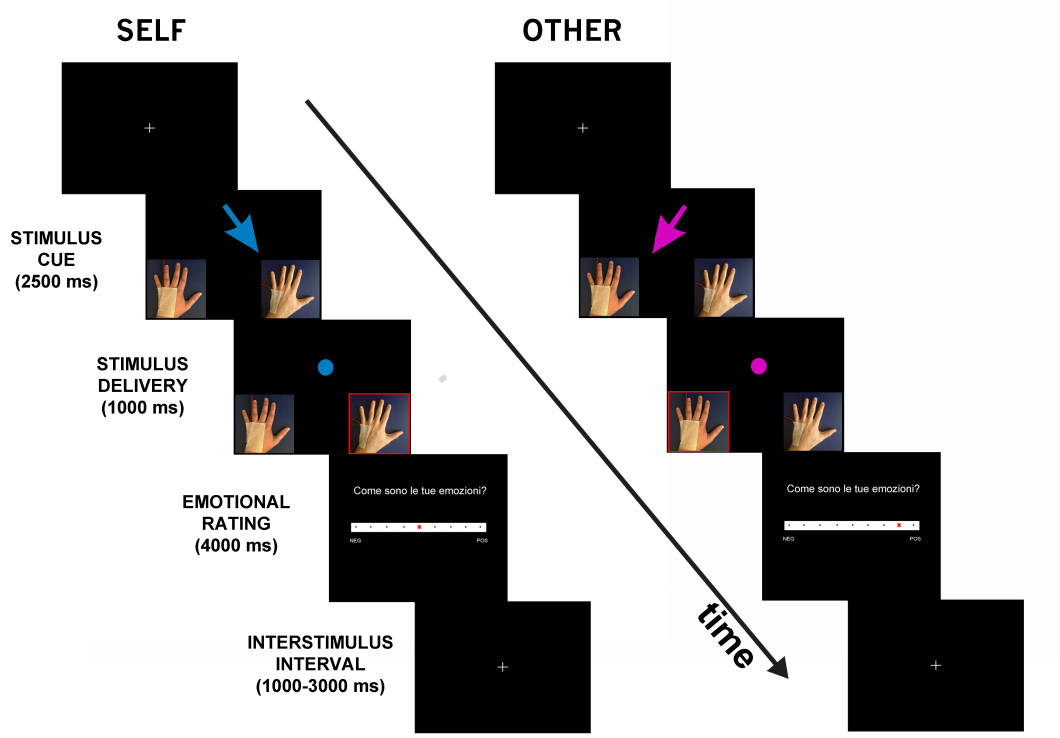

Figure 1 fMRI design for the physical pain task. In each trial, participants were first presented with colored arrows as cues indicating the target, either the participant (self) or his partner (other) and the intensity (painful or non-painful) of the incoming stimulation. Specifically, dark colors indicated a painful stimulus, whereas light colors were paired with non-painful stimuli (in the figure only dark-colored cues are shown). The arrows also pointed at participant's or his partner's hand, whose photos were taken before the experiment. The actual delivery of the stimulus was signaled by a dot of the same color of the arrow, appearing after 2500 ms. Participants judged their own emotion on a 9-points Likert scale, displayed for 4000 ms, immediately after the stimulation period (1000 ms). Interstimulus interval was randomly jittered (1000–3000 ms).

fMRI acquisition and pre-processing

A 3 Tesla Philips Achieva whole-body MR Scanner at the Hospital 'Santa Maria della Misericordia' (Udine, Italy), equipped with an 8- channel head coil, was used for MRI scanning. Structural images were acquired as 180 T1-weighted transverse images (0.75 mm slice thickness). Functional images were acquired using a T2*-weighted echo-planar imaging (EPI) sequence with 33 transverse slices covering the whole brain (slice thickness 3.2 mm; interslice gap 0.3 mm; TR/ TE = 2000/35 ms; flip angle = 90°, field of view = 230 × 230 mm^2; matrix size = 128 × 128, SENSE factor 2).

Data were analyzed with SPM8 (Wellcome Department of Imaging Neuroscience, London, UK). All functional volumes were realigned to the first volume, segmented in gray matter, white matter and cerebrospinal fluid tissues, spatially normalized to the

standard EPI template, and smoothed using a Gaussian kernel with full width at half maximum (FWHM) of 10 mm^3 (6 mm smoothing at first, 8 mm at second level). Following pre-processing, statistical analysis was carried out using a general linear model approach. High-pass temporal filtering with a cut-off of 128 s was used to remove low-frequency drifts.

fMRI analysis

Whole-brain analysis

In the first-level analysis data were analyzed separately for each subject. Two separate regressors (stimulation period and rating) were defined for each condition ('self pain', 'self no-pain', 'other pain' and 'other no-pain') for a total of eight regressors for each run. Residual effects of head motion were corrected by including the six estimated motion parameters of each participant as regressors of no interest in the design matrix.

Neural activation related to conditions of interest was determined by entering the parameter estimates for the stimulation period regressors into a flexible factorial design ANOVA model (as implemented in SPM8), for random effect inference at the group level (Penny and Holmes, 2004). Linear contrasts of the repeated measure ANOVA with two within-subject factors [TARGET (self and other) and INTENSITY (pain and no-pain)] and one between-subject factor [GROUP (Controls, Placebo Responders, Placebo Non-responders)] were used to assess main effects and interactions.

Regressors of interest were convolved with the canonical hemodynamic response function. The Anatomy Toolbox version 1.6 (Eickhoff et al., 2005) was used for anatomical and cytoarchitectonic labelling. A statistical threshold of $P < 0.05$ corrected for multiple spatial comparisons at cluster-level was used, except for *a priori* hypothesized regions where small volume corrections were applied. The selection of the *a priori* regions was based on a recent meta-analysis investigating brain mechanisms of placebo analgesia (Atlas and Wager, 2014, tables 5-6, pages 52-53). Since these tables did not report any coordinates of the somatosensory cortices (S1, S2) and dorsolateral prefrontal cortex (DLPFC, or middle frontal gyrus) that have consistently been reported as brain regions modulated by placebo analgesia both during anticipation of pain and pain itself (e.g. Price et al., 2007; Atlas et al., 2012), we integrated the *a priori* regions list with coordinates of S1 and S2 found in Study 1 and coordinates of DLPFC from results of a more general meta-analysis included in the same paper by Atlas and Wager.

Regions of Interest (ROIs) were constructed by creating spheres of 10 mm radius for cortical regions (15 mm for DLPFC) and of 5 mm radius for subcortical regions, centered on the peak coordinates reported in the meta-analysis (see **Table 1** and **Table 2** for a detailed list of the ROIs). Small volume corrections were applied to each single contrast jointly using coordinates from both the tables. Only clusters involving $k > 9$ and $k > 4$ contiguous voxels were reported, for cortical and subcortical regions respectively.

ROI analysis

The peak coordinates used for the small volume correction were also used to build up the ROIs. The spheres had 10 mm and 5 mm radius for cortical and subcortical regions, respectively. All spheres were defined using the SPM-toolbox Marsbar (http://marsbar.sourceforge.net) and parameter estimates were extracted using the toolbox REX (http://web.mit.edu/swg).

Given that meta-analysis approach is quite conservative, we also built for each ROI a symmetrical sphere in the contralateral hemisphere, in order to not neglect other possible meaningful activations. The coordinates are reported in **Table 1** and **Table 2**.

A series of $2 \times 2 \times 2$ ANOVAs with factors TARGET (self, other), INTENSITY (high, low) and GROUP were conducted for each ROI in order to compare mean activations between control vs. responders, controls vs. non-responders and responders vs. non-responders respectively.

Name of the Region of Interest	Center of the sphere			Radius of the sphere
	x	y	z	
anterior insula 1	±38	-2	-16	10 mm
anterior insula 2	±42	10	2	10 mm
anterior insula 3	±38	8	-14	10 mm
middle insula 1	±44	-4	-8	10 mm
middle insula 2	±34	4	-4	10 mm
middle insula 3	±40	-6	6	10 mm
mid-posterior insula	±36	-10	-4	10 mm
posterior insula 1	±42	-18	2	10 mm
posterior insula 2	±48	-16	10	10 mm
putamen 1	±26	-12	2	5 mm
putamen 2, contiguous with anterior insula	±30	14	-2	5 mm
amygdala 1	±26	-6	-10	5 mm
amygdala 2, contiguous with putamen	±26	4	-12	5 mm
postcentral gyrus (S1)	22	-46	66	10 mm
rolandic operculum (S2)	40	-16	16	10 mm

Table 1 List of the ROIs used to investigate differences between groups, based on the meta-analysis by Atlas and Wager, 2013 and on Study 1 for the somatosensory cortices. In the table the name of the ROI, the peak coordinate and the diameter of the spheres are reported. The coordinates refer to areas showing decreased activity after placebo induction during painful stimulation.

Table 2 List of coordinates used to build ROIs to investigate differences between the groups in brain areas whose activity during pain is increased by placebo. The letter outside the brackets indicates to which hemisphere belongs the original coordinate in the meta-analysis by Atlas and Wager, 2013.

Name of the Region of Interest	Center of the sphere			Radius of the sphere
	x	y	z	
L (R) pregenual ACC 1	±2	40	0	10 mm
L (R) pregenual ACC 2	±12	28	4	10 mm
L (R) pregenual ACC 3	±4	32	10	10 mm
L (R) pregenual ACC 4	±4	42	12	10 mm
R (L) pregenual ACC 5	±4	38	18	10 mm
– – subgenual ACC	0	20	-6	10 mm
L (R) subgenual ACC 1	±8	34	-6	10 mm
R (L) subgenual ACC 2	±4	34	-8	10 mm
R (L) rostro-dorsal ACC	±6	28	24	10 mm
R (L) rostral ACC 1	±2	22	8	10 mm
R (L) rostral ACC 2	±12	24	12	10 mm
R (L) rostral ACC 3	±10	44	12	10 mm
L (R) ventromedial PFC	±12	46	-10	10 mm
L (R) medial OFC 1 (middle orbital gyrus)	±2	26	-14	10 mm
L (R) medial OFC 2 (rectal gyrus)	±6	36	-16	10 mm
L (R) inferior frontal gyrus 1	±46	24	0	10 mm
L (R) inferior frontal gyrus 2	±40	24	12	10 mm
L (R) anterior insula 1	±38	18	2	10 mm
L (R) anterior insula 2	±38	18	-10	10 mm
L (R) anterior insula 3	±40	10	-4	10 mm
L (R) anterior insula 4	±30	28	-2	10 mm
L (R) anterior insula 5	±40	32	2	10 mm
L (R) ventral striatum 1	±6	6	-8	5 mm
L (R) ventral striatum 2	±8	-2	-2	5 mm
– – PAG (midbrain surrounding-)	0	-32	-12	5 mm
L (R) thalamus (midbrain surrounding-)	±6	-20	-4	5 mm
R (L) middle frontal gyrus (DLPFC) 1	±42	20	36	15 mm
R (L) middle frontal gyrus (DLPFC) 2	±36	26	30	15 mm

RESULTS

Behavioral results

Analysis of emotional ratings

Participants were stimulated with current intensities ranging from 0.1 to 3.5 mA (overall mean of non-painful stimulations: 0.3 (SD = 0.1); overall mean of painful stimulations: 1.2 (SD = 0.6)). Independent samples *t*-tests showed that mean intensities of painful stimulations (controls: (Mean/SE) = 1.319/0.170; responders: (Mean/SE) = 1.231/0.119; non-responders: (Mean/SE) = 1.063/0.082) did not differ between groups (controls vs. responders: $t_{35} = -0.385$, P = 0.702; controls vs. non-responders: $t_{35} = -1.213$, P = 0.233; responders vs. non-responders: $t_{30} = 1.020$, P = 0.316). Instead, a difference in the mean intensities of non-painful stimulations was found between responders and non-responders (responders: Mean/SE = 0.325/0.030; non-responders: Mean/SE = 0.231/0.024; planned comparison: $t_{30} = 2.475$, P = 0.019), whereas there was no difference between controls and responders (controls: Mean/SE = 0.314/0.035; planned comparison: $t_{35} = 0.223$, P = 0.825) and controls and non-responders (planned comparison: $t_{35} = -1.822$, P = 0.077).

Emotional ratings were first analyzed through a repeated measure 2 × 2 × 3 ANOVA with two within-subject factors, TARGET (self, other) and INTENSITY (pain, no-pain) and one between-subject factor, GROUP (controls, responders, non-responders) using SPSS 20 (IBM software). This analysis was mainly meant to explore the main effects of the single factors. Means and standard errors of emotional ratings given by each group in every condition are reported in **Figure 2**.

Overall, the task was effective in inducing negative emotions in the pain condition. In fact, participants rated the painful stimulations compared with the non-painful ones as more unpleasant (main effect of INTENSITY, $F_{(1,50)} = 180.196$, P = 0.000); furthermore, they judged stimuli applied to their partner's hands as more unpleasant than stimuli applied to their own hands (main effect of TARGET, $F_{(1,50)} = 5.307$, P = 0.029). Finally, a main effect of GROUP was found ($F_{(2,50)} = 6.510$, P = 0.003).

To better investigate the main effect of GROUP and its interaction with the within-subject factors and consequently analyze differences between groups, a series of 2 × 2 × 2 ANOVAs with factors TARGET (self, other), INTENSITY (pain, no-pain) and GROUP were conducted, comparing every time mean emotional ratings of controls vs.

responders, controls vs. non-responders and responders vs. non-responders, respectively.

Controls – responders comparison

The ANOVA comparing controls and responders showed an interaction between INTENSITY and GROUP ($F_{(1,35)}$ = 14.664, P = 0.002) indicating that the controls gave more negative ratings during 'pain' than 'no-pain' compared to responders (*Pain:* controls – responders (mean/SE) = −1.366/0.400; planned comparison; $F_{(1,35)}$ = 11.679, P = 0.002. *No-pain:* controls – responders (mean/SE = −0.096/0.404; planned comparison: $F_{(1,35)}$ = 0.056, P = 0.814). Post-hoc analysis showed that this was true both for the 'self' and 'other' condition [*Self pain*: controls – responders (mean/SE) = −1.553/0.461; planned comparison; $F_{(1,35)}$ = 11.588, P = 0.002. *Other pain* = −1.180/0.573; planned comparison; $F_{(1,35)}$ = 4.901, P = 0.033]. Furthermore, a three-way interaction TARGET × INTENSITY × GROUP ($F_{(1,35)}$ = 4.265, P = 0.046) was found, indicating that responders in the self condition showed a tendency to judge more similarly painful and non-painful stimulations, compared to the other condition and compared to both conditions in controls (*Controls*: self pain – self no-pain (mean/SE) = −2.262/0.357; planned comparison; $F_{(1,35)}$ = 63.938, P = 0.000; other-pain – other no pain (mean/SE) = −2.193/0.267; planned comparison; $F_{(1,35)}$ = 83.434, P = 0.000. *Responders:* self pain – self no-pain (mean/SE) = −0.683/0.147; planned comparison: $F_{(1,35)}$ = 4.433, P = 0.042; other pain – other no-pain (mean/SE) = −1.231/0.228; planned comparison; $F_{(1,35)}$ = 20.041, P = 0.000).

Controls – non-responders comparison

The ANOVA comparing controls and non-responders showed an interaction between TARGET and GROUP ($F_{(1,35)}$ = 4.940, P = 0.033) indicating that controls judged less negatively the stimulations in the 'self' condition than in the 'other', while non-responders did not present this difference (*Controls*: self – other (mean/SE) = 0.634/0.212; planned comparison; $F_{(1,35)}$ = 8.895, P = 0.005. *Non-responders:* self – other (mean/SE) = −0.084/0.243; planned comparison: $F_{(1,35)}$ = 0.120, P = 0.731). Post-hoc *t*-tests showed that emotional ratings given by non-responders during first-hand painful stimulations were more negative than the ones given by controls (t_{35} = 2.987, P = 0.005).

Non-responders – responders comparison

The ANOVA comparing non-responders and responders showed an interaction between INTENSITY and GROUP ($F_{(1,30)}$ = 41.211, P = 0.000) indicating that non-responders gave more negative ratings during 'pain' condition compared to responders (*Pain:* non-responders – responders (mean/SE) = −2.184/0.373; planned comparison; $F_{(1,30)}$ = 34.273, P = 0.000. *No-pain:* non-responders – responders (mean/SE) = −0.351/0.398; planned comparison: $F_{(1,30)}$ = 0.775, P = 0.386).

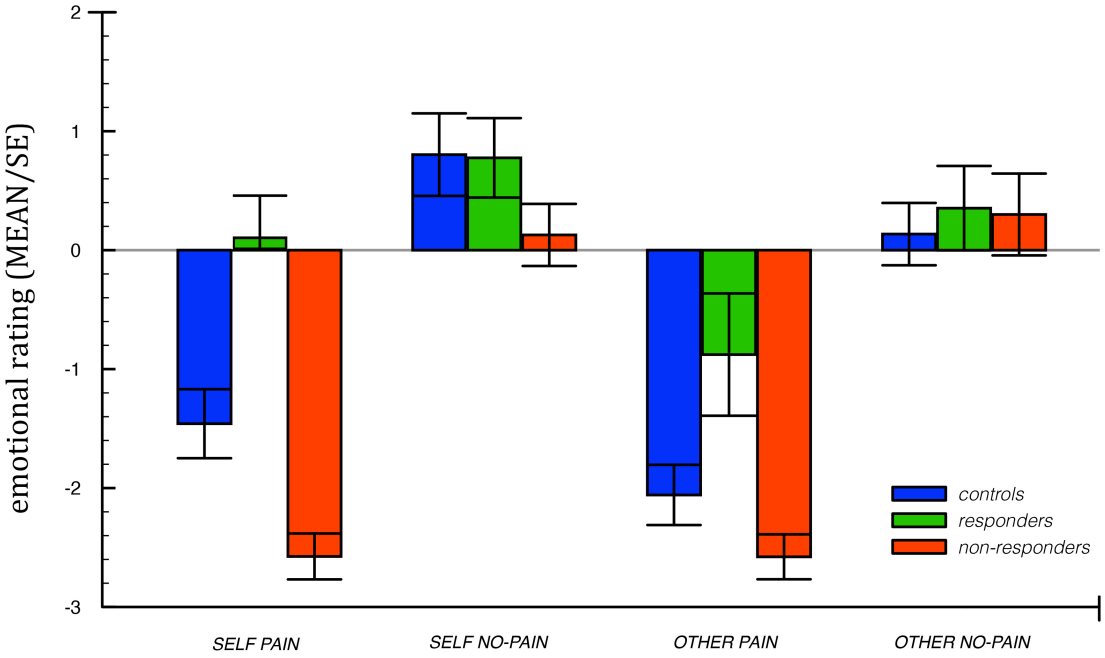

Figure 2 Emotional ratings given by each group in the physical pain task. Graphs represent mean and standard errors.

fMRI results

Whole-brain analysis results

Representative statistical maps obtained from the contrasts: self pain > self no-pain, other pain > other no-pain for each group, are reported in **Figure 3**.

Controls – responders comparison

Self pain: controls > responders. Comparison of hemodynamic responses of controls and responders groups to painful trials in the 'self' condition revealed that controls

showed more activity in some of the regions classically associated with placebo-induced pain reductions: anterior and middle cingulate cortex, left thalamus, left pallidum, left hippocampus ($P < 0.05$, cluster-level corrected), left anterior and posterior insular cortex, left putamen and left amygdala ($P < 0.05$ FWE, SVC). Note that a postcentral gyrus (S1) region was also activated, but only with $k = 8$ ($P < 0.05$ FWE, SVC). Controls also showed increased activation in regions associated with placebo-induced increases: bilateral rectus gyrus, and right middle orbitofrontal gyrus ($P < 0.05$ cluster-level corrected), right medial orbitofrontal gyrus (vmPFC), rostral anterior cingulate cortex, and bilateral inferior frontal gyrus ($P < 0.05$ FWE, SVC). Other significantly more activated brain areas were: left superior orbitofrontal gyrus, right superior frontal gyrus, right superior medial frontal gyrus, right superior temporal pole, bilateral middle temporal gyrus, bilateral supplementary motor area, left paracentral lobule, bilateral precuneus, left fusiform gyrus, right inferior occipital gyrus, and left calcarine gyrus ($P < 0.05$, cluster-level corrected, see **Table 1** in Appendix III).

Self pain: responders > controls. Comparison of hemodynamic responses of responders and controls groups to painful trials in the 'self' condition revealed that responders showed more activity in some of the regions associated with placebo-induced increases: right inferior frontal gyrus ($P > 0.05$, cluster-level corrected), right middle frontal gyrus (DLPFC), rostral anterior cingulate cortex, bilateral anterior insular cortex, periaquedutal gray matter and right ventral striatum ($P < 0.05$ FWE, SVC). Other significantly more activated brain areas were: left precuneus, left calcarine gyrus, and cerebellum ($P < 0.05$, cluster-level corrected, see **Table 2** in Appendix III).

Self no-pain: controls > responders. Comparison of hemodynamic responses of controls and responders groups to non-painful trials in the 'self' condition revealed that controls showed more activity in some of the regions classically associated with placebo-induced pain reductions: left rolandic operculum and bilateral superior temporal gyrus ($P < 0.05$, cluster-level corrected), right middle insular cortex, left posterior insular cortex and left putamen ($P < 0.05$ FWE, SVC). Controls also showed increased activation in regions associated with placebo-induced increases: left thalamus, and right anterior insular cortex ($P < 0.05$ FWE, SVC). Other significantly more activated brain areas were: right inferior frontal gyrus, right superior temporal gyrus,

bilateral middle temporal gyrus, and right inferior occipital gyrus ($P < 0.05$, cluster-level corrected, see **Table 3** in Appendix III),

Self no-pain: responders > controls. Comparison of hemodynamic responses of responders and controls groups to non-painful trials in the 'self' condition revealed that responders showed more activity in two of the regions associated with placebo-induced increases: the periaquedutal gray matter and the right inferior frontal gyrus ($P < 0.05$ FWE, SVC, see **Table 4** in Appendix III).

Other pain: controls > responders. Comparison of hemodynamic responses of control and responder groups to painful trials in the 'other' condition revealed that controls showed more activity in some of the regions classically associated with placebo-induced pain reductions*:* bilateral superior temporal gyrus ($P < 0.05$, cluster-level corrected), left posterior insular cortex, left putamen and left amygdala ($P < 0.05$ FWE, SVC). Controls also showed increased activation in regions associated with placebo-induced increases: left thalamus, and left rectal gyrus ($P < 0.05$ FWE, SVC). Other significantly more activated brain areas were: bilateral middle temporal gyrus, left precentral gyrus, left postcentral gyrus, left precuneus, bilateral fusiform gyrus, bilateral lingual gyrus, right superior occipital gyrus, right middle occipital gyrus, and right inferior occipital gyrus ($P < 0.05$, cluster-level corrected, see **Table 5** in Appendix III).

Other pain: responders > controls. Comparison of hemodynamic responses of responders and controls groups to painful trials in the 'other' condition revealed that responders showed more activity in two of the regions associated with placebo-induced increases: left thalamus and left middle orbitofrontal gyrus/rectal gyrus ($P < 0.05$ FWE, SVC, see **Table 6** in Appendix III).

Other no-pain: controls > responders. Comparison of hemodynamic responses of control and responder groups to non-painful trials in the 'other' condition revealed that controls showed more activity in two of the regions classically associated with placebo-induced pain reductions: left posterior insula and left rolandic operculum ($P < 0.05$ FWE, SVC). Controls also showed increased activation in one of the regions associated with placebo-induced increases, the left middle frontal gyrus (DLPFC, $P < 0.05$ FWE, SVC, see **Table 7** in Appendix III).

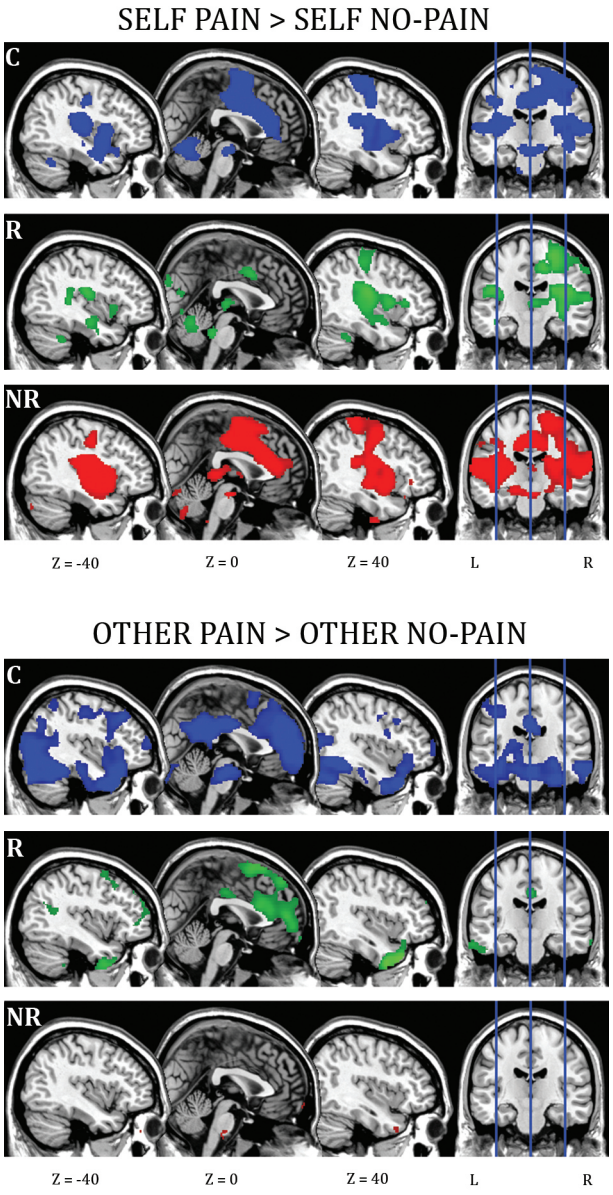

Figure 3 Top part: neural activations for the first-person experience of physical pain (contrast: self pain > self no-pain) in each group. Bottom part: neural activations for empathy for physical pain (contrast: other pain > other no-pain). Statistical maps are superimposed on a standard T1 template. Maps are thresholded at $P < 0.005$ uncorrected, for illustrative purposes. C = controls, R = responders, NR = non-responders.

Other no-pain: responders > controls. Comparison of hemodynamic responses of responder and control groups to non-painful trials in the 'other' condition revealed that responders showed higher activity in one of the regions associated with placebo-induced increases, the right inferior frontal gyrus ($P < 0.05$ FWE, SVC). Controls also showed increased activation in one region associated with placebo-induced pain reductions, the right putamen ($P < 0.05$ FWE, SVC, see **Table 8** in Appendix III).

Controls – non-responders comparison

Self pain: controls > non-responders. Comparison of hemodynamic responses of control and non-responder groups to painful trials in the 'self' condition revealed that controls showed more activity in one of the regions classically associated with placebo-induced pain reductions: the left anterior insular cortex ($P < 0.05$ FWE, SVC). Other significantly more activated brain areas were: right middle occipital gyrus, right inferior occipital gyrus and left calcarine gyrus ($P < 0.05$, cluster-level corrected, see **Table 9** in Appendix III).

Self pain: non-responders > controls. Comparison of hemodynamic responses of non-responder and control groups to painful trials in the 'self' condition revealed that non-responders showed more activity in some of the regions associated to placebo-induced increases: right middle frontal gyrus (DLPFC, $P < 0.05$, cluster-level corrected), and left middle frontal gyrus (DLPFC), rostral anterior cingulate cortex, and bilateral inferior frontal gyrus extending into the anterior insular cortex ($P < 0.05$ FWE, SVC). Non-responders also showed increased activation in regions associated with placebo-induced pain reductions: left putamen, left amygdala ($P < 0.05$, cluster-level corrected), right anterior insular cortex, left middle insular cortex, right amygdala ($P < 0.05$ FWE, SVC). Other significantly more activated brain areas were: right superior frontal gyrus, right superior orbitofrontal gyrus, bilateral superior medial frontal gyrus, right supplementary motor area, left lingual gyrus, cerebellum, left parahippocampal gyrus ($P < 0.05$, cluster-level corrected, see **Table 10** in Appendix III).

Self no-pain: controls > non-responders. Comparison of hemodynamic responses of control and non-responder groups to non-painful trials in the 'self' condition revealed that controls showed more activity in two of the regions classically associated with placebo-induced pain reductions: left anterior insular cortex and left middle insular cortex ($P < 0.05$ FWE, SVC). Controls also showed increased activation in one region associated with placebo-induced increases, the left middlfe frontal gyrus (DLPFC, $P < 0.05$ FWE, SVC). Other significantly more activated brain areas were: left middle occipital gyrus, bilateral inferior occipital gyrus, left calcarine gyrus and left fusiform gyrus ($P < 0.05$, cluster-level corrected, see **Table 11** in Appendix III).

Self no-pain: non-responders > controls. Comparison of hemodynamic responses of non-responder and control groups to non-painful trials in the 'self' condition revealed that non-responders showed more activity in four of the regions associated with placebo-induced increases: right middle frontal gyrus (DLPFC, $P < 0.05$, cluster-level corrected), and left middle frontal gyrus (DLPFC), rostral anterior cingulate cortex, right anterior insular cortex, and bilateral inferior frontal gyrus ($P < 0.05$ FWE, SVC). Non-responders also showed increased activation in one region associated with placebo-induced pain reductions, the bilateral amygdala ($P < 0.05$ FWE, SVC). Other significantly more activated brain areas were: left lingual gyrus, left calcarine gyrus, cerebellum, and parahippocampal gyrus ($P < 0.05$, cluster-level corrected, see **Table 12** in Appendix III).

Other pain: controls > non-responders. Comparison of hemodynamic responses of control and non-responder groups to painful trials in the 'other' condition revealed that controls showed more activity only in one of the regions classically associated with placebo-induced pain reductions, the left anterior insular cortex ($P < 0.05$ FWE, SVC). Controls also showed increased activation in two regions associated with placebo-induced increases: the left middle frontal gyrus (DLPFC), and the right medial orbitofrontal gyrus ($P < 0.05$ FWE, SVC). Other brain areas activated were: right inferior occipital gyrus, left calcarine gyrus, right fusiform gyrus, right lingual gyrus and cerebellum ($P < 0.05$, cluster-level corrected, see **Table 13** in Appendix III).

Other pain: non-responders > controls. Comparison of hemodynamic responses of non-responder and control groups to painful trials in the 'other' condition revealed that responders showed more activity in two of the regions associated with placebo-induced increases: the left middle frontal gyrus (DLPFC), and the left inferior frontal gyrus ($P < 0.05$ FWE, SVC). Non-responders also showed increased activation in one region associated with placebo-induced pain reductions, the right amygdala ($P < 0.05$ FWE, SVC). Other brain areas activated were: left lingual gyrus, left calcarine gyrus, left fusiform gyrus, cerebellum ($P < 0.05$, cluster-level corrected see **Table 14** in Appendix III).

Other no-pain: controls > non-responders. Comparison of hemodynamic responses of control and non-responder groups to non-painful trials in the 'other' condition revealed that controls did not show any more active area than non-responders.

Other no-pain: non-responders > controls. Comparison of hemodynamic responses of non-responder and control groups to non-painful trials in the 'other' condition revealed that non-responders showed higher activity in some of the regions associated with placebo-induced increases: right middle frontal gyrus (DLPFC), and left middle frontal gyrus (DLPFC), bilateral middle orbitofrontal gyrus, and bilateral inferior frontal gyrus ($P < 0.05$, cluster-level corrected), right medial orbitofrontal gyrus (vmPFC), left anterior insular cortex, rostral anterior cingulate cortex and left ventral striatum ($P < 0.05$ FWE, SVC). Non-responders also showed increased activation in some regions associated with placebo-induced pain reductions: right anterior insular cortex, bilateral middle insula, left posterior insular cortex, bilateral amygdala and bilateral putamen ($P < 0.05$ FWE, SVC). Other significantly more activated brain areas were: bilateral superior frontal gyrus, left superior medial frontal gyrus, left superior orbitofrontal gyrus, left inferior orbitofrontal gyrus, inferior frontal operculum, left precentral gyrus, right inferior temporal gyrus, left supramarginal gyrus, left middle temporal gyrus, right fusiform gyrus, bilateral lingual gyrus, precuneus, cuneus, left superior occipital gyrus, left calcarine gyrus, cerebellum, vermis, and right hippocampus ($P < 0.05$, cluster-level corrected, see **Table 15** in Appendix III).

Non-responders – responders comparison

Self pain: non-responders > responders. Comparison of hemodynamic responses of non-responder and responder groups to painful trials in the 'self' condition revealed that non-responders showed more activity in some of the regions classically associated with placebo-induced pain reductions: anterior-middle cingulate cortex, left middle insular cortex, left pallidum, left putamen and bilateral amygdala ($P < 0.05$, cluster-level corrected), right rolandic operculum (S2), left anterior insular cortex and left posterior insular cortex ($P < 0.05$ FWE, SVC). Non-responders also showed increased activation in some regions associated with placebo-induced increases: left middle frontal gyrus (DLPFC), right middle orbitofrontal gyrus, rectus gyrus, left thalamus ($P < 0.05$, cluster-level corrected), and right middle frontal gyrus (DLPFC), bilateral anterior

insular cortex, bilateral inferior frontal gyrus, rostral anterior cingulate cortex, and left ventral striatum ($P < 0.05$ FWE, SVC). Other significantly more activated brain areas were: bilateral superior orbitofrontal gyrus, bilateral superior medial frontal gyrus, right superior frontal gyrus, right precentral gyrus, left middle temporal gyrus, bilateral precuneus, left superior parietal gyrus, bilateral lingual gyrus, right inferior occipital gyrus, cerebellum, and right pallidum ($P < 0.05$, cluster-level corrected, see **Table 16** in Appendix III).

Self pain: responders > non-responders. Comparison of hemodynamic responses of responder and non-responder groups to painful trials in the 'self' condition revealed that responders showed more activity in three the regions associated to placebo-induced increases: rostral anterior cingulate cortex, bilateral anterior insular cortex, right inferior frontal gyrus, bilateral thalamus and periaquedutal gray matter ($P < 0.05$ FWE, SVC). Other brain areas activated were: right middle temporal pole, right inferior temporal gyrus, right fusiform gyrus, right inferior occipital gyrus, and cerebellum ($P < 0.05$, cluster-level corrected, see **Table 17** in Appendix III).

Self no-pain: non-responders > responders. Comparison of hemodynamic responses of non-responder and responder groups to non-painful trials in the 'self' condition revealed that non-responders showed more activity in three of the regions classically associated with placebo-induced pain reductions: right anterior insula and right putamen ($P < 0.05$, cluster-level corrected), and left amygdala ($P < 0.05$ FWE, SVC). Non-responders also showed increased activation in some regions associated with placebo-induced increases: right middle orbitofrontal gyrus (mOFC) and right anterior insular cortex ($P < 0.05$, cluster-level corrected), and bilateral middle frontal gyrus (DLPFC), left inferior frontal gyrus, and rostral anterior cingulate cortex ($P < 0.05$ FWE, SVC). Other significantly more activated brain areas were: right superior frontal gyrus, left middle temporal gyrus, left inferior temporal gyrus, right precuneus, bilateral lingual gyrus, right calcarine gyrus, cerebellum, and right pallidum ($P < 0.05$, cluster-level corrected, see **Table 18** in Appendix III).

Self no-pain: responders > non-responders. Comparison of hemodynamic responses of responder and non-responder groups to non-painful trials in the 'self' condition revealed that responders showed more activity in two regions associated with placebo-induced

increases: right anterior insular cortex and periaquedutal gray matter ($P < 0.05$ FWE, SVC, see **Table 19** in Appendix III).

Other pain: non-responders > responders. Comparison of hemodynamic responses of non-responder and responder groups to painful trials in the 'other' condition revealed that non-responders showed more activity in some of the regions classically associated with placebo-induced pain reductions: left superior temporal gyrus, left amygdala and left hippocampus ($P < 0.05$, cluster-level corrected), left middle insular cortex, left posterior insular cortex and right amygdala ($P < 0.05$ FWE, SVC). Non-responders also showed increased activation in two regions associated with placebo-induced increases: the bilateral thalamus ($P < 0.05$, cluster-level corrected), and the left middle frontal gyrus (DLPFC, $P > 0.05$ FWE, SVC). Other significantly more activated brain areas were: right inferior frontal gyrus, left middle temporal gyrus, bilateral inferior temporal gyrus, right fusiform gyrus, left precuneus, bilateral lingual gyrus, left calcarine gyrus, right superior occipital gyrus, right middle occipital gyrus, cerebellum, right hippocampus ($P < 0.05$, cluster-level corrected, see **Table 20** in Appendix III).

Other pain: responders > non-responders. Comparison of hemodynamic responses of responder and non-responder groups to painful trials in the 'other' condition revealed that responders showed more activity in two of the regions associated with placebo-induced increases: rostral anterior cingulate cortex and right inferior frontal gyrus ($P < 0.05$ FWE, SVC, see **Table 21** in Appendix III).

Other no-pain: non-responders > responders. Comparison of hemodynamic responses of non-responder and responder groups to non-painful trials in the 'other' condition revealed that non-responders showed more activity in some of the regions classically associated with placebo-induced pain reductions: left hippocampus and bilateral inferior frontal gyrus ($P < 0.05$, cluster-level corrected), left posterior insular cortex and bilateral amygdala ($P < 0.05$ FWE, SVC). Non-responders also showed increased activation in some regions associated with placebo-induced increases: bilateral middle frontal gyrus (DLPFC), left thalamus ($P < 0.05$ SVC), left inferior frontal gyrus, right anterior insular cortex, rostral anterior cingulate cortex ($P < 0.05$ FWE, SVC). Other significantly more activated brain areas were: bilateral superior frontal gyrus, bilateral superior medial frontal gyrus, right supplementary motor area, left precentral gyrus, left

postcentral gyrus, left middle temporal gyrus, left superior parietal gyrus, right fusiform gyrus, left precuneus, bilateral cuneus, bilateral lingual gyrus, right calcarine gyrus, cerebellum, and right hippocampus ($P < 0.05$, cluster-level corrected, see **Table 22** in Appendix III).

Other no-pain: responders > non-responders. Comparison of hemodynamic responses of responder and non-responder groups to non-painful trials in the 'other' condition revealed that responders did not show any more active area than non-responders.

ROI analysis results

Placebo-induced reductions ROIS

Controls – responders comparison

When comparing control and responder groups in the peak coordinates associated with decreased activity as effect of placebo, left anterior insula, left amygdala, and left putamen showed different activity´s patterns in the two groups (**Figure 4**).

A significant interaction INTENSITY × GROUP was found for left anterior insula 1, ($F_{(1,35)} = 4.458$, $P = 0.042$, **Figure 4A**), left anterior insula 3 ($F_{(1,35)} = 4.201$, $P = 0.048$, **Figure 4B**) and left amygdala 2 ($F_{(1,35)} = 5.782$, $P = 0.022$, **Figure 4D**), while a significant interaction TARGET × INTENSITY × GROUP was found for left amygdala 1 ($F_{(1,35)} = 8.983$, $P = 0.005$, **Figure 4C**) and right primary somatosensory cortex ($F_{(1,35)} = 4.481$, $P = 0.041$, **Figure 4E**). The general pattern showed that responders did not present any modulation of activity in these areas according to the intensity of the stimulations, whereas controls showed higher activity during painful stimulations.

Post-hoc *t*-tests showed increased activity in 'pain' compared to 'no-pain' condition only in the controls group for left anterior insula 1 [*Controls*: self pain – self no-pain (mean/SE) = 0.713/0.197; planned comparison; $F_{(1,35)} = 14.637$, $P = 0.001$; other pain – other no-pain (mean/SE) = 0.463/0.119; planned comparison; $F_{(1,35)} = 11.258$, $P = 0.002$. *Responders*: self pain – self no-pain (mean/SE) = 0.386/0.196; planned comparison; $F_{(1,35)} = 3.277$, $P = 0.079$; other pain – other no-pain (mean/SE) = -0.019/0.183; planned comparison; $F_{(1,35)} = 0.014$, $P = 0.907$], left anterior insula 3 [*Controls*: self pain – self no-pain (mean/SE) = 0.735/0.188; planned comparison; $F_{(1,35)} = 16.770$, $P = 0.000$; other pain – other no-pain (mean/SE) = 0.600/0.125; planned

comparison; $F_{(1,35)}$ = 19.187, P = 0.000. *Responders*: self pain – self no-pain (mean/SE) = 0.369/0.192; planned comparison; $F_{(1,35)}$ = 3.219, P = 0.081; other pain – other no-pain (mean/SE) = 0.190/0.174; planned comparison; $F_{(1,35)}$ = 1.465, P = 0.234] and left amygdala 2 [*Controls*: self pain – self no-pain (mean/SE) = 0.077/0.128; planned comparison; $F_{(1,35)}$ = 0.043, P = 0.838; other pain – other no-pain (mean/SE) = 0.567/0.100; planned comparison; $F_{(1,35)}$ = 30.564, P = 0.000 *Responders*: self pain – self no-pain (mean/SE) = –0.028/0.123; planned comparison; $F_{(1,35)}$ = 0.043, P = 0.838; other pain – other no-pain (mean/SE) = 0.088/0.122; planned comparison; $F_{(1,35)}$ = 0.560, P = 0.459].

This difference was also found, although in the 'other' condition only, for left amygdala 1 [*Controls*: other pain – other no-pain (mean/SE) = 0.465/0.096; planned comparison; $F_{(1,35)}$ = 22.960, P = 0.000; *Responders*: other pain – other no-pain (mean/SE) = -0.094/0.112 planned comparison; $F_{(1,35)}$ = 0.710, P = 0.405], and for right primary somatosensory cortex [*Controls*: other pain – other no-pain (mean/SE) = –0.235/0.115; planned comparison; $F_{(1,35)}$ = 4.212, P = 0.048; *Responders*: other pain – other no-pain (mean/SE) = 0.160/0.131 planned comparison; $F_{(1,35)}$ = 1.479, P = 0.232] explaining the significance of the three-way interaction.

No areas of the right hemisphere showed any significant interaction with factor group.

Controls − non-responders comparison

The ANOVA comparing the control group and the group of participants in which placebo treatment was ineffective, showed a three-way interaction TARGET × INTENSITY × GROUP in several ROIs (**Figure 5**) mostly indicating that participants in the control group had higher activation in cortical and subcortical regions both during direct and vicarious experience of pain, compared to no-pain, while non-responders had higher activation only when directly undergoing painful stimulations, but not during vicarious experience.

In particular, in the left hemisphere, seven ROIs displayed the significant three-way interaction: middle insula 2 ($F_{(1,35)}$ = 5.540, P = 0.024, **Figure 5A**), middle insula 3 ($F_{(1,35)}$ = 5.712, P = 0.022, **Figure 5B**), mid-posterior insula ($F_{(1,35)}$ = 7.734, P = 0.009, **Figure 5C**), putamen 1 ($F_{(1,35)}$ = 8.589, P = 0.006, **Figure 5D**), putamen 2 ($F_{(1,35)}$ = 11.811, P = 0.002, **Figure 5E**), amygdala 1 ($F_{(1,35)}$ = 10.535, P = 0.003, **Figure 5F**), amygdala 2 ($F_{(1,35)}$ = 10.773, P = 0.002, **Figure 5G**).

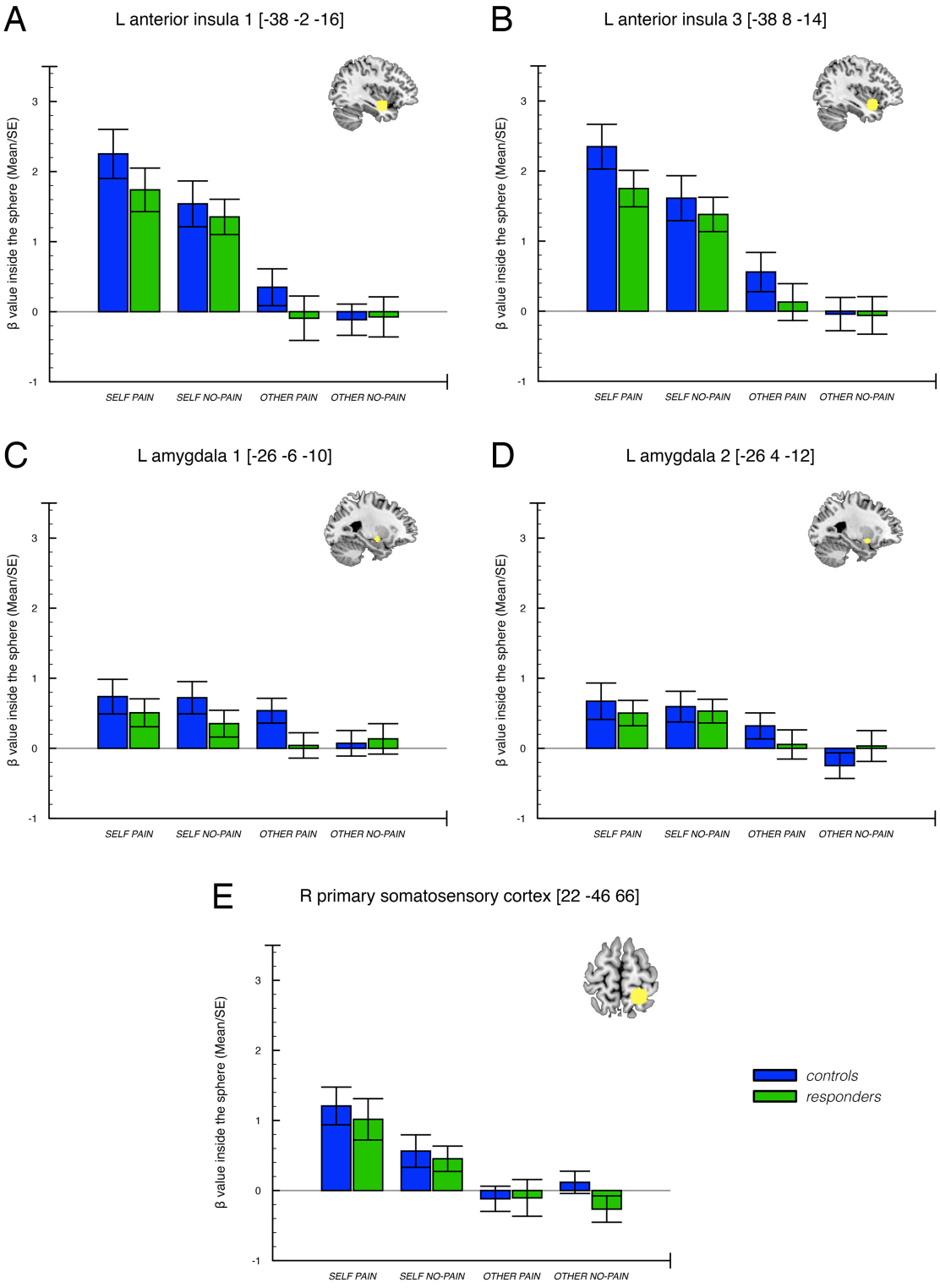

Figure 4 Mean β-values for the ROIs showing significant statistical difference between controls and responders. (A-B, E) sphere radius: 10 mm. (C-D) sphere radius: 5 mm.

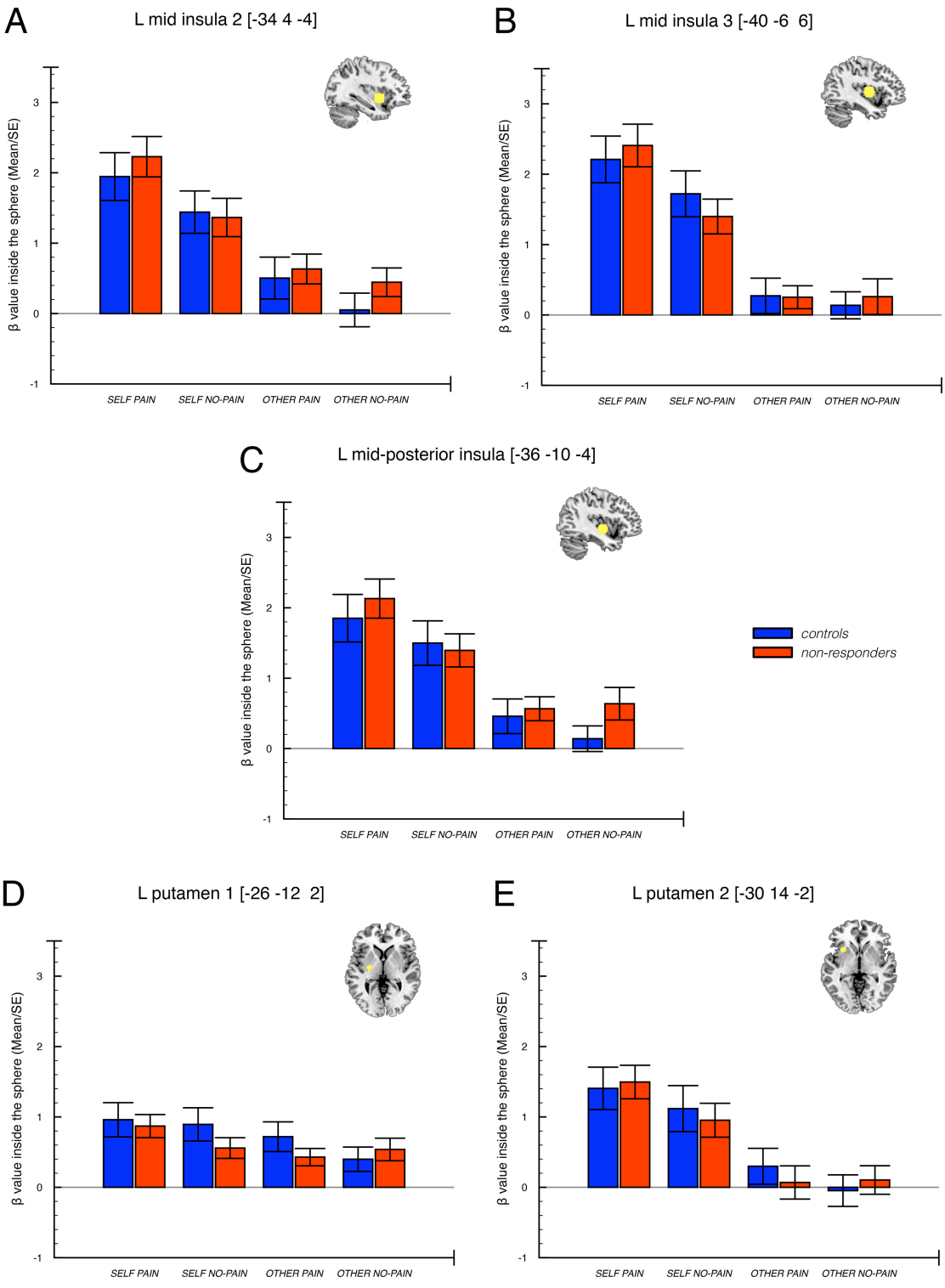

Figure 5 Mean β-values over all the voxels inside left-hemisphere ROIs showing significant statistical difference between controls and non-responders. (A-C) sphere radius: 10 mm. (D-G) sphere radius: 5 mm. F and G are on the next page.

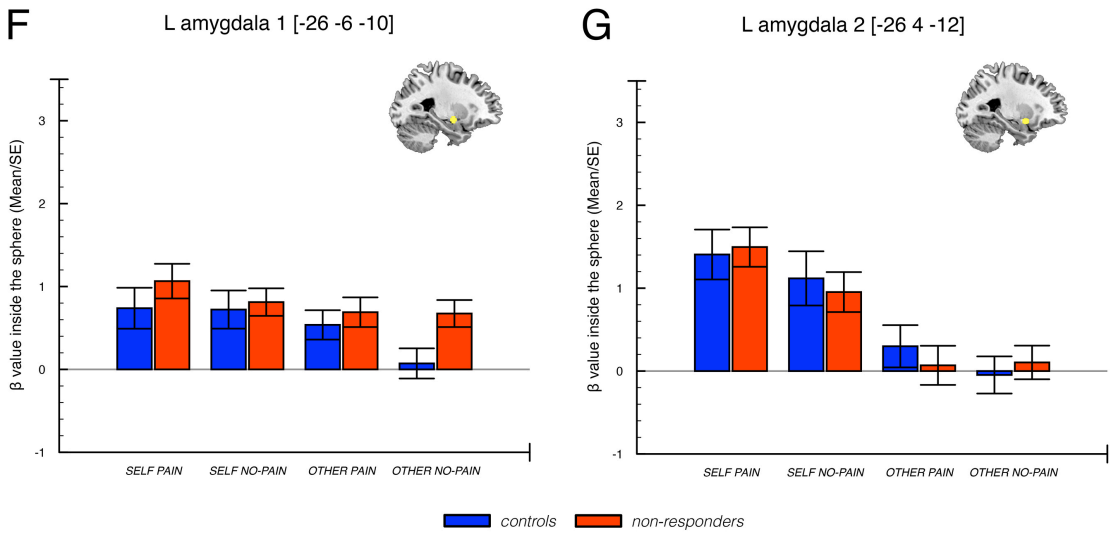

As anticipated, post-hoc *t*-tests revealed that across all ROIs the 'other' condition showed a consistent pattern for which there was an effect of intensity ('pain' bigger than 'no-pain') in the control group, which was absent in the non-responders: left middle insula 2 [*Controls*: other pain – other no-pain (mean/SE) = 0.453/0.105; planned comparison; $F_{(1,35)}$ = 16.121, P = 0.000. *Non-responders*: other pain – other no-pain (mean/SE) = 0.188/0.140; planned comparison; $F_{(1,35)}$ = 2.125, P = 0.154); left middle insula 3 [*Controls*: other pain – other no-pain (mean/SE) = 0.135/0.109; planned comparison; $F_{(1,35)}$ = 1.255, P = 0.270. *Non-responders*: other pain – other no-pain (mean/SE) = −0.008/0.154; planned comparison; $F_{(1,35)}$ = 0.003, P = 0.955]; left mid-posterior insula [*Controls*: other pain – other no-pain (mean/SE) = 0.319/0.100; planned comparison; $F_{(1,35)}$ = 22.960, P = 0.000. *Non-responders*: other pain – other no-pain (mean/SE) = −0.071/0.151; planned comparison; $F_{(1,35)}$ = 0.710, P = 0.405]; left putamen 1 [*Controls*: other pain – other no-pain (mean/SE) = 0.320/0.079; planned comparison; $F_{(1,35)}$ = 12.286, P = 0.001. *Non-responders*: other pain – other no-pain (mean/SE) = -0.109/0.121; planned comparison; $F_{(1,35)}$ = 1.082, P = 0.305; left putamen 2 [*Controls*: other pain – other no-pain (mean/SE) = 0.346/0.115; planned comparison; $F_{(1,35)}$ = 10.444, P = 0.003. *Non-responders*: other pain – other no-pain (mean/SE) = −0.035/0.109; planned comparison; $F_{(1,35)}$ = 0.080, P = 0.779]; left amygdala 1 [*Controls*: (mean/SE) = 0.465/0.096; planned other pain – other no-pain comparison; $F_{(1,35)}$ = 20.466, P = 0.000. *Non-responders*: other pain – other no-pain (mean/SE) = 0.016/0.127; planned comparison; $F_{(1,35)}$ = 0.018, P = 0.893]; left amygdala 2 [*Controls*: other pain – other no-pain (mean/SE) = 0.567/0.100; planned comparison; $F_{(1,35)}$ =

25.054, P = 0.000. *Non-responders*: other pain – other no-pain (mean/SE) = 0.000/0.148; planned comparison; $F_{(1,35)} = 0.000$, P = 0.999]. In the left middle insula 3 the interaction was explained by a trend of the same kind present in the controls, although it did even not reach the significance level [*Controls*: other pain – other no-pain (mean/SE) = 0.135/0.109; planned comparison; $F_{(1,35)} = 1.255$, P = 0.270. *Non-responders*: other pain – other no-pain (mean/SE) = -0.008/0.154; planned comparison; $F_{(1,35)} = 0.003$, P = 0.955].

In the 'self' condition instead, three different patterns of modulation of activity of these areas were found. Higher activity in 'pain' compared to 'no-pain' was found in both groups in left mid-posterior insula [*Controls*: self pain – self no-pain (mean/SE) = 0.353/0.160; planned comparison; $F_{(1,35)} = 5.622$, P = 0.023. *Non-responders*: self pain – self no-pain (mean/SE) = 0.736/0.151; planned comparison; $F_{(1,35)} = 18.643$, P = 0.000], left middle insula 2 [*Controls*: self pain – self no-pain (mean/SE) = 0.505/0.150; planned comparison; $F_{(1,35)} = 11.888$, P = 0.001. *Non-responders*: self pain – self no-pain (mean/SE) = 0.864/0.161; planned comparison; $F_{(1,35)} = 26.567$, P = 0.000], left posterior insula 1 [*Controls*: self pain – self no-pain (mean/SE) = 0.555/0.191; planned comparison; $F_{(1,35)} = 9.622$, P = 0.004. *Non-responders*: self pain – self no-pain (mean/SE) = 0.903/0.185; planned comparison; $F_{(1,35)} = 19.395$, P = 0.000], and left putamen 2 [*Controls*: self pain – self no-pain (mean/SE) = 0.288/0.100; planned comparison; $F_{(1,35)} = 6.848$, P = 0.013. *Non-responders*: self pain – self no-pain (mean/SE) = 0.542/0.139; planned comparison; $F_{(1,35)} = 18.506$, P = 0.000].

There was no effect of intensity in the 'self' condition in left amygdala 1 [*Controls*: self pain – self no-pain (mean/SE) = 0.016/0.129; planned comparison; $F_{(1,35)} = 0.015$, P = 0.904. *Non-responders*: self pain – self no-pain (mean/SE) = 0.253/0.153; planned comparison; $F_{(1,35)} = 2.844$, P = 0.101] and left amygdala 2 [*Controls*: self pain – self no-pain (mean/SE) = 0.077/0.128; planned comparison; $F_{(1,35)} = 0.315$, P = 0.578. *Non-responders*: self pain – self no-pain (mean/SE) = 0.298/0.168; planned comparison; $F_{(1,35)} = 3.630$, P = 0.065]. In left putamen 1 the effect of the intensity in the 'self' was found in the non-responders group ('pain' bigger than 'no-pain') but not in the controls [*Controls*: self pain – self no-pain (mean/SE) = 0.066/0.128; planned comparison; $F_{(1,35)} = 0.307$, P = 0.583. *Non-responders*: self pain – self no-pain (mean/SE) = 0.312/0.123; planned comparison; $F_{(1,35)} = 5.173$, P = 0.029].

In the right hemisphere, four ROIs displayed a significant three-way interaction TARGET × INTENSITY × GROUP: anterior insula 3 ($F_{(1,35)} = 4.759$, P = 0.036,

Figure 6A), middle insula 2 ($F_{(1,35)}$ = 4.794, P = 0.035, **Figure 6B**), mid-posterior insula ($F_{(1,35)}$ = 4.920 , P = 0.033, **Figure 6C**), amygdala 2 ($F_{(1,35)}$ = 8.501, P = 0.006, **Figure 6D**).

Post-hoc t-tests again revealed consistency across all ROIs but one (mid-posterior insula) for the 'other' condition, displaying an interaction with intensity in the control group ('pain' bigger than 'no-pain') which non-responders group did not show: right anterior insula 3 [*Controls*: other pain – other no-pain (mean/SE) = 0.281/0.117; planned comparison; $F_{(1,35)}$ = 6.177, P = 0.018. *Non-responders*: other pain – other no-pain (mean/SE) = -0.009/0.123; planned comparison; $F_{(1,35)}$ = 0.005, P = 0.945]; right middle insula 2 [*Controls*: other pain – other no-pain (mean/SE) = 0.242/0.109; planned comparison; $F_{(1,35)}$ = 4.402, P = 0.043. *Non-responders*: other pain – other no-pain (mean/SE) = -0.081/0.142; planned comparison; $F_{(1,35)}$ = 0.376, P = 0.543]; right amygdala 2 [*Controls*: other pain – other no-pain (mean/SE) = 0.292/0.090; planned comparison; $F_{(1,35)}$ = 7.545, P = 0.009. *Non-responders*: other pain – other no-pain (mean/SE) = -0.136/0.143; planned comparison; $F_{(1,35)}$ = 1.251, P = 0.271]. In the right mid-posterior insula none of the two groups showed an interaction with the factor intensity in the 'other' condition [*Controls*: other pain – other no-pain (mean/SE) = 0.179/0.101; planned comparison; $F_{(1,35)}$ = 2742, P = 0.101. *Non-responders*: other pain – other no-pain (mean/SE) = -0.141/0.135; planned comparison; $F_{(1,35)}$ = 1.295, P = 0.263]; instead, the interaction was explained by a significant difference between the groups in the 'other no-pain' condition [*other no-pain*: Non-responders – Controls (mean/SE) = 0.516/0.333; planned comparison; $F_{(1,35)}$ = 4.982, P = 0.032).

Again, 'self' condition did not show interaction with the group factor in all the ROIs, although the interaction with the intensity was found different for the different ROIs. In particular, all ROIs showed a bigger activity during 'pain' than 'no-pain', amygdala 2 apart in which there was no difference (despite a trend approaching to significance in the non-responders): right anterior insula 3 [*Controls*: self pain – self no-pain (mean/SE) = 0.459/0.200; planned comparison; $F_{(1,35)}$ = 6.846, P = 0.013. *Non-responders*: self pain – self no-pain (mean/SE) = 0.722/0.156; planned comparison; $F_{(1,35)}$ = 12.917, P = 0.001]; right middle insula 2 [*Controls*: self pain – self no-pain' (mean/SE) = 0.419/0.178; planned comparison; $F_{(1,35)}$ = 7.508, P = 0.010. *Non-responders*: self pain – self no-pain (mean/SE) = 0.561/0,126; planned comparison; $F_{(1,35)}$ = 10.274, P = 0.003]; right mid/posterior insula [*Controls*: self pain – self no-pain (mean/SE) = 0.436/0.183; planned comparison; F(1,35) = 7.983, P = 0.008. *Non-*

responders: self pain – self no-pain' (mean/SE) = 0.610/0,119; planned comparison; $F_{(1,35)}$ = 11.914, P = 0.001]; right amygdala 2 [*Controls*: self pain – self no-pain' (mean/SE) = 0.170/0.148; planned comparison; $F_{(1,35)}$ = 1.556, P = 0.221. *Non-responders*: self pain – self no-pain (mean/SE) = 0.309/0,136; planned comparison; $F_{(1,35)}$ = 3.927, P = 0.055].

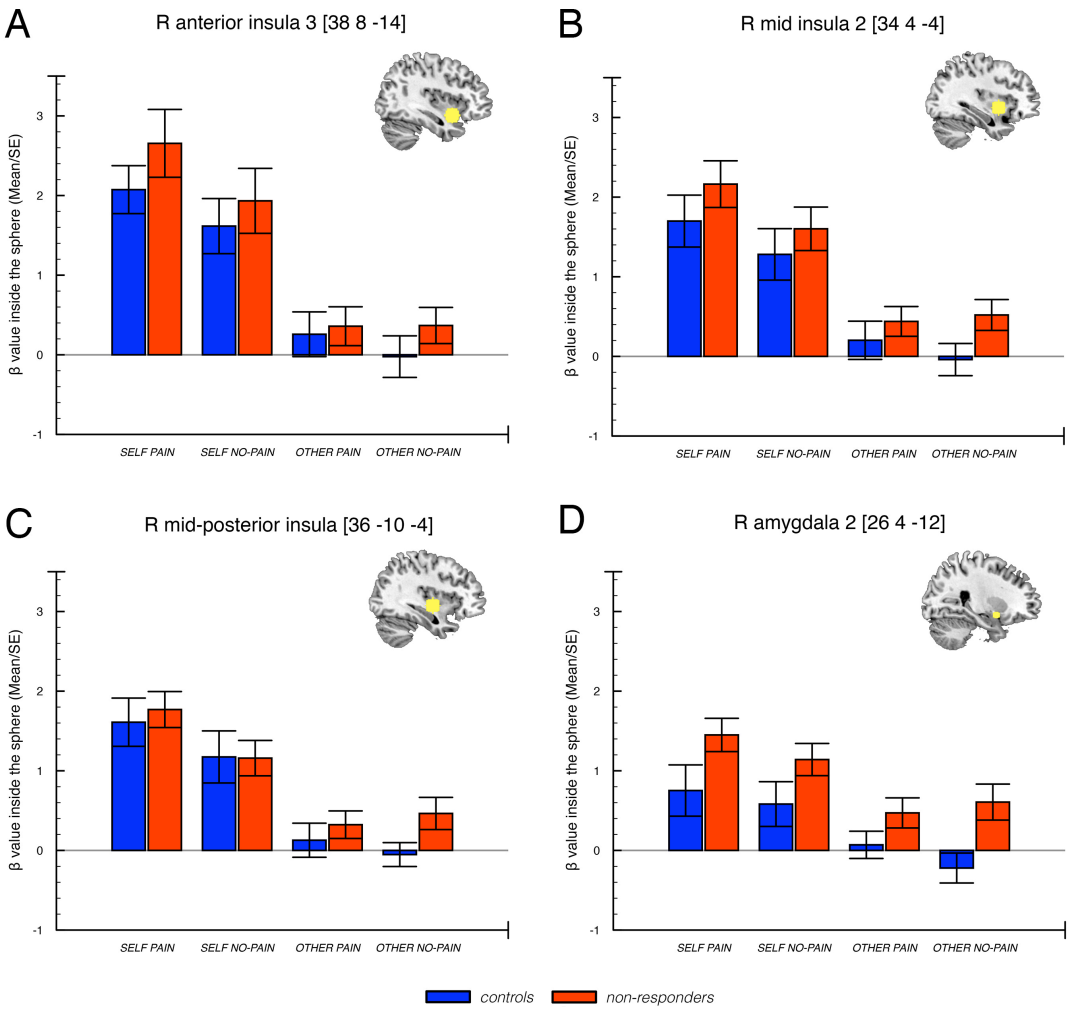

Figure 6 Mean β values over all the voxels inside right-hemisphere ROIs showing statistical interaction with the GROUP factor in the ANOVA comparing controls and non-responders groups. (A-C) sphere radius: 10 mm. (D) sphere radius: 5 mm.

Non-responders − responders comparison

The ANOVAs comparing the activity inside ROIs between the two groups that underwent a placebo manipulation but responded in a different manner showed that the

difference was located in the insula (**Figure 7**). Overall, in this region non-responders presented higher activity than responders, and the difference was primarily due to the different activity during the condition in which participants received direct painful stimulations ('self pain').

Indeed, in the left hemisphere middle insula 1 [-44 -4 -8] presented a significant two-way interaction INTENSITY × GROUP ($F_{(1,30)}$ = 5.385, P = 0.027, **Figure 7A**), while a significant three-way interaction TARGET × INTENSITY × GROUP was found for middle insula 3 [-40 -6 6] ($F_{(1,30)}$ = 4.831, P = 0.036, **Figure 7B**), posterior insula 1 [-42 -18 2] ($F_{(1,30)}$ = 7.103, P = 0.012, **Figure 7C**), and posterior insula 2 [-48 -16 10] ($F_{(1,30)}$ = 7.521, P = 0.010, **Figure 7D**).

Post-hoc *t*-tests revealed that activity in left middle insula 1 in the non-responders depended on intensity [*Non-responders*: pain – no-pain (mean/SE) = 0.658/0.218; planned comparison; $F_{(1,30)}$ = 26.824, P = 0.000] while this difference was absent in the responders [*Responders*: pain – no-pain (mean/SE) = 0.241/0.175; planned comparison; $F_{(1,30)}$ = 3.600, P = 0.067]. A similar pattern explained the three-way interaction in the left posterior insula 1, yet the difference was there only for the 'self' condition [*Non-responders*: self pain – self no-pain (mean/SE) = 0.903/0.185; planned comparison; $F_{(1,30)}$ = 28.537, P = 0.000. *Responders*: self pain – self no-pain (mean/SE) = 0.307/0.152; planned comparison; $F_{(1,30)}$ = 3.292, P = 0.080]. In the left middle insula 3 the significant three-way interaction was explained by a trend toward significance in the direct comparison between the activity in the two groups during 'self pain', with non-responders showing greater activity [*Non-responders*: self pain (mean/SE) = 2.408/0.303; *Responders*: self pain (mean/SE) = 1.552/0.312. Planned comparison; $F_{(1,30)}$ = 3.882, P = 0.058] In the left posterior insula 2 the same difference was found [*Non-responders*: self pain (mean/SE) = 2.732/0.387; *Responders*: self pain (mean/SE) = 1.515/0.377. Planned comparison; $F_{(1,30)}$ = 5.059, P = 0.032] together with a difference in the 'other no-pain' condition [*Non-responders*: other no pain (mean/SE) = 0.341/0.174; *Responders*: other no pain (mean/SE) = -0.360/0.272. Planned comparison; $F_{(1,30)}$ = 4.734, P = 0.038].

No areas of the right hemisphere showed any interaction with the group factor.

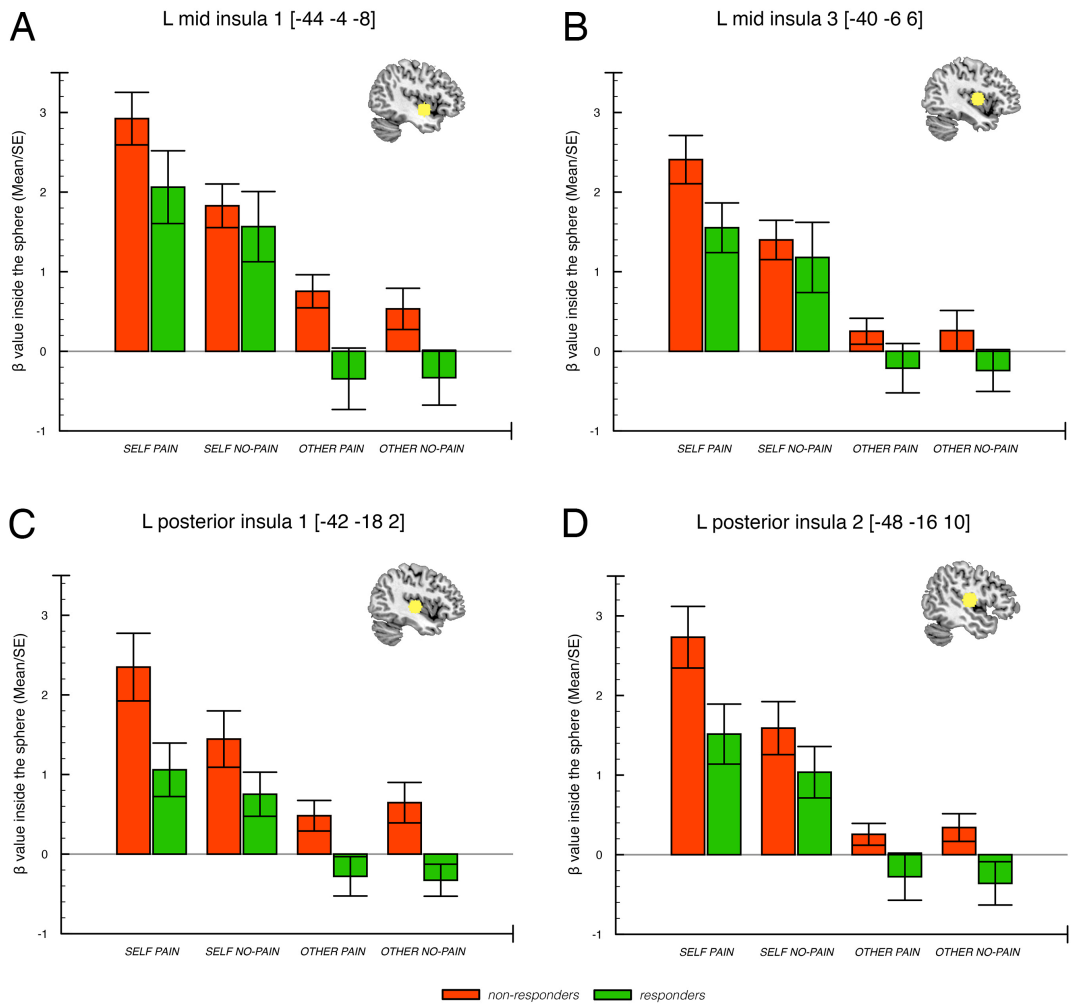

Figure 7 Mean β values over all the voxels inside ROIs showing statistical interaction with the GROUP factor in the ANOVA comparing responders and non-responders groups. (A-D) sphere radius: 10 mm.

Placebo-induced increases ROIS

Controls – responders comparison

The 2 × 2 × 2 ANOVA comparing controls and responders groups in the areas associated with increasing activity as effect of placebo showed an interaction TARGET × GROUP in three ROIs inside the rostral anterior cingulate cortex (rACC) and a three-way interaction INTENSITY × TARGET × GROUP in two ROIs centered in the right dorsolateral prefrontal cortex (DLPFC, **Figure 8**). The general pattern in the rACC indicated that participants in the control group generally presented higher activity in the 'self' than in the 'other' condition, while responders did not show this modulation. In particular, the three ROIs were: left rostro-dorsal ACC [-6 28 24] ($F_{(1,35)}$ = 4.623, P =

0.039, **Figure 8A**), left pregenual ACC 3 [-4 32 10] ($F_{(1,35)}$ = 5.938, P = 0.020, **Figure 8B**), right pregenual ACC 3[4 32 10] ($F_{(1,35)}$ = 5.627, P = 0.023, **Figure 8C**).

As anticipated, post-hoc *t*-tests revealed that activity in the controls depended on target ('self' bigger than 'other'), while this effect was absent in the responders. This was particularly clear for ROIs inside pregenual ACC, i.e. left pregenual ACC 3 [*Controls*: self – other (mean/SE) = 0.418/0.134; planned comparison; $F_{(1,35)}$ = 9.759, P = 0.004. *Responders*: self – other (mean/SE) = −0.078/0.153 planned comparison; $F_{(1,35)}$ = 0.258, P = 0.615] and right pregenual ACC 3 [*Controls*: self– other (mean/SE) = 0.452/0.137; planned comparison; $F_{(1,35)}$ = 10.866, P = 0.002. *Responders*: self – other (mean/SE) = −0.043/0.157; planned comparison; $F_{(1,35)}$ = 0.074, P = 0.788]. A similar pattern explained the interaction for the left rostro-dorsal ACC, although in this case also the difference between activity during the 'self' and 'other' condition in the responders reached statistical significance [*Controls*: self – other (mean/SE) = 0.888/0.159; planned comparison; $F_{(1,35)}$ = 31.309, P = 0.000. *Responders*: self – other (mean/SE) = 0.369/0.182; planned comparison; $F_{(1,35)}$ = 4.121, P = 0.050].

The two ROIs that presented the three-way interaction in the DLPFC were: right middle frontal gyrus 1 [42 20 36] ($F_{(1,35)}$ = 5.118, P = 0.030, **Figure 8D**), and right middle frontal gyrus 2 [36 26 30] ($F_{(1,35)}$ = 4.164, P = 0.049, **Figure 8E**).

Post-hoc *t*-tests revealed that activity in the controls depended on intensity (in opposite directions according to the target), while this effect was absent in the responders. This was true both for right middle frontal gyrus 1 [*Controls*: self pain – self no-pain (mean/SE) = −0.387/0.138; planned comparison; $F_{(1,35)}$ = 7.820, P = 0.008; other pain – other no-pain (mean/SE) = 0.257/0.096; planned comparison; $F_{(1,35)}$ = 7.178, P = 0.011. *Responders*: self pain – self no-pain (mean/SE) = −0.164/0.158; planned comparison; $F_{(1,35)}$ = 1.065, P = 0.309; other pain – other no-pain (mean/SE) = −0.092/0.110; planned comparison; $F_{(1,35)}$ = 0.706, P = 0.407] and for right middle frontal gyrus 2 [*Controls*: self pain – self no-pain (mean/SE) = −0.266/0.124; planned comparison; $F_{(1,35)}$ = 4.642, P = 0.038; other pain – other no-pain (mean/SE) = 0.158/0.071; planned comparison; $F_{(1,35)}$ = 4.972, P = 0.032. *Responders*: self pain – self no-pain (mean/SE) = −0.082/0.142; planned comparison; $F_{(1,35)}$ = 0.331, P = 0.568; other pain – other no-pain (mean/SE) = −0.049/0.081; planned comparison; $F_{(1,35)}$ = 0.357, P = 0.554].

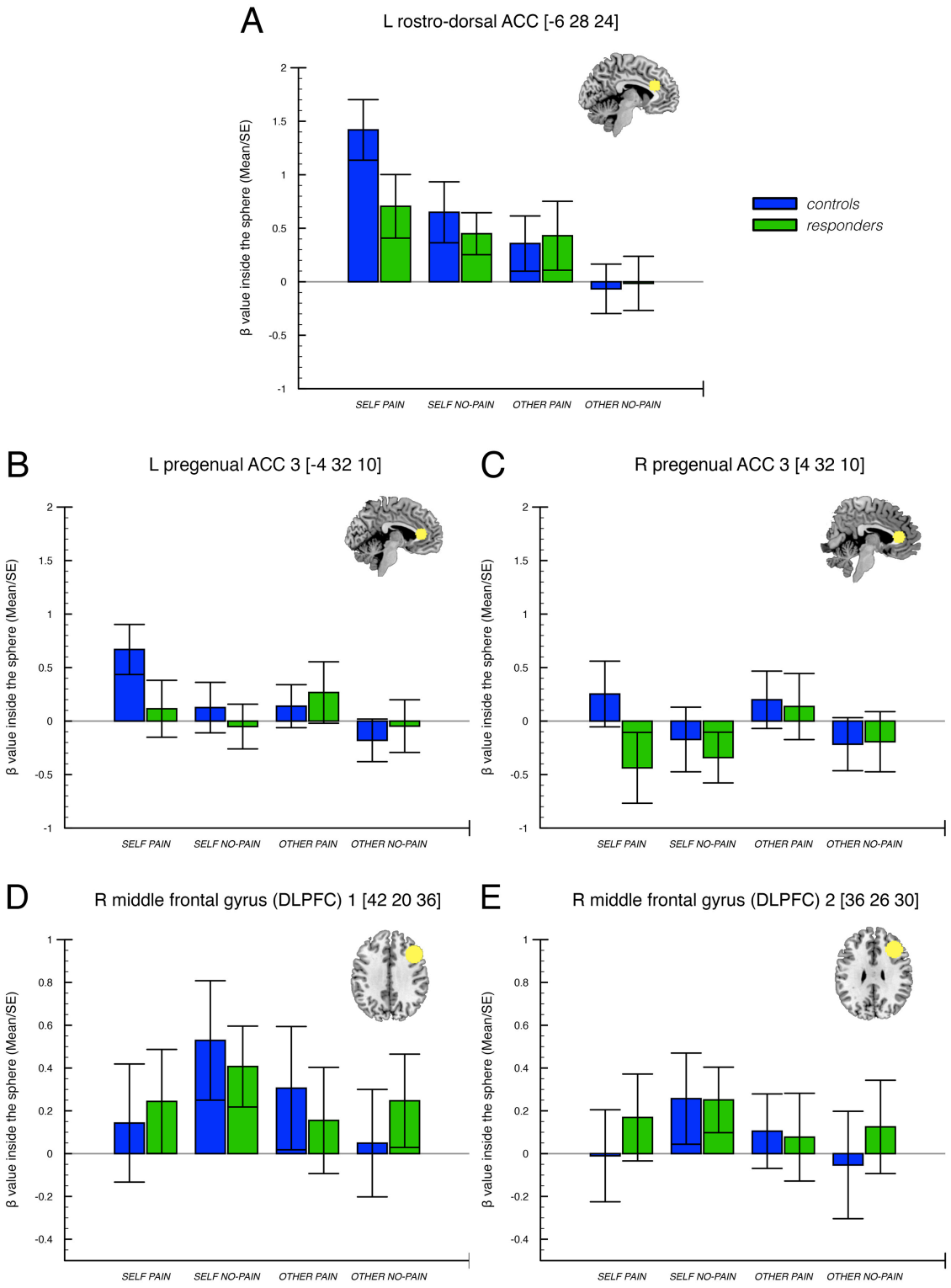

Figure 8 Mean β-values for the ROIs showing significant statistical difference between controls and responders. (A-C) sphere radius: 10 mm. (D-E) sphere radius: 15 mm.

Controls – Non-responders comparison

The ANOVA comparing the control group and the group of participants in which placebo treatment was ineffective, showed a INTENSITY × GROUP interaction for one ROI inside DLPFC, the right middle frontal gyrus 1 [42 20 36] ($F_{(1,35)}$ = 4.786, P = 0.035, **Figure 9D**). Other three ROIs inside DLPFC showed an INTENSITY × TARGET × GROUP interaction: left middle frontal gyrus 1 [−42 20 36] ($F_{(1,35)}$ = 6.592, P = 0.015, **Figure 9B**), left middle frontal gyrus 2 [−36 26 30] ($F_{(1,35)}$ = 6.776, P = 0.013, **Figure 9C**), and right middle frontal gyrus 2 [36 26 30] ($F_{(1,35)}$ = 5.329, P = 0.027, **Figure 9E**). Finally, a INTENSITY × TARGET × GROUP interaction was also found for one ROI inside the rostral anterior cingulate cortex, the right rostral ACC 3 [10 44 12] ($F_{(1,35)}$ = 4.909, P = 0.034, **Figure 9A**).

As for the activity inside the DLPFC, the general pattern showed that non-responders modulate their activity according to the intensity of the stimulations in the 'other' condition only ('no-pain' bigger than 'pain'), while controls mostly presented an inverse modulation according to the target: 'no-pain' bigger than 'pain' in the self condition, 'pain' bigger than 'no-pain' in the 'other' condition. Post hoc *t*-test revealed that this was particularly true for right middle frontal gyrus 2 [*Controls*: self pain – self no-pain (mean/SE) = −0.266/0.124; planned comparison; $F_{(1,35)}$ = 4.642, P = 0.038; other pain – other no-pain (mean/SE) = 0.158/0.071; planned comparison; $F_{(1,35)}$ = 4.972, P = 0.032. *Non-responders*: self pain – self no-pain (mean/SE) = −0.234/0.125; planned comparison; $F_{(1,35)}$ = 3.490, P = 0.070; other pain – other no-pain (mean/SE) = −0.215/0.073; planned comparison; $F_{(1,35)}$ = 8.606, P = 0.006] and left middle frontal gyrus 1 [*Controls*: self pain – self no-pain (mean/SE) = −0.272/0.128; planned comparison; $F_{(1,35)}$ = 4.553, P = 0.040; other pain – other no-pain (mean/SE) = 0.338/0.102; planned comparison; $F_{(1,35)}$ = 11.054, P = 0.002. *Non-responders*: self pain – self no-pain (mean/SE) = −0.270/0.146; planned comparison; $F_{(1,35)}$ = 3.411, P = 0.073; other pain – other no-pain (mean/SE) = −0.250/0.116; planned comparison; $F_{(1,35)}$ = 4.599, P = 0.039]. In left middle frontal gyrus 2 non-responders did not present any modulation of activity, while controls presented a modulation in the 'other' condition only [*Controls*: self pain – self no-pain (mean/SE) = −0.140/0.111; planned comparison; $F_{(1,35)}$ = 1.569, P = 0.219; other pain – other no-pain (mean/SE) = 0.264/0.084; planned comparison; $F_{(1,35)}$ = 9.860, P = 0.003. *Responders*: self pain – self no-pain (mean/SE) = −0.057/0.128; planned comparison; $F_{(1,35)}$ = 0.202, P = 0.656; other pain – other no-pain (mean/SE) = −0.157/0.096; planned comparison; $F_{(1,35)}$ = 2.658, P = 0.112]. Conversely,

in right middle frontal gyrus 1 the INTENSITY × GROUP interaction indicated that controls did not present any modulation according to intensity [*Controls*: pain – no-pain (mean/SE) = −0.065/0.075; planned comparison; $F_{(1,35)}$ = 0.743, P = 0.395], whereas non-responders presented less increasing activity during painful stimulations [*Non-responders*: pain – no-pain (mean/SE) = −0.315/0.086; planned comparison; $F_{(1,35)}$ = 13.369, P = 0.001].

As for the right rostral ACC 3, post hoc t-test showed that participants in the control group activated more this area in 'pain' compared to 'no-pain' condition, no matter the target [*Controls*: self pain – self no-pain (mean/SE) = 0.228/0.116; planned comparison; $F_{(1,35)}$ = 4.503, P = 0.041; other pain – other no-pain (mean/SE) = 0.462/0.092; planned comparison; $F_{(1,35)}$ = 28.414, P = 0.000], while participants in the non-responders group had this modulation of activity only in the self [*Non-responders*: self pain – self no-pain (mean/SE) = 0.356/0.108; planned comparison; $F_{(1,35)}$ = 8.439, P = 0.007; other pain – other no-pain (mean/SE) = 0.088/0.091; planned comparison; $F_{(1,35)}$ = 0.790, P = 0.380].

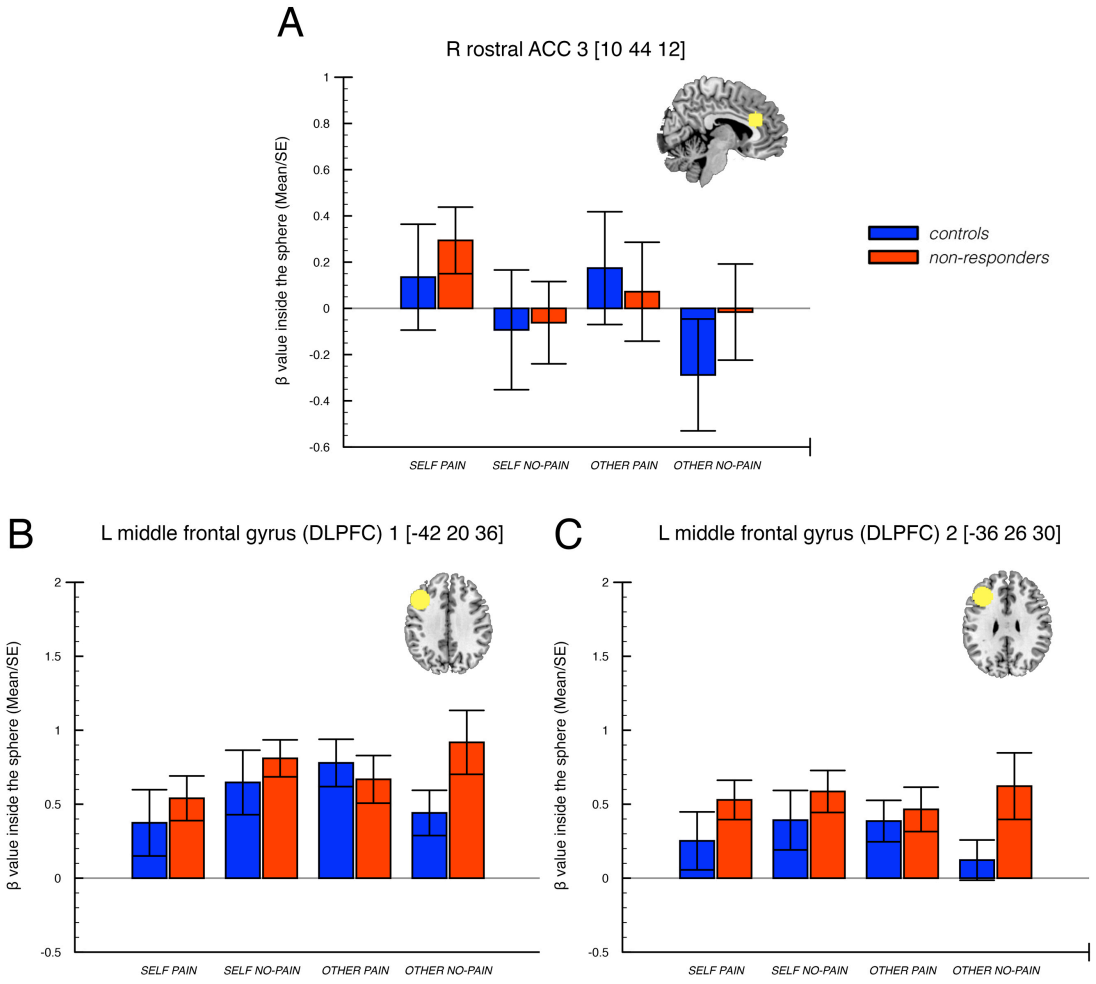

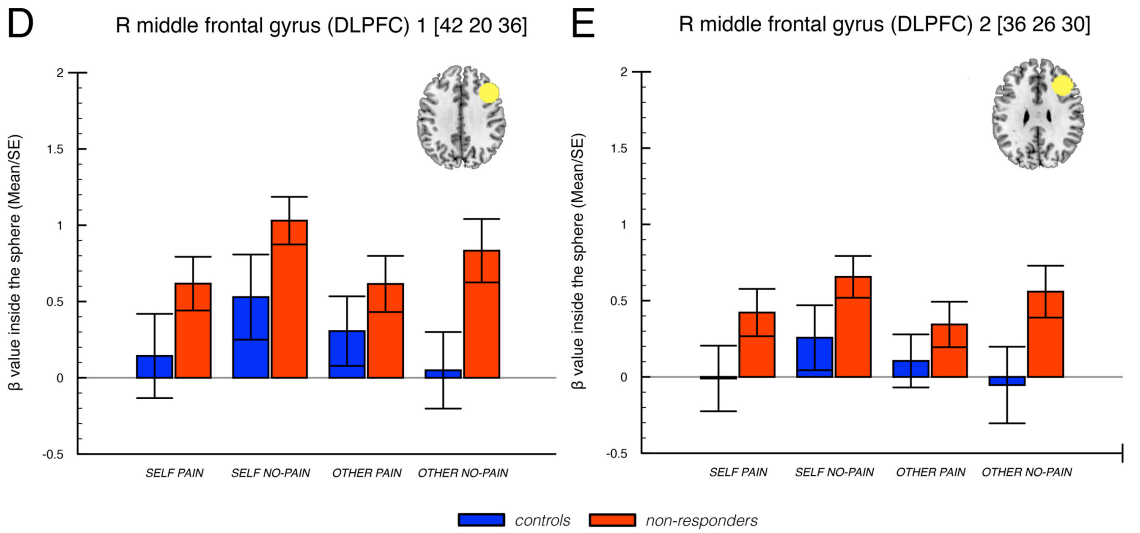

Figure 9 Mean β-values for the only ROI showing significant statistical difference between controls and non-responders. (A) Sphere radius: 10 mm. (B-E) Sphere radius: 15 mm.

Non-responders – responders comparison

The ANOVAs comparing the activity inside ROIs between the two groups that responded differently to a placebo manipulation showed that the difference was located in different parts of the anterior cingulate cortex (**Figures 10-11**). Overall, in this region non-responders presented a modulation of activity according to the intensity of the stimulations ('pain' bigger than 'no-pain') only in the 'self' condition, while responders presented the same kind of modulation ('pain' bigger than 'no-pain) in the 'other' condition only.

Indeed, a significant three-way interaction TARGET × INTENSITY × GROUP was found for ten ROIs located in both the hemispheres: left rostral ACC 2 [−12 24 12] ($F_{(1,30)}$ = 4.909, P = 0.034, **Figure 10A**), left rostro-dorsal ACC [−6 28 24] ($F_{(1,30)}$ = 10.266, P = 0.003, **Figure 10B**), left pregenual ACC 1 [−2 40 0] ($F_{(1,30)}$ = 4.425, P = 0.044, **Figure 10C**), left pregenual ACC 3 [−4 32 10] ($F_{(1,30)}$ = 4.172, P = 0.050, **Figure 10D**), left pregenual ACC 4 [−4 42 12] ($F_{(1,30)}$ = 4.116, P = 0.051, **Figure 10E**), left pregenual ACC 5 [−4 38 18] ($F_{(1,30)}$ = 6.619, P = 0.015, **Figure 10F**), right rostral ACC 2 [12 24 12] ($F_{(1,30)}$ = 4.292, P = 0.047, **Figure 11A**), right rostro-dorsal ACC [6 28 24] ($F_{(1,30)}$ = 8.753, P = 0.006, **Figure 11B**), right pregenual ACC 3 [4 32 10] ($F_{(1,30)}$ = 4.119, P = 0.051, **Figure 11C**), right pregenual ACC 5 [4 38 18] ($F_{(1,30)}$ = 5.490, P = 0.026, **Figure 11D**).

Post-hoc *t*-tests revealed a consistent pattern for the 'self' condition, with non-responders showing an interaction with the intensity that responders did not present. In detail this was found for: left rostral ACC 2 [*Non-responders*: self pain – self no-pain (mean/SE) = 0.244/0.085; planned comparison; $F_{(1,30)} = 9.180$, P = 0.005. *Responders*: self pain – self no-pain (mean/SE) = 0.005/0.075; planned comparison; $F_{(1,30)} = 0.004$, P = 0.948], left rostro-dorsal ACC [*Non-responders*: self pain – self no-pain (mean/SE) = 0.835/0.165; planned comparison; $F_{(1,30)} = 24.288$, P = 0.000. *Responders*: self pain – self no-pain (mean/SE) = 0.256/0.174; planned comparison; $F_{(1,30)} = 2.282$, P = 0.141], left pregenual ACC 1 [*Non-responders*: self pain – self no-pain (mean/SE) = 0.385/0.128; planned comparison; $F_{(1,30)} = 6.266$, P = 0.018. *Responders*: self pain – self no-pain (mean/SE) = −0.085/0.176; planned comparison; $F_{(1,30)} = 0.308$, P = 0.583], left pregenual ACC 3 [*Non-responders*: self pain – self no-pain (mean/SE) = 0.501/0.102; planned comparison; $F_{(1,30)} = 16.197$, P = 0.000. *Responders*: self pain – self no-pain (mean/SE) = 0.164/0.144; planned comparison; $F_{(1,30)} = 1.759$, P = 0.195], left pregenual ACC 4 [*Non-responders*: self pain – self no-pain (mean/SE) = 0.610/0.136; planned comparison; $F_{(1,30)} = 13.372$, P = 0.001. *Responders*: self pain – self no-pain (mean/SE) = 0.228/0.193; planned comparison; $F_{(1,30)} = 1.874$, P = 0.181], left pregenual ACC 5 [*Non-responders*: self pain – self no-pain (mean/SE) = 0.701/0.143; planned comparison; $F_{(1,30)} = 17.622$, P = 0.000. *Responders*: self pain – self no-pain (mean/SE) = 0.227/0.120; planned comparison; $F_{(1,30)} = 1.843$, P = 0.185], right rostral ACC 2 [*Non-responders*: self pain – self no-pain (mean/SE) = 0.261/0.097; planned comparison; $F_{(1,30)} = 7.434$, P = 0.011. *Responders*: self pain – self no-pain (mean/SE) = 0.042/0.094; planned comparison; $F_{(1,30)} = 0.194$, P = 0.663], right rostro-dorsal ACC [*Non-responders*: self pain – self no-pain (mean/SE) = 0.910/0.182; planned comparison; $F_{(1,30)} = 21.129$, P = 0.000. *Responders*: self pain – self no-pain (mean/SE) = 0.360/0.187; planned comparison; $F_{(1,30)} = 3.313$, P = 0.079], right pregenual ACC 3 [*Non-responders*: self pain – self no-pain (mean/SE) = 0.550/0.114; planned comparison; $F_{(1,30)} = 16.402$, P = 0.000. *Responders*: self pain – self no-pain (mean/SE) = 0.212/0.154; planned comparison; $F_{(1,30)} = 2.436$, P = 0.129], right pregenual ACC 5 [*Non-responders*: self pain – self no-pain (mean/SE) = 0.713/0.155; planned comparison; $F_{(1,30)} = 16.283$, P = 0.000. *Responders*: self pain – self no-pain (mean/SE) = 0.277/0.196; planned comparison; $F_{(1,30)} = 2.461$, P = 0.127].

In the 'other' condition, instead, the majority of ROIs (eight out of ten) showed the reverse pattern, with responders showing an interaction with the intensity that non-

responders did not present. These eight ROIs were: left rostro-dorsal ACC [*Non-responders*: other pain – other no-pain (mean/SE) = 0.122/0.120; planned comparison; $F_{(1,30)}$ = 0.649, P = 0.427. *Responders*: other pain – other no-pain (mean/SE) = 0.445/0.178; planned comparison; $F_{(1,30)}$ = 8.604, P = 0.006], left pregenual ACC 1 [*Non-responders*: other pain – other no-pain (mean/SE) = 0.215/0.097; planned comparison; $F_{(1,30)}$ = 2.158, P = 0.152. *Responders*: other pain – other no-pain (mean/SE) = 0.312/0.183; planned comparison; $F_{(1,30)}$ = 4.518, P = 0.042], left pregenual ACC 3 [*Non-responders*: other pain – other no-pain (mean/SE) = 0.123/0.098; planned comparison; $F_{(1,30)}$ = 0.810, P = 0.375. *Responders*: other pain – other no-pain (mean/SE) = 0.314/0.167; planned comparison; $F_{(1,30)}$ = 5.269, P = 0.029], left pregenual ACC 4 [*Non-responders*: other pain – other no-pain (mean/SE) = 0.245/0.128; planned comparison; $F_{(1,30)}$ = 2.452, P = 0.128. *Responders*: other pain – other no-pain (mean/SE) = 0.498/0.181; planned comparison; $F_{(1,30)}$ = 10.137, P = 0.003], left pregenual ACC 5 [*Non-responders*: other pain – other no-pain (mean/SE) = 0.151/0.122; planned comparison; $F_{(1,30)}$ = 0.861, P = 0.361. *Responders*: other pain – other no-pain (mean/SE) = 0.497/0.196; planned comparison; $F_{(1,30)}$ = 9.281, P = 0.005], right rostro-dorsal ACC [*Non-responders*: other pain – other no-pain (mean/SE) = 0.100/0.108; planned comparison; $F_{(1,30)}$ = 0.370, P = 0.548. *Responders*: other pain – other no-pain (mean/SE) = 0.559/0.197; planned comparison; $F_{(1,30)}$ = 11.607, P = 0.002], right pregenual ACC 3 [*Non-responders*: other pain – other no-pain (mean/SE) = 0.137/0.105; planned comparison; $F_{(1,30)}$ = 0.829, P = 0.370. *Responders*: other pain – other no-pain (mean/SE) = 0.389/0.185; planned comparison; $F_{(1,30)}$ = 6.701, P = 0.015], right pregenual ACC 5 [*Non-responders*: other pain – other no-pain (mean/SE) = 0.142/0.125; planned comparison; $F_{(1,30)}$ = 0.643, P = 0.005. *Responders*: other pain – other no-pain (mean/SE) = 0.543/0.217; planned comparison; $F_{(1,30)}$ = 9.423, P = 0.005]. In the last two ROIs, located in the rostral ACC, both the groups did not show interaction with intensity: left rostral ACC 2 [*Non-responders*: other pain – other no-pain (mean/SE) = −0.041/0.059; planned comparison; $F_{(1,30)}$ = 0.302, P = 0.587. *Responders*: other pain – other no-pain (mean/SE) = 0.029/0.087; planned comparison; $F_{(1,30)}$ = 0.147, P = 0.704], right rostral ACC 2 [*Non-responders*: other pain – other no-pain (mean/SE) = −0.055/0.068; planned comparison; $F_{(1,30)}$ = 0.453, P = 0.506. *Responders*: other pain – other no-pain (mean/SE) = 0.131/0.092; planned comparison; $F_{(1,30)}$ = 2.607, P = 0.117].

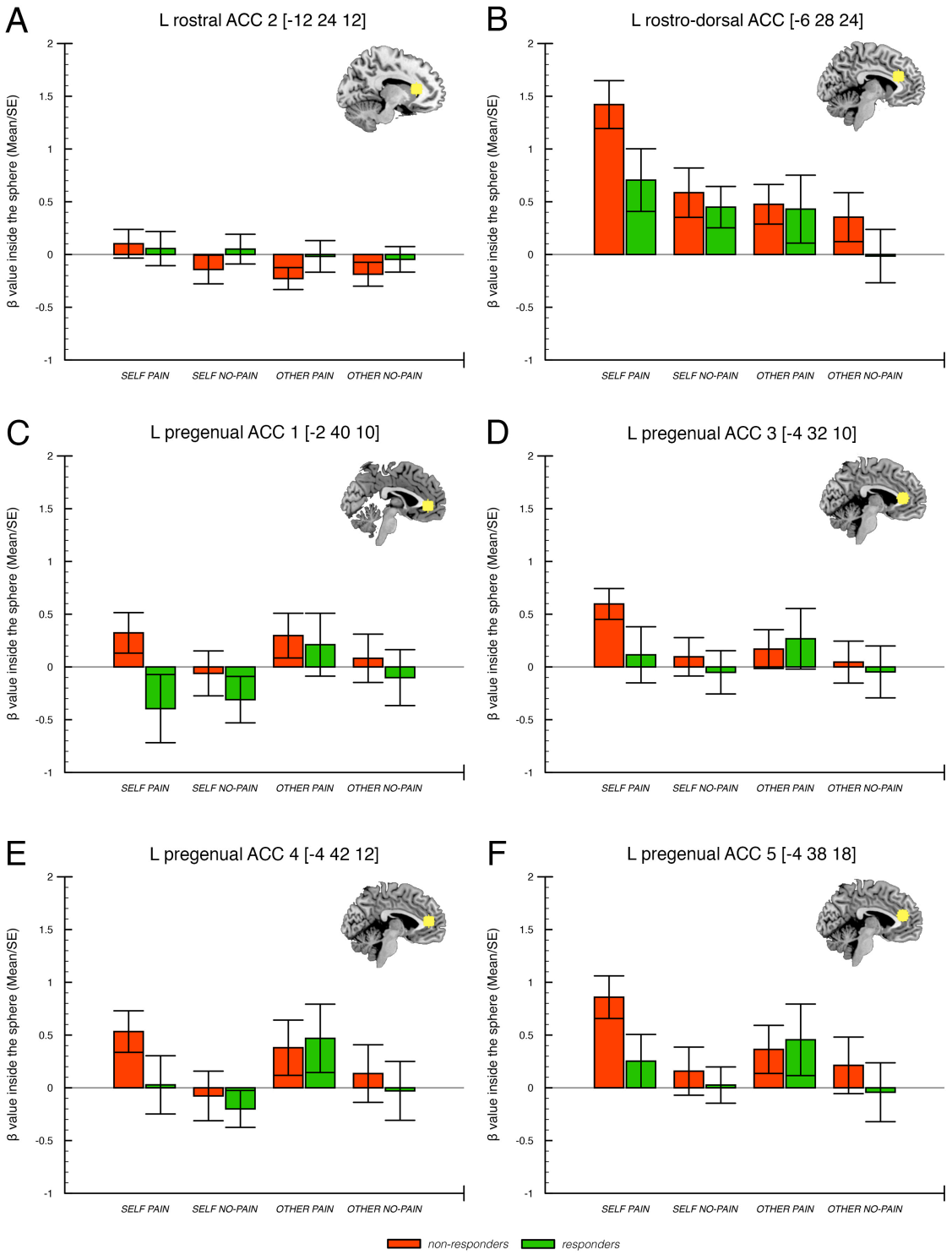

Figure 10 Mean β values over all the voxels inside left-hemisphere ROIs showing statistical interaction with the GROUP factor in the ANOVA comparing responders and non-responders groups. (A-F) sphere radius: 10 mm.

.

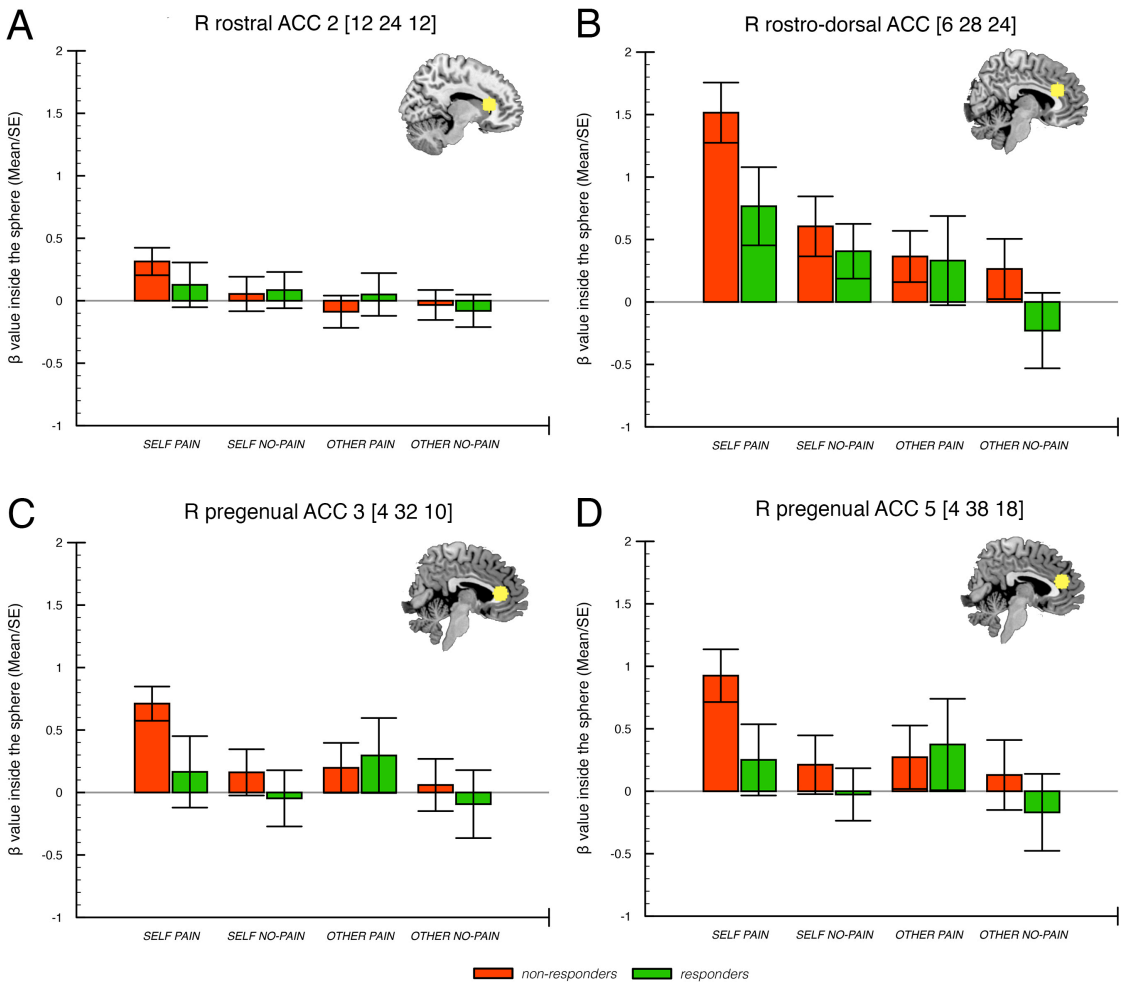

Figure 11 Mean β values over all the voxels inside right-hemisphere ROIs showing statistical interaction with the GROUP factor in the ANOVA comparing responders and non-responders groups. (A-D) sphere radius: 10 mm.

DISCUSSION

Empathic skills are at the core of human sociality. Many psychologists (and scholars in general) are persuaded that this ability to cooperate with and understand others is one of the main reasons behind the success of the human species (Zaki and Ochsner 2012; Tomasello, 2009). Therefore, research in the field of Social Neuroscience is putting a lot of effort in trying to understand the neural underpinnings of empathy, and in fact advances in this field have provided important new insights into the brain basis of empathy (see Bernhardt and Singer, 2012 for a review). Instead, hardly anything is known about the neurochemical mechanisms that modulate empathic responses. Discovering which neuromolecules are implicated in empathy would be crucial to better

understand, for instance, how empathic abilities can be modulated not only in an endogenous way, but also through external interventions.

In this study we first aimed at indirectly assessing the role of the opioid system in empathy for pain. For this purpose we induced a placebo analgesia effect in a group of participants to supposedly enhance the activity of the endogenous opioid system and measure behavioral and neurophysiological changes occurring in comparison to participants with baseline activation of this system.

In order to observe how empathic responses were modulated by endogenous opioid release, we first needed to prove the efficacy of our placebo manipulation on participants' first-hand experiences of physical pain.

As already pointed out, placebo effect does not occur in every person and in every circumstance (Colloca et al., 2013); therefore, a critical point of this work was the assignment of participants in the placebo group to the responder and non-responder subgroups.

The post-hoc subdivision we used was based on participants' behavioral responses to first-hand painful and non-painful stimulations. It proved to be successful in sorting responders and non-responders, as demonstrated by the fact that the emotional ratings following pain given by the former group were significantly less negative than controls' ratings, whereas the latter group did not differ from control group in the emotional ratings following pain.

At the neural level, when painfully stimulated, participants in the control group compared to placebo responders displayed increased activation in cortical and subcortical regions belonging to the affective component of the pain-network, i.e. anterior insula (aINS) and the anterior part of the mid cingulate cortex (aMCC). This is in line with many studies reporting the existence of a correlation between reduction of activity in these areas and placebo effect magnitude (see Koban et al., 2013 for a review). Controls also exhibited higher activity than responders in the amygdala. This could be interpreted considering amygdala pivotal role in negative emotion processing and also reckoning its specific involvement in pain processing (see Simons et al., 2014 for a recent meta-analysis). Amygdala higher activation in the controls could also reflect a general higher vigilance and uncertainty during anticipation and/or during pain itself (Davis and Whalen, 2001), whereas responders were comforted by the belief of the analgesic treatment. Region of interest analysis confirmed this pattern, by showing that responders did not present change of activity in amygdala between pain and no-pain,

while controls presented higher activation during pain compared to no-pain. The same pattern applied to aINS, confirming that the difference between controls and responders in first-hand experience of pain was mainly related to affective processing areas. In fact, we also found an effect on somatosensory areas contralateral to the stimulation side, with controls showing higher activity in the right primary somatosensory cortex (S1). Despite this difference was found within a cluster with only 8 voxels (just below the selected threshold for cortical ROIs, $k > 9$), this confirms that placebo effect also acts decreasing activity in somatosensory areas (Wager et al., 2004; Bingel et al., 2006; Price et al., 2007).

Responders, on the contrary, presented higher activity than controls during painful stimulations in areas like right dorsolateral prefrontal cortex (DLPFC), subgenual anterior cingulate cortex (sACC), aINS, inferior frontal gyrus, periaquedutal gray matter (PAG), and ventral striatum. The DLPFC has been implicated in several studies on placebo analgesia, and several authors have suggested that its recruitment might reflect expectation of pain relief or the generation and maintenance of cognitive representations that are used to create the placebo effect (Krummenacher et al., 2010; Wager et al., 2011). In particular, DLPFC is thought to initiate the placebo response through a top-down modulation of other cortical and subcortical areas, like rACC (including sACC) and PAG, other two areas we have found more active in responders compared to controls. PAG and sACC have consistently been linked with pain regulation processes, for example through endogenous opioid release (Eippert et al., 2009; Wager et al., 2007; Zubieta et al., 2005). In particular, PAG has been traditionally linked to pain control and learning in animals (McNally et al., 2004), and it has been recently assigned with a prominent role in representing aversive prediction errors during pain experience in humans (Roy et al., 2014). Subgenual ACC (and rACC in general) activity has been found to correlate with lower ratings of pain intensity and pain unpleasantness (Zubieta et al. 2005), and is believed to play a key role in the recruitment of a subcortical antinociceptive network, that also involves PAG (Bindel et al., 2006).

It should be noticed however, that we found activated areas belonging to rACC also in the opposite contrast (‘controls more than responders’). Actually, activity in this contrast was localized more dorsally (in the vicinity of the aMCC/dACC,) in respect to the ROI more active in the responders, suggesting that the function of those areas could be related more to pain responses than pain relief (Shackman et al., 2011). Finally, also ventral striatum activation should be considered with particular regard. Since this

subcortical region has been linked with dopamine binding and reward processing (Scott et al., 2002; Scott et al., 2008), it strengthens the possibility that opioid-mediated analgesia could also represent a reward response (de la Fuente-Fernandez, 2009).

Once verified that our placebo manipulation worked in responders, we could look at the impact of placebo effect on empathic responses by comparing the two groups in the behavioral and neurophysiological responses to the condition in which their partner was painfully stimulated. Behaviorally, the pattern of results replicates what we found for the 'self' condition, meaning that responders presented less negative emotional ratings than controls. On the neurophysiological level, the most relevant results come from the region of interest analysis. In fact, by comparing the mean activity around coordinates centered in the left aINS and bilateral pregenual (pACC), we found a different modulation of these areas in the two groups. Specifically, in the left anterior insula both groups showed increased activation when the self was stimulated compared to the condition in which their partner was stimulated. In this latter case, instead, only controls showed higher activation during painful stimulation of their partners compared to non-painful stimulation, whereas responders responded equally to both the conditions (other pain and other no-pain), essentially showing no change in activity. It is well known that anterior insula is one of the core regions of the empathy network (Bernhardt and Singer, 2012) and has a central role in the integration of interoceptive and affective information (Craig 2009). The representation of such information in this region not only allows the self to understand his own feeling and to predict the bodily effects of anticipated emotional stimuli to the body, but it may also serve as the visceral correlate of a prospective simulation of how something may feel for others (Singer and Lamm, 2009). Therefore, the differential activity found for the two groups could be interpreted as a difference in being negative affected from the state of the other person with responders not showing increased empathy for their partner being painfully stimulated compared to baseline (no-pain condition), differently from controls.

In empathic responses aINS activation usually goes with aMCC activation. In this case we did not find significant different activity between the two groups, as revealed both from whole-brain analysis and ROI analysis in the more dorsal parts of the ACC (e.g., left rostro-dorsal ACC). Instead, we found a different modulation in a more rostral part of the anterior cingulate cortex: the pregenual ACC (pACC), an area that like sACC, has been implicated in emotion regulation processes (Etkin et al., 2011) and has consistently been found to play a central role in opioid-mediated placebo responses

(Eippert et al., 2009; Wager et al., 2007). In this ROI controls presented an activity pattern for which they activated bilaterally this area more during the trials in which they were directly stimulated compared to the empathy condition. The fact that responders did not present this modulation could indicate that they were able to generalize the pain relief associated with the activity of this area in the self to the empathy condition. This interpretation, however, is weakened by the fact that mean activity in responders during first-hand painful stimulations was significantly lower than controls (for both left and right pACC) and in the case of right pACC responders presented deactivation rather than activation. Therefore, an alternative hypothesis is that pACC is not coding for pain relief but for anxiety. In fact, pACC seems to have a two-phase activity during placebo effect: during anticipation of pain pACC activity has been shown to decrease as related to less anxiety (Porro et al., 2003; Wager et al., 2009), whereas during pain has been shown to increase as an indicator of emotional stimulus processing and pain relief (Petrovic et al., 2002; Bingel et al., 2006; Eippert et al., 2009). Unfortunately, our GLM design did not allow us to disentangle brain activity in the two phases, since anticipation and pain phase were too close in time. As a consequence, we were not able to clearly distinguish differences of activity in this area in the two groups, leaving open the question regarding the contribution of placebo-related areas to the modulation of empathic responses.

A second goal of this study was to investigate possible differences in neural activations between responders and non-responders to a placebo analgesia induction, trying to replicate the results of studies having already looked into this difference (e.g, Elsenbruch et al., 2012) and extend the investigation to the empathic responses.

For this purpose, we first looked at the comparison between control and non-responder participants, in order to understand if the unsuccessful placebo induction in the latter participants elicited responses comparable to controls.

Indeed, when comparing the emotional ratings, we found a difference in terms of negative emotions concerning the 'self' condition, in which non-responders presented more negative ratings than controls, especially during painful trials.

These data seem in agreement with data coming from the neural level. Indeed, the contrast between the activity in the two groups during painful trials showed that non-responders generally presented higher activation in pain- and negative affect-related areas (bilateral amygdala, bilateral putamen, bilateral middle insula and right anterior insula), while in the opposite contrast we found a significant activation in the left

anterior insula only. Interestingly, the non-responders also presented higher activity in areas like the middle frontal gyrus (dorsolateral prefrontal cortex, DLPFC), pregenual ACC and subgenual anterior cingulate cortex. These areas are typically activated in participants experiencing successful placebo induction. In particular, the dorsolateral prefrontal cortex is a region that is involved in executive functions and general top-down control (Miller and Cohen, 2001) and has been found consistently across studies both during pain anticipation and during painful stimulation itself (Craggs et al., 2008; Watson et al., 2009; Atlas et al., 2012). The same studies also found increased activity in rACC (both p- and s- ACC), an area that is known to be important in emotional regulation (Etkin et al., 2011). We provide two alternative explanations for this pattern. First, despite displaying the signs of an unsuccessful placebo analgesia effect, non-responders were participants that anyhow underwent a placebo induction, and likely their expectation of experiencing pain relief is still able to initiate a top-down process; on the other hand the evidence coming from sensory inputs through a bottom-up way is somehow stronger, resulting in a failure of the top-down modulation. This account is in agreement with the results of a study comparing responders with non-responders to expectation-mediated placebo analgesia in a rectal pain model (Elsenbruch, 2012) in which researchers found that responders demonstrated greater placebo-induced decreases in activation of the DLPFC. A second possible explanation lays in the observation that prefrontal regions mediate not only descending pain inhibition but also facilitation of transmission of nociceptive information (Tracey and Mantyh, 2007; Wiech et al., 2008), for instance during nocebo hyperalgesia (Kong et al., 2008).

As for the differences in the empathic responses between controls and non-responders, the results of the ROI analysis clearly showed that non-responders were generally less empathic than controls. Indeed, non-responders did not modulate the activity in areas like anterior insula, mid insula, posterior insula, putamen and amygdala according to the intensity of the stimulation in the other condition. In other words, differently from controls, non-responders always seemed tuned into their own situation, activating areas related to negative emotions (anterior insula, amygdala) and pain (mid-posterior insula) with the same intensity, independently on the painfulness of the stimulation delivered to their partner.

Finally, the comparison between responders and non-responders showed that on the behavioral level the impact of the placebo induction on the two groups was dramatically different. In fact, non-responders presented emotional ratings consistently more

negative during all the conditions, but the one in which their partner received non-painful stimulations.

As for the first-person experience of pain, the different behavior of the groups was explained by the difference of activity found in affective areas like the anterior insula, the anterior part of the mid anterior cingulate cortex (aMCC) and the amygdala, where non-responders presented greater activation than responders. Non-responders also presented higher activity than responders in the secondary somatosensory cortex (S2) contralateral to the shocked hand, confirming that a successful placebo response is also capable of modulating activity in the somatosensory cortices (Wager et al., 2004; Bingel et al., 2006; Price et al., 2007). Interestingly, replicating what was found in comparison to controls, non-responders presented a higher activity also in the network recruited in placebo responses. In fact, an increased activity compared to responders was found in the middle frontal gyrus (DLPFC) and in the rostral parts of the anterior cingulate cortex, i.e. pregenual and subgenual ACC. These data are in keeping with what was found by Elsenbruch and colleagues (2012) that found a higher activation in DLPFC in responders compared to non-responders only in the condition in which participants were informed to be treated with an inert substance. Therefore, one possible interpretation of this pattern in our data is that non-responders show overcompensation of activity in this area in an attempt to continuously match their expectancy of pain relief with their actual sensory states. Furthermore, whole-brain and ROI analysis conjointly showed that non-responders presented a modulation of activity according to intensity in the rostral parts of the anterior cingulate cortex (sACC, pACC), suggesting that these participants tried to regulate their emotions during painful stimulations. The pACC activation during painful stimulation under condition of placebo analgesia is thought to engage in top-down modulation of regions that are involved in opioid-mediated anti-nociceptive responses, such as the amygdala (that we found in fact more active in non-responders than responders) and PAG (Bingel et al., 2006). The role of the sACC, instead, is less clear, since it has also been associated with sadness (Phan, 2002), although positive emotions, which can regulate and diminish negative emotions, also have been associated with both sACC and pACC (Wager et al., 2008).

The two groups also presented differences in neural responses related to empathy for pain. Although during painful stimulations delivered to their partner non-responders gave more negative ratings than responders, on the neural level non-responders showed less empathy than responders. In fact, analysis inside the ROIs showed a different

activity in the two groups in the anterior cingulate cortex, especially in the rostro-dorsal part, where non-responders did not show any modulation of activity according to the intensity of the stimulation delivered to the partner, differently from responders. The rostro-dorsal ACC corresponds to the classical area of the anterior cingulate cortex found in many studies investigating empathy for pain (Bernhardt and Singer, 2012). Interestingly, responders also presented higher activity in the sACC that, as already mentioned, has also been associated to emotion regulation and positive emotions (Wager et al., 2008), suggesting that when comparing the subgroups, the general reduced empathic response of the responders is still able to trigger some regulatory processes compared to the non-responders. Therefore, we hypothesize that the difference in behavioral empathic responses between the two groups can be explained by the fact the non-responders are not displaying more negative affect as a higher concern for the other, but as a result of generalization of their egocentric negative state to the condition of the other.

Taken all together, the results of our experiment show that using a well established protocol of placebo analgesia induction, we managed to identify participants who effectively responded by reducing their negative emotion reports following pain and participants who did not respond to the manipulation and presented reports of negative emotion comparable or even more intense than participants belonging to a control group. On the brain level, this difference was mirrored in a different activity in response to pain between the three groups, with responders benefiting from placebo analgesia and therefore displaying lower activity than the two other groups (controls, non-responders) in brain areas associated with pain and negative affect (aINS, aMCC, amygdala). Conversely, they showed higher activity than the two other groups in brain areas associated with emotion regulation (sACC), pain control (PAG) and reward (ventral striatum).

Successful placebo induction was also associated with behavioral and neurophysiological changes during empathy for pain. In particular, responders showed significantly reduced negative emotions following painful stimulations to their partner compared to both controls and non-responders. On the neural level, in the comparison with controls this difference was generally associated with a reduction of activity in an empathy-related area, the anterior insula. Interestingly, and contrary to what we expected, on the neural level responders displayed more empathy-related activity than non-responders (activity in aMCC depending on the intensity), despite their less

negative reports of negative affect. In the light of the design of the task, which presented participants with intermingled trials of self and other in the same block, a possible explanation could be that non-responders generalized their negative affect (as measured through behavioral ratings), mainly due to the ineffectiveness of the analgesic treatment in relieving pain, to the other condition without really empathizing (at the level of brain activity) with their partner. Future research should investigate this effect, for instance, by administering participants with the two conditions in different blocks.

Finally, it should be noticed that effects observed in the responders on both first-hand and vicarious experiences of pain could be associated with an increased activity of the endogenous opioid system, but that the experimental design could not answer directly this question. Future studies should investigate if modulations of empathic responses obtained with the same or a similar protocol are opioid-specifics, for example by reverting the induced analgesia with the administration of an opioid-antagonist (e.g., naloxone).

Conclusions

The work presented in this thesis aimed at clarifying some aspects concerning the neural bases of empathy and related phenomena like prosocial behavior.

In summary, Study 1 provides evidence that experiences of social rejection can activate regions of the brain so far observed during experiences of physical pain and possibly responsible for coding the intensity of the threatening event (secondary somatosensory cortex and posterior insula). Furthermore, for the first time, we showed that this pattern of brain activation extends to the witnessing of the same type of social pain in others. Our findings provide fresh support to models of empathy proposing a partial sharing of the affective experiences of others based on one's own emotional representations in similar experiences (Singer and Lamm, 2009). Finally, the version of the Cyberball task developed in Study 1 represents a more ecological tool for the investigation of social pain that could be used in settings and populations (e.g. in autism and children) where other ways of powerful social exclusion such as romantic rejection or bereavement could not be used.

Study 2 investigated the neurophysiological underpinnings of altruistic behavior in a more ecological context than what has been used in past research. The highly realistic scenario created with virtual reality, combined with the Independent Component Analysis of fMRI data, allowed us to observe brain activity during a flowing stressful experience that required social decision-making. For the first time, we were able to disentangle the interplay of dedicated brain networks in the engagement (or not) of prosocial behavior, bringing new evidence of the mechanisms of altruistic behavior in a close-to-real-life situation. Specifically, an increased functional connectivity in the salience network, comprising the anterior insula (aINS) and the anterior mid cingulate cortex (aMCC), was observed in the selfish group compared to the prosocial one. Conversely, higher ICA weights in the medial prefrontal cortex and temporo-parietal junction (TPJ) were observed in the prosocial group.

Study 3 aimed at examining how empathic responses to physical pain are modulated by placebo analgesia, possibly as a consequence of enhanced release of endogenous opioids. By comparing the behavioral and neurophysiological responses of a group of participants under the effect of placebo analgesia (*responders)* both with a natural history group (no pill) and a group of participants with apparent negative response to

the placebo induction (*non-responders*), we were able to show for the first time that placebo effect modulates empathic responses by decreasing the neural activity of the anterior insula, a brain region consistently implicated in empathic responses to several affective states (see Bernhardt and Singer, 2012 for a review). In particular, aINS seems to play a major role in representing and integrating internal and emotional feeling states (Craig, 2009), and its role in empathic responses might extend to represent the correlates of a prospective simulation of how something may feel for others (Singer and Lamm, 2009).

Considered as a whole, the work presented in the thesis demonstrates that anterior insula and anterior cingulate cortex represent key brain structures for neural processing of human social emotions. Changes in the level of recruitment of these areas across tasks and conditions has shown to dramatically impact on behavioral output in several settings, spanning from prosocial behavior to empathic responses to social pain, and physical pain (both under normal conditions and expectation of analgesia).

The results of our studies represent new insights into the brain mechanisms of empathy and prosocial behavior, extending prior knowledge on the contextual and individual factors that intervene in modulating and shaping such social behaviors. Nevertheless, there is still much to do to reach a complete understanding of the results of human evolution in terms of neural implementation of social emotions, and this long road necessarily goes through an improvement of the investigation techniques. For instance, the research group lead by Tor Wager has recently published a research in which they have applied a newly developed fMRI-analysis method (multivariate pattern analysis, MVPA) to data collected from participants undergoing physically and socially painful stimulations (Woo et al., 2014). This technique allows analyzing neural activity with a more fine-grained precision than the usual univariate GLM analysis, as it detects patterns of activity that are sensitive to population codes distributed across large numbers of individual neurons. Through this approach they were able to show that physical pain and social rejection do not share neural representations within core pain-processing brain regions and that co-localization of neural representations of the two pains at the gross anatomical level is an artifact due to low resolution power of classical univariate GLM analysis.

Beyond a doubt, their work represents a breakthrough in the recent research line on the hypothesized shared neural representation of physical and social pain (see Eisenberger 2012, for a review), and it exhorts to interpret more carefully our data on shared neural

representations for physical and social pain both for first-hand and empathic experiences. Nevertheless, as the authors themselves reckon in their publication, the social pain task they used was not fully matching the physical pain task in important features like, for instance, the temporal setting of the actual pain. Indeed, presenting participants with ex-partner photos refers to past experiences and only indirectly to present circumstance, whereas administered physical pain is experienced 'here and now'. Differently from their work, our experiment used a social rejection task, the Cyberball, that is more contingent and in the present. Therefore, possible follow-up research on neural overlap of physical and social pain, especially in the case of empathic experiences, should benefit from the integration of the two approaches, one oriented to match as much as possible the contextual features of the experiences, and the other meant to detect with much more accuracy the actual neural overlap in terms of population codes.

A similar strategy could be applied to extend the findings on the role of the opioid system in empathy for physical pain to responses to vicarious experiences of social pain. In other words, by combining placebo analgesia induction in participants administered with first-hand and empathic experiences of physical and social pain in a within-subject design with multivariate pattern analysis of the fMRI data we could finally understand to which extent there are common neural substrates for the two kinds of pain and test this possible overlap on the neurochemical level. Obviously, in order to check for the specific role of the opioid system, the design should also involve a group of participants undergoing placebo induction but whose enhanced opioid system activity should be reversed by the administration of an opioid-antagonist (e.g., naloxone).

Finally, despite an increasing number of studies suggest that empathic concern drives and motivates prosocial behavior (see for instance the very recent work from FeldmannHall and colleagues, 2015, showing that trait empathic concern, and not trait personal distress, motivates costly altruism) a definitive answer to a question that philosophers, psychologists and neuroscientists have broadly debated in the last decades is still lacking: how do empathic responses relate to altruistic behavior? In our study we have showed that an increased activity of the salience network throughout a stressful experience predicts later selfish over altruistic behavior. Interestingly, what has been referred to as 'salience network' comprises aINS and aMCC, two cortical areas that both previous and our research have found at the core of empathic responses. Therefore, it would be interesting to investigate how prosocial behavior is influenced by different

levels of activation of the endogenous opioid system, which in turn would impact the neurophysiology of the saliency/empathy network by targeting opioid-receptors in these brain regions. In this framework, we could also test if both empathic responses and prosocial behavior depend on the activation of the opioid system, and consequently, on the individual differences in terms of density of opioid receptors in empathy-related regions. Indeed, several genetic correlational studies have shown that genetic variation of the mu opioid receptor (MOR) expression are associated with differences in the individual sensitivity to both physical and social pain (Fillingim et al., 2005; Sia et al., 2008; Way et al., 2009) and with reduced activity in pain related brain regions (including MCC) (Way et al. 2009; Lotsch et al., 2006). Since a robust body of research has demonstrated shared representations for first-hand and vicarious experiences of affective states, it is very likely that genetic profile in terms of subtypes, amount and distribution of opioid receptors could be associated with different propensity to empathize and behave prosocially. The results of a research of this type could strongly impact on both the scientific community and the public opinion: in fact, the understanding of the mechanisms (neurochemical and neurophysiological) beyond these processes could help us to gain knowledge about the reasons for pathology such as sociopathy, autism and alexithymia, conditions observed early in life and associated with severe deficits in social competence and understanding of other people's mental and emotional states.

References

Allison, T., et al. (2000). "Social perception from visual cues: role of the STS region." *Trends Cogn Sci* **4**(7): 267-278.

Amanzio, M. and F. Benedetti (1999). "Neuropharmacological dissection of placebo analgesia: expectation-activated opioid systems versus conditioning-activated specific subsystems." *J Neurosci* **19**(1): 484-494.

Amodio, D. M. and C. D. Frith (2006). "Meeting of minds: the medial frontal cortex and social cognition." *Nat Rev Neurosci* **7**(4): 268-277.

Anderson, S. W., et al. (1999). "Impairment of social and moral behavior related to early damage in human prefrontal cortex." *Nat Neurosci* **2**(11): 1032-1037.

Arbabshirani, M. R., et al. (2013). "Functional network connectivity during rest and task conditions: a comparative study." *Hum Brain Mapp* **34**(11): 2959-2971.

Atlas, L. Y. and T. D. Wager (2014). A meta-analysis of brain mechanisms of placebo analgesia: Consistent findings and unanswered questions. *Placebo*, Springer**:** 37-69.

Atlas, L. Y., et al. (2012). "Dissociable influences of opiates and expectations on pain." *J Neurosci* **32**(23): 8053-8064.

Avenanti, A., et al. (2005). "Transcranial magnetic stimulation highlights the sensorimotor side of empathy for pain." *Nat Neurosci* **8**(7): 955-960.

Bastiaansen, J. A., et al. (2009). "Evidence for mirror systems in emotions." *Philos Trans R Soc Lond B Biol Sci* **364**(1528): 2391-2404.

Batson, C. D., et al. (1991). "Empathic joy and the empathy-altruism hypothesis." *J Pers Soc Psychol* **61**(3): 413-426.

Batson, C. D., et al. (1987). "Distress and empathy: two qualitatively distinct vicarious emotions with different motivational consequences." *J Pers* **55**(1): 19-39.

Baumgartner, U., et al. (2006). "High opiate receptor binding potential in the human lateral pain system." *NeuroImage* **30**(3): 692-699.

Beckmann, C. F. (2012). "Modelling with independent components." *NeuroImage* **62**(2): 891-901.

Beeney, J. E., et al. (2011). "I feel your pain: emotional closeness modulates neural responses to empathically experienced rejection." *Social Neuroscience* **6**(4): 369-376.

Bell, A. J. and T. J. Sejnowski (1995). "An information-maximization approach to blind separation and blind deconvolution." *Neural Comput* **7**(6): 1129-1159.

Benedetti, F. (1996). "The opposite effects of the opiate antagonist naloxone and the cholecystokinin antagonist proglumide on placebo analgesia." *Pain* **64**(3): 535-543.

Benedetti, F., et al. (2005). "Neurobiological mechanisms of the placebo effect." *The Journal of neuroscience : the official journal of the Society for Neuroscience* **25**(45): 10390-10402.

Bernhardt, B. C. and T. Singer (2012). "The neural basis of empathy." *Annu Rev Neurosci* **35**: 1-23.

Bingel, U., et al. (2006). "Mechanisms of placebo analgesia: rACC recruitment of a subcortical antinociceptive network." *Pain* **120**(1-2): 8-15.

Bohil, C. J., et al. (2011). "Virtual reality in neuroscience research and therapy." *Nat Rev Neurosci* **12**(12): 752-762.

Bolling, D. Z., et al. (2012). "Differential brain responses to social exclusion by one's own versus opposite-gender peers." *Soc Neurosci* **7**(4): 331-346.

Bolling, D. Z., et al. (2011). "Dissociable brain mechanisms for processing social exclusion and rule violation." *NeuroImage* **54**(3): 2462-2471.

Bowlby, J. (1969). "Attachment and loss, volume i: Attachment."

Bowles, S. (2006). "Group competition, reproductive leveling, and the evolution of human altruism." *Science* **314**(5805): 1569-1572.

Boyd, R. (2006). "Evolution. The puzzle of human sociality." *Science* **314**(5805): 1555-1556.

Bressler, S. L. and V. Menon (2010). "Large-scale brain networks in cognition: emerging methods and principles." *Trends Cogn Sci* **14**(6): 277-290.

Byrne, R. W. and L. A. Bates (2007). "Sociality, evolution and cognition." *Curr Biol* **17**(16): R714-723.

Bzdok, D., et al. (2013). "Segregation of the human medial prefrontal cortex in social cognition." *Front Hum Neurosci* **7**: 232.

Calhoun, V. D., et al. (2001a). "fMRI activation in a visual-perception task: network of areas detected using the general linear model and independent components analysis." *NeuroImage* **14**(5): 1080-1088.

Calhoun, V. D., et al. (2001b). "Spatial and temporal independent component analysis of functional MRI data containing a pair of task-related waveforms." *Hum Brain Mapp* **13**(1): 43-53.

Calhoun, V. D., et al. (2008). "Modulation of temporally coherent brain networks estimated using ICA at rest and during cognitive tasks." *Hum Brain Mapp* **29**(7): 828-838.

Calhoun, V. D., et al. (2009). "A review of group ICA for fMRI data and ICA for joint inference of imaging, genetic, and ERP data." *NeuroImage* **45**(1 Suppl): S163-172.

Celone, K. A., et al. (2006). "Alterations in memory networks in mild cognitive impairment and Alzheimer's disease: an independent component analysis." *J Neurosci* **26**(40): 10222-10231.

Chen, S., et al. (2008). "Group independent component analysis reveals consistent resting-state networks across multiple sessions." *Brain Res* **1239**: 141-151.

Cheng, Y., et al. (2010). "Love hurts: an fMRI study." *NeuroImage* **51**(2): 923-929.

Chittaro, L. and N. Zangrando (2010). The persuasive power of virtual reality: effects of simulated human distress on attitudes towards fire safety. *Persuasive Technology. Lecture Notes in Computer Science*. T. Ploug, P. Hasle and H. Oinas-Kukkonen. Heidelberg, Springer. **6137:** 58-69.

Cole, D. M., et al. (2010). "Advances and pitfalls in the analysis and interpretation of resting-state FMRI data." *Front Syst Neurosci* **4**(8): 1-15.

Colloca, L., et al. (2013). "Placebo analgesia: psychological and neurobiological mechanisms." *Pain* **154**(4): 511-514.

Craggs, J. G., et al. (2008). "The dynamic mechanisms of placebo induced analgesia: Evidence of sustained and transient regional involvement." *Pain* **139**(3): 660-669.

Craig, A. D. (2003). "Interoception: the sense of the physiological condition of the body." *Curr Opin Neurobiol* **13**(4): 500-505.

Craig, A. D. (2009). "How do you feel--now? The anterior insula and human awareness." *Nat Rev Neurosci* **10**(1): 59-70.

Critchley, H. D. (2004). "The human cortex responds to an interoceptive challenge." *Proc Natl Acad Sci U S A* **101**(17): 6333-6334.

Cziko, G. A. (1989). "Unpredictability and indeterminism in human behavior: Arguments and implications for educational research." *Educational researcher* **18**(3): 17-25.

Damoiseaux, J. S., et al. (2006). "Consistent resting-state networks across healthy subjects." *Proc Natl Acad Sci U S A* **103**(37): 13848-13853.

Davis, K. D. (2000). "The neural circuitry of pain as explored with functional MRI." *Neurological research* **22**(3): 313-317.

Davis, M. (1980). "A multidimensional approach to individual differences in empathy." *JSAS Catalog of Selected Documents* **10**: 85.

Davis, M. and P. J. Whalen (2001). "The amygdala: vigilance and emotion." *Molecular Psychiatry* **6**(1): 13-34.

de la Fuente-Fernandez, R. (2009). "The placebo-reward hypothesis: dopamine and the placebo effect." *Parkinsonism Relat Disord* **15 Suppl 3**: S72-74.

de Vignemont, F. and T. Singer (2006). "The empathic brain: how, when and why?" *Trends Cogn Sci* **10**(10): 435-441.

Decety, J. (2011). "The neuroevolution of empathy." *Ann N Y Acad Sci* **1231**: 35-45.

Decety, J. and C. Lamm (2006). "Human empathy through the lens of social neuroscience." *ScientificWorldJournal* **6**: 1146-1163.

Decety, J. and C. Lamm (2007). "The role of the right temporoparietal junction in social interaction: how low-level computational processes contribute to meta-cognition." *Neuroscientist* **13**(6): 580-593.

Decety, J. and J. A. Sommerville (2003). "Shared representations between self and other: a social cognitive neuroscience view." *Trends Cogn Sci* **7**(12): 527-533.

Denny, B. T., et al. (2012). "A meta-analysis of functional neuroimaging studies of self- and other judgments reveals a spatial gradient for mentalizing in medial prefrontal cortex." *J Cogn Neurosci* **24**(8): 1742-1752.

Dewall, C. N., et al. (2010). "Acetaminophen reduces social pain: behavioral and neural evidence." *Psychol Sci* **21**(7): 931-937.

Drevets, W. C., et al. (2008). "The subgenual anterior cingulate cortex in mood disorders." *CNS Spectr* **13**(8): 663-681.

Dunbar, R. I. and S. Shultz (2007). "Evolution in the social brain." *Science* **317**(5843): 1344-1347.

Eagly, A. H. (2009). "The his and hers of prosocial behavior: an examination of the social psychology of gender." *Am Psychol* **64**(8): 644-658.

Eagly, A. H. and S. W. Becker (2005). "Comparing the heroism of women and men." *Am Psychol* **60**(4): 343-344.

Eickhoff, S. B., et al. (2005). "A new SPM toolbox for combining probabilistic cytoarchitectonic maps and functional imaging data." *NeuroImage* **25**: 1325-1335.

Eippert, F., et al. (2009). "Activation of the opioidergic descending pain control system underlies placebo analgesia." *Neuron* **63**(4): 533-543.

Eisenberg, N. and R. Lennon (1983). "Sex differences in empathy and related capacities." *Psychol Bull* **94**(1): 100-131.

Eisenberg, N. and P. A. Miller (1987). "The relation of empathy to prosocial and related behaviors." *Psychol Bull* **101**(1): 91-119.

Eisenberger, N. I. (2012). "The pain of social disconnection: examining the shared neural underpinnings of physical and social pain." *Nature reviews. Neuroscience* **13**(6): 421-434.

Eisenberger, N. I., et al. (2003). "Does rejection hurt? An FMRI study of social exclusion." *Science* **302**(5643): 290-292.

Elsenbruch, S., et al. (2012). "Neural mechanisms mediating the effects of expectation in visceral placebo analgesia: an fMRI study in healthy placebo responders and nonresponders." *Pain* **153**(2): 382-390.

Etkin, A., et al. (2011). "Emotional processing in anterior cingulate and medial prefrontal cortex." *Trends in Cognitive Sciences* **15**(2): 85-93.

Fahrenfort, J. J., et al. (2012). "Neural correlates of dynamically evolving interpersonal ties predict prosocial behavior." *Front Neurosci* **6**: 28.

Fan, Y., et al. (2011). "Is there a core neural network in empathy? An fMRI based quantitative meta-analysis." *Neuroscience and Biobehavioral Reviews* **35**(3): 903-911.

Fehr, E. and U. Fischbacher (2003). "The nature of human altruism." *Nature* **425**(6960): 785-791.

FeldmanHall, O., et al. (2015). "Empathic concern drives costly altruism." *NeuroImage* **105**: 347-356.

FeldmanHall, O., et al. (2012a). "Differential neural circuitry and self-interest in real vs hypothetical moral decisions." *Soc Cogn Affect Neurosci* **7**(7): 743-751.

FeldmanHall, O., et al. (2012b). "What we say and what we do: the relationship between real and hypothetical moral choices." *Cognition* **123**(3): 434-441.

Fillingim, R. B., et al. (2005). "The A118G single nucleotide polymorphism of the mu-opioid receptor gene (OPRM1) is associated with pressure pain sensitivity in humans." *J Pain* **6**(3): 159-167.

Fine, P. G. and R. K. Portenoy (2004). "Chapter 2: The Endogenous Opioid System." *A Clinical Guide to Opioid Analgesia. New York: McGraw Hill*.

Fisher, H. E., et al. (2010). "Reward, addiction, and emotion regulation systems associated with rejection in love." *J Neurophysiol* **104**(1): 51-60.

Frith, C. D. and U. Frith (2006). "The neural basis of mentalizing." *Neuron* **50**(4): 531-534.

Frith, C. D. and T. Singer (2008). "The role of social cognition in decision making." *Philos Trans R Soc Lond B Biol Sci* **363**(1511): 3875-3886.

Glick, P. and S. T. Fiske (1997). "Hostile and benevolent sexism measuring ambivalent sexist attitudes toward women." *Psychology of Women Quarterly* **21**(1): 119-135.

Gracely, R. H., et al. (1983). "Placebo and naloxone can alter post-surgical pain by separate mechanisms." *Nature* **306**(5940): 264-265.

Greene, J. D., et al. (2001). "An fMRI investigation of emotional engagement in moral judgment." *Science* **293**(5537): 2105-2108.

Grevert, P., et al. (1983). "Partial antagonism of placebo analgesia by naloxone." *Pain* **16**(2): 129-143.

Groen, Y., et al. (2013). "Are there sex differences in ERPs related to processing empathy-evoking pictures?" *Neuropsychologia* **51**(1): 142-155.

Hall, K. T., et al. (2012). "Catechol-O-methyltransferase val158met polymorphism predicts placebo effect in irritable bowel syndrome." *PLoS ONE* **7**(10): e48135.

Han, S., et al. (2005). "Distinct neural substrates for the perception of real and virtual visual worlds." *NeuroImage* **24**(3): 928-935.

Harrison, B. J., et al. (2008a). "Consistency and functional specialization in the default mode brain network." *Proc Natl Acad Sci U S A* **105**(28): 9781-9786.

Harrison, B. J., et al. (2008b). "Modulation of brain resting-state networks by sad mood induction." *PLoS One* **3**(3): e1794.

Hein, G. and R. T. Knight (2008). "Superior temporal sulcus--It's my area: or is it?" *J Cogn Neurosci* **20**(12): 2125-2136.

Hein, G., et al. (2011). "Skin conductance response to the pain of others predicts later costly helping." *PLoS One* **6**(8): e22759.

Hein, G., et al. (2010). "Neural responses to ingroup and outgroup members' suffering predict individual differences in costly helping." *Neuron* **68**(1): 149-160.

Hein, G. and T. Singer (2008). "I feel how you feel but not always: the empathic brain and its modulation." *Curr Opin Neurobiol* **18**(2): 153-158.

Iannetti, G. D. and A. Mouraux (2010). "From the neuromatrix to the pain matrix (and back)." *Exp Brain Res* **205**(1): 1-12.

Izuma, K., et al. (2010). "The roles of the medial prefrontal cortex and striatum in reputation processing." *Soc Neurosci* **5**(2): 133-147.

Jackson, P., et al. (2005). "How do we perceive the pain of others? A window into the neural processes involved in empathy." *NeuroImage* **24**(3): 771-779.

Jackson, P. L., et al. (2006). "Empathy examined through the neural mechanisms involved in imagining how I feel versus how you feel pain." *Neuropsychologia* **44**(5): 752-761.

Kelly, C., et al. (2012). "A convergent functional architecture of the insula emerges across imaging modalities." *NeuroImage* **61**(4): 1129-1142.

Kersting, A., et al. (2009). "Neural activation underlying acute grief in women after the loss of an unborn child." *Am J Psychiatry* **166**(12): 1402-1410.

Keysers, C., et al. (2010). "Somatosensation in social perception." *Nat Rev Neurosci* **11**(6): 417-428.

Kingstone, A., et al. (2008). "Cognitive Ethology: a new approach for studying human cognition." *Br J Psychol* **99**(Pt 3): 317-340.

Koban, L., et al. (2013). "Brain predictors of individual differences in placebo responding." *Placebo and pain (89–101). Elsevier/Academic Press, Burlington, MA*.

Koenigs, M., et al. (2007). "Damage to the prefrontal cortex increases utilitarian moral judgements." *Nature* **446**(7138): 908-911.

Kong, J., et al. (2008). "A functional magnetic resonance imaging study on the neural mechanisms of hyperalgesic nocebo effect." *J Neurosci* **28**(49): 13354-13362.

Krill, A. and S. M. Platek (2009). "In-group and out-group membership mediates anterior cingulate activation to social exclusion." *Front Evol Neurosci* **1**: 1.

Kross, E., et al. (2011). "Social rejection shares somatosensory representations with physical pain." *Proceedings of the National Academy of Sciences of the United States of America* **108**(15): 6270-6275.

Krummenacher, P., et al. (2010). "Prefrontal cortex modulates placebo analgesia." *Pain* **148**(3): 368-374.

Kurth, F., et al. (2010). "A link between the systems: functional differentiation and integration within the human insula revealed by meta-analysis." *Brain Structure and Function* **in press**.

Laird, A. R., et al. (2011). "Behavioral interpretations of intrinsic connectivity networks." *J Cogn Neurosci* **23**(12): 4022-4037.

Lamm, C., et al. (2011). "Meta-analytic evidence for common and distinct neural networks associated with directly experienced pain and empathy for pain." *NeuroImage* **54**(3): 2492-2502.

Lamm, C. and T. Singer (2010). "The role of anterior insular cortex in social emotions." *Brain Struct Funct* **214**(5-6): 579-591.

Legrain, V., et al. (2011). "The pain matrix reloaded: a salience detection system for the body." *Prog Neurobiol* **93**(1): 111-124.

Levine, J. D. and N. C. Gordon (1984). "Influence of the method of drug administration on analgesic response." *Nature* **312**(5996): 755-756.

Li, Y. O., et al. (2007). "Estimating the number of independent components for functional magnetic resonance imaging data." *Hum Brain Mapp* **28**(11): 1251-1266.

Lieberman, M. D. (2012). "A geographical history of social cognitive neuroscience." *NeuroImage* **61**(2): 432-436.

Lotsch, J., et al. (2006). "The human mu-opioid receptor gene polymorphism 118A > G decreases cortical activation in response to specific nociceptive stimulation." *Behav Neurosci* **120**(6): 1218-1224.

Mar, R. A., et al. (2007). "Detecting agency from the biological motion of veridical vs animated agents." *Soc Cogn Affect Neurosci* **2**(3): 199-205.

Markett, S., et al. (2013). "Intrinsic connectivity networks and personality: The temperament dimension harm avoidance moderates functional connectivity in the resting brain." *Neuroscience* **240**: 98-105.

Masten, C. L., et al. (2011a). "An fMRI investigation of responses to peer rejection in adolescents with autism spectrum disorders." *Dev Cogn Neurosci* **1**(3): 260-270.

Masten, C. L., et al. (2009). "Neural correlates of social exclusion during adolescence: understanding the distress of peer rejection." *Soc Cogn Affect Neurosci* **4**(2): 143-157.

Masten, C. L., et al. (2011b). "An fMRI investigation of empathy for 'social pain' and subsequent prosocial behavior." *NeuroImage* **55**(1): 381-388.

Masten, C. L., et al. (2012). "Time spent with friends in adolescence relates to less neural sensitivity to later peer rejection." *Soc Cogn Affect Neurosci* **7**(1): 106-114.

Mathur, V. A., et al. (2010). "Neural basis of extraordinary empathy and altruistic motivation." *NeuroImage* **51**(4): 1468-1475.

Mayberg, H. S., et al. (1999). "Reciprocal limbic-cortical function and negative mood: converging PET findings in depression and normal sadness." *Am J Psychiatry* **156**(5): 675-682.

McKeown, M. J., et al. (1998). "Analysis of fMRI data by blind separation into independent spatial components." *Hum Brain Mapp* **6**(3): 160-188.

McNally, G. P., et al. (2004). "Opioid receptors in the midbrain periaqueductal gray regulate extinction of pavlovian fear conditioning." *J Neurosci* **24**(31): 6912-6919.

Meyer, M. L., et al. (2012). "Empathy for the social suffering of friends and strangers recruits distinct patterns of brain activation." *Social cognitive and affective neuroscience*.

Michalska, K. J., et al. (2013). "Age-related sex differences in explicit measures of empathy do not predict brain responses across childhood and adolescence." *Dev Cogn Neurosci* **3**: 22-32.

Miller, E. K. and J. D. Cohen (2001). "An integrative theory of prefrontal cortex function." *Annu Rev Neurosci* **24**: 167-202.

Mitchell, J. P., et al. (2005a). "General and specific contributions of the medial prefrontal cortex to knowledge about mental states." *NeuroImage* **28**(4): 757-762.

Mitchell, J. P., et al. (2005b). "The link between social cognition and self-referential thought in the medial prefrontal cortex." *J Cogn Neurosci* **17**(8): 1306-1315.

Moll, J., et al. (2006). "Human fronto-mesolimbic networks guide decisions about charitable donation." *Proc Natl Acad Sci U S A* **103**(42): 15623-15628.

Moor, B. G., et al. (2012). "Social exclusion and punishment of excluders: neural correlates and developmental trajectories." *NeuroImage* **59**(1): 708-717.

Morishima, Y., et al. (2012). "Linking brain structure and activation in temporoparietal junction to explain the neurobiology of human altruism." *Neuron* **75**(1): 73-79.

Mouraux, A., et al. (2011). "A multisensory investigation of the functional significance of the "pain matrix"." *NeuroImage* **54**(3): 2237-2249.

Mutschler, I., et al. (2009). "Functional organization of the human anterior insular cortex." *Neurosci Lett* **457**(2): 66-70.

Nichols, T., et al. (2005). "Valid conjunction inference with the minimum statistic." *NeuroImage* **25**(3): 653-660.

Onoda, K., et al. (2009). "Decreased ventral anterior cingulate cortex activity is associated with reduced social pain during emotional support." *Soc Neurosci* **4**(5): 443-454.

Paciello, M., et al. (2013). "High cost helping scenario: The role of empathy, prosocial reasoning and moral disengagement on helping behavior." *Personality and Individual Differences* **55**(1): 3-7.

Pecina, M., et al. (2013). "Personality trait predictors of placebo analgesia and neurobiological correlates." *Neuropsychopharmacology* **38**(4): 639-646.

Penny, W. D. and A. Holmes (2004). Random-effects analysis. *Human Brain Function*. W. Penny, Holmes, A., Friston, K.J. San Diego, Elsevier**:** 843–850.

Perl, E. R. (2007). "Ideas about pain, a historical view." *Nat Rev Neurosci* **8**(1): 71-80.

Petrovic, P., et al. (2002). "Placebo and opioid analgesia-- imaging a shared neuronal network." *Science* **295**(5560): 1737-1740.

Peyron, R., et al. (2000). "Functional imaging of brain responses to pain. A review and meta-analysis (2000)." *Neurophysiologie Clinique* **30**: 263-288.

Phan, K. L., et al. (2002). "Functional neuroanatomy of emotion: a meta-analysis of emotion activation studies in PET and fMRI." *NeuroImage* **16**(2): 331-348.

Porro, C. A., et al. (2003). "Functional activity mapping of the mesial hemispheric wall during anticipation of pain." *NeuroImage* **19**(4): 1738-1747.

Premkumar, P. (2012). "Are you being rejected or excluded? Insights from neuroimaging studies using different rejection paradigms." *Clin Psychopharmacol Neurosci* **10**(3): 144-154.

Preston, S. D. and F. B. M. de Waal (2002). "Empathy: its ultimate and proximate bases." *Behav Brain Sci* **25**: 1-72.

Preuschoff, K., et al. (2008). "Human insula activation reflects risk prediction errors as well as risk." *J Neurosci* **28**(11): 2745-2752.

Price, D. D., et al. (2007). "Placebo analgesia is accompanied by large reductions in pain-related brain activity in irritable bowel syndrome patients." *Pain* **127**(1-2): 63-72.

Rameson, L. T., et al. (2012). "The neural correlates of empathy: experience, automaticity, and prosocial behavior." *J Cogn Neurosci* **24**(1): 235-245.

Rilling, J., et al. (2002). "A neural basis for social cooperation." *Neuron* **35**(2): 395-405.

Risko, E. F., et al. (2012). "Social attention with real versus reel stimuli: toward an empirical approach to concerns about ecological validity." *Front Hum Neurosci* **6**: 143.

Riva, P., et al. (2011). "Gender effects in pain detection: speed and accuracy in decoding female and male pain expressions." *Eur J Pain* **15**(9): 985 e981-985 e911.

Roy, M., et al. (2014). "Representation of aversive prediction errors in the human periaqueductal gray." *Nat Neurosci* **17**(11): 1607-1612.

Schubert, T., et al. (2001). "The experience of presence: Factor analytic insights." *Presence: Teleoperators and virtual environments* **10**(3): 266-281.

Scott, D. J., et al. (2008). "Placebo and nocebo effects are defined by opposite opioid and dopaminergic responses." *Arch Gen Psychiatry* **65**(2): 220-231.

Scott, L., et al. (2002). "Selective up-regulation of dopamine D1 receptors in dendritic spines by NMDA receptor activation." *Proc Natl Acad Sci U S A* **99**(3): 1661-1664.

Seeley, W. W., et al. (2007). "Dissociable intrinsic connectivity networks for salience processing and executive control." *J Neurosci* **27**(9): 2349-2356.

Shackman, A. J., et al. (2011). "The integration of negative affect, pain and cognitive control in the cingulate cortex." *Nat Rev Neurosci* **12**(3): 154-167.

Shirer, W. R., et al. (2012). "Decoding subject-driven cognitive states with whole-brain connectivity patterns." *Cereb Cortex* **22**(1): 158-165.

Sia, A. T., et al. (2008). "A118G single nucleotide polymorphism of human mu-opioid receptor gene influences pain perception and patient-controlled intravenous morphine consumption after intrathecal morphine for postcesarean analgesia." *Anesthesiology* **109**(3): 520-526.

Silk, J. B. (2007). "Social components of fitness in primate groups." *Science* **317**(5843): 1347-1351.

Simons, L. E., et al. (2014). "The human amygdala and pain: evidence from neuroimaging." *Hum Brain Mapp* **35**(2): 527-538.

Singer, T. (2012). "The past, present and future of social neuroscience: a European perspective." *NeuroImage* **61**(2): 437-449.

Singer, T., et al. (2009). "A common role of insula in feelings, empathy and uncertainty." *Trends Cogn Sci* **13**(8): 334-340.

Singer, T. and C. Lamm (2009). "The social neuroscience of empathy." *Ann N Y Acad Sci* **1156**: 81-96.

Singer, T., et al. (2004). "Empathy for pain involves the affective but not the sensory components of pain." *Science* **303**: 1157-1161.

Singer, T., et al. (2008). "Effects of oxytocin and prosocial behavior on brain responses to direct and vicariously experienced pain." *Emotion* **8**(6): 781-791.

Slater, M., et al. (2010). "First person experience of body transfer in virtual reality." *PLoS One* **5**(5): e10564.

Smelser, N. J. and P. B. Baltes (2001). *International encyclopedia of the social & behavioral sciences*, Elsevier Amsterdam.

Smith, S. M., et al. (2009). "Correspondence of the brain's functional architecture during activation and rest." *Proc Natl Acad Sci U S A* **106**(31): 13040-13045.

Spiers, H. J. and E. A. Maguire (2007). "Decoding human brain activity during real-world experiences." *Trends Cogn Sci* **11**(8): 356-365.

Stein, N., et al. (2012). "White matter integrity of the descending pain modulatory system is associated with interindividual differences in placebo analgesia." *Pain* **153**(11): 2210-2217.

Strobel, A., et al. (2008). "Novelty and target processing during an auditory novelty oddball: a simultaneous event-related potential and functional magnetic resonance imaging study." *NeuroImage* **40**(2): 869-883.

Tomasello, M. (2009). *The cultural origins of human cognition*, Harvard University Press.

Torta, D. M. and F. Cauda (2011). "Different functions in the cingulate cortex, a meta-analytic connectivity modeling study." *NeuroImage* **56**(4): 2157-2172.

Tracey, I. and P. W. Mantyh (2007). "The cerebral signature for pain perception and its modulation." *Neuron* **55**(3): 377-391.

Uddin, L. Q., et al. (2009). "Functional connectivity of default mode network components: correlation, anticorrelation, and causality." *Hum Brain Mapp* **30**(2): 625-637.

Vogeley, K. and G. R. Fink (2003). "Neural correlates of the first-person-perspective." *Trends Cogn Sci* **7**(1): 38-42.

Vogeley, K., et al. (2004). "Neural correlates of first-person perspective as one constituent of human self-consciousness." *J Cogn Neurosci* **16**(5): 817-827.

Vogt, B. A. (2005). "Pain and emotion interactions in subregions of the cingulate gyrus." *Nat Rev Neurosci* **6**: 533-544.

Vorst, H. and B. Bermond (2001). "Validity and reliability of the Bermond–Vorst Alexithymia Questionnaire." *Personality and Individual Differences* **30**(3): 413-434.

Wager, T. D., et al. (2011). "Predicting individual differences in placebo analgesia: contributions of brain activity during anticipation and pain experience." *J Neurosci* **31**(2): 439-452.

Wager, T. D., et al. (2008). "The neuroimaging of emotion." *The handbook of emotion* **3**: 249-271.

Wager, T. D., et al. (2004). "Placebo-induced changes in FMRI in the anticipation and experience of pain." *Science* **303**(5661): 1162-1167.

Wager, T. D., et al. (2007). "Placebo effects on human mu-opioid activity during pain." *Proc Natl Acad Sci U S A* **104**(26): 11056-11061.

Wager, T. D., et al. (2009). "Brain mediators of cardiovascular responses to social threat: part I: Reciprocal dorsal and ventral sub-regions of the medial prefrontal cortex and heart-rate reactivity." *NeuroImage* **47**(3): 821-835.

Watson, A., et al. (2009). "Placebo conditioning and placebo analgesia modulate a common brain network during pain anticipation and perception." *Pain* **145**(1-2): 24-30.

Way, B. M., et al. (2009). "Variation in the mu-opioid receptor gene (OPRM1) is associated with dispositional and neural sensitivity to social rejection." *Proc Natl Acad Sci U S A* **106**(35): 15079-15084.

Waytz, A., et al. (2012). "Response of dorsomedial prefrontal cortex predicts altruistic behavior." *J Neurosci* **32**(22): 7646-7650.

Wiech, K., et al. (2008). "Neurocognitive aspects of pain perception." *Trends Cogn Sci* **12**(8): 306-313.

Williams, A. C. (2002). "Facial expression of pain: an evolutionary account." *Behav Brain Sci* **25**(4): 439-455; discussion 455-488.

Williams, K. D., et al. (2000). "Cyberostracism: effects of being ignored over the Internet." *Journal of Personality and Social Psychology* **79**(5): 748-762.

Woo, C. W., et al. (2014). "Separate neural representations for physical pain and social rejection." *Nat Commun* **5**: 5380.

Zaki, J. and K. Ochsner (2012). "The neuroscience of empathy: progress, pitfalls and promise." *Nat Neurosci* **15**(5): 675-680.

Zubieta, J. K., et al. (2005). "Placebo effects mediated by endogenous opioid activity on mu-opioid receptors." *J Neurosci* **25**(34): 7754-7762.

Zubieta, J. K. and C. S. Stohler (2009). "Neurobiological mechanisms of placebo responses." *Ann N Y Acad Sci* **1156**: 198-210.

Appendix I

Table 1

Main effect of physical pain: Self (Pain > No Pain)

(cluster-level corrected, p < 0.05)

	Cluster Size	x	y	z	Z score
Right Supplementary Motor Area	114426	12	4	62	6.55*
		6	-4	66	6.40*
Left Ant Mid Cingulate Cortex	114426	-4	22	28	7.07*
		-2	38	12	6.52*
Right Ant Mid Cingulate Cortex	114426	4	20	30	6.93*
Left Post Mid Cingulate Cortex	114426	-4	-2	42	7.21*
		-12	-38	48	6.36*
		-10	-32	44	6.27*
Right Post Mid Cingulate Cortex	114426	6	-18	46	7.40*
		6	4	42	7.17*
Left Mid/Anterior Insula	114426	-40	6	6	6.60*
Right Mid/Anterior Insula	114426	48	8	2	6.46*
Right Rolandic Operculum	114426	40	-16	16	6.55*
Right Precentral Gyrus	114426	34	-26	56	6.75*
		42	-24	66	6.65*
		26	-12	68	6.60*
		54	0	48	5.73*
Left Postcentral Gyrus	114426	-22	-46	64	6.80*
Right Postcentral Gyrus	114426	22	-46	66	7.11*
		36	-30	72	6.70*
Left Superior Temporal Gyrus	114426	-56	-2	-2	6.86*
		-56	-40	20	6.07*
		-62	-20	12	5.86*

Right Superior Temporal Gyrus	114426	54	-2	2	6.57*
		60	-34	24	5.91*
		60	-22	16	5.84*
Right Superior Temporal Gyrus		48	-32	24	5.76*
Right Superior Temporal Pole	114426	54	16	-8	6.75*
Thalamus	114426	0	-12	10	7.05*
Vermis	114426	-2	-64	14	6.31*

* FWE corrected ($p < 0.05$)

Table 2

Conjunction physical pain: Self ∩ Other (Pain > No Pain)

(cluster-level corrected, p < 0.05)

	Cluster Size	x	y	z	Z score
Right Mid Superior Frontal Gyrus	2412	4	50	32	3.98
Left Superior Frontal Gyrus	2412	-18	44	32	3.01
		-22	46	38	2.83
Left perigenual Ant Cingulate Cortex	2412	-4	48	18	4.85*
Left Gyrus Rectus					
Left Anterior Insula	2412	-2	58	-18	3.02
Right Inferior Orbitofrontal	713	-30	16	-18	4.04
Gyrus/Anterior Insula	731	52	28	-10	3.85
Right Mid Temporal Gyrus		44	28	-18	3.42
	731	54	6	-30	2.71
Right Superior Temporal Pole		50	18	-24	2.71
	713	-42	24	-18	3.84
		-46	24	-16	3.76
		-38	26	-32	3.06
Right Mid Temporal Pole	731	42	28	-22	3.41
	713	-38	20	-34	3.07
	731	42	14	-32	3.39
		52	12	-26	2.74

* FWE corrected (p < 0.05)

Table 3

Main effect of physical pain: Other (Pain > No Pain)

(cluster-level corrected, p < 0.05)

	Cluster Size	x	y	z	Z score
Left Mid Superior Frontal Gyrus	7859	-10	56	28	6.13*
		-4	44	42	5.53*
Right Mid Superior Frontal Gyrus	7859	6	48	46	5.59*
		6	60	8	5.02*
		10	34	58	3.55
Left Mid Superior Frontal Gyrus	7859	-12	36	56	5.64*
Left perigenual Ant Cingulate Cortex	7859	-2	54	12	5.07*
Right Gyrus Rectus					
Left Anterior Insula	7859	2	62	-22	3.17
Left Inferior Orbitofrontal Gyrus	3461	-28	16	-18	4.04
Right Inferior Orbitofrontal	3461	-44	38	-20	4.27
Gyrus/Anterior Insula	2004	-52	30	-14	4.37
Right Precentral Gyrus					
Left Superior Temporal Pole					
	3461	-44	30	-26	4.38
		-38	26	-32	3.06
Right Mid Temporal Pole		-32	28	-34	2.98
Left Inferior Temporal Gyrus	2004	46	12	-34	4.16
	3461	-42	10	-38	4.49*
		-54	-8	-34	4.07
Right Inferior Temporal Gyrus		-64	-28	-16	3.93
	2004	52	-8	-46	5.17*
Left Angular Gyrus		52	4	-42	4.78*

Left Angular Gyrus	1632	-54	-66	34	5.06*
Right Cerebellum	1632	-46	-60	28	5.01*
	913	32	-88	-36	4.50*
		14	-90	-34	3.66
		50	-70	-46	3.46

* FWE corrected ($p < 0.05$)

Table 4

Main effect of social pain: Self (Exclusion > Inclusion)

(cluster-level corrected, p < 0.05)

	Cluster Size	x	y	z	Z score
Right subgenual Anterior Cingulate	2253	4	32	-6	3.25
Cortex		8	38	-6	3.15
Left Mid Orbitofrontal Gyrus	2253	-4	52	-12	4.25
Left Posterior Insula	1321	-34	-16	18	5.59*
Right Posterior Insula	1773	40	-16	14	4.36
Left Rolandic Operculum	1321	-56	-2	10	3.38
Right Superior Temporal Gyrus	1773	56	-8	4	4.10
		70	-16	-2	3.60
		-12	-60	16	4.62*
Left Mid Temporal Gyrus	1321	-58	-16	-6	3.36
Left Calcarine Gyrus	741	-18	-54	12	4.50*
Left Caudate	2253	-10	4	20	3.23
Right Caudate	2253	10	14	16	3.75

* FWE corrected ($p < 0.05$)

Table 5

Main effect of social pain: Other (Exclusion > Inclusion)

(cluster-level corrected, p < 0.05)

	Cluster Size	x	y	z	Z score
Right Superior Frontal Gyrus	32698	50	0	4	3.69
Left Mid Frontal Gyrus	32698	-26	12	54	3.31
		-24	12	44	3.28
Left subgenual Anterior Cingulate	32698	-4	26	-4	3.26
Cortex		-10	28	-8	3.19
Right Ant Mid Cingulate Cortex	32698	6	10	30	3.85
Right Ant Mid Cingulate Cortex	32698	2	10	42	4.15
		4	-36	46	3.06
Left Superior Orbitofrontal Gyrus	32698	-14	32	-18	3.58
Right Superior Orbitofrontal Gyrus	32698	14	48	-20	3.58
Left Mid Orbifrontal Gyrus	32698	-28	40	-16	3.74
Right Mid Orbitofrontal Gyrus	32698	12	44	-6	3.75
Left Posterior Insula	32698	-28	16	4	3.54
Right Mid Posterior Insula		-44	-22	-4	3.53
	32698	36	28	12	3.71
Left Rolandic Operculum		40	-2	8	3.08
Right Rolandic Operculum	32698	-44	-4	4	4.16
Left Gyrus Rectus	32698	50	0	4	4.51*
Right Gyrus Rectus	32698	-10	44	-20	3.50
	32698	8	-32	16	3.75
Right Supplementary Motor Area		6	40	-18	3.26
Left Precentral Gyrus	32698	2	-2	56	3.68
	32698	-50	4	24	3.67
	32698	-24	-26	62	3.47

Right Postcentral Gyrus	32698	-18	-18	70	3.14
	32698	64	-14	18	4.11
Left Superior Parietal Gyrus		22	-44	62	3.70
Left Inferior Parietal Gyrus	32698	-24	-40	62	3.62
Right Superior Temporal Pole	32698	-56	-28	42	3.43
Left Superior Temporal Gyrus	32698	22	8	-18	3.29
	32698	-56	-8	-4	4.43*
Right Superior Temporal Gyrus		-50	2	-12	4.28
	32698	64	-12	2	4.42*
Left Mid Temporal Gyrus		46	-16	-2	3.34
Left Supramarginal Gyrus	32698	-62	-32	10	3.57
	32698	-60	24	24	4.07
Right Supramarginal Gyrus		-50	-24	28	4.03
	32698	50	-24	34	4.44*
		66	-20	28	4.06
Left Fusiform Gyrus		64	-18	26	4.03
Left Calcarine Gyrus	32698	-34	-40	-14	4.48*
	32698	-20	-52	10	4.49*
Right Calcarine Gyrus		-14	-64	10	3.78
Left Caudate	32698	20	-54	12	3.34
Right Caudate	32698	16	-12	22	3.15
	32698	4	8	-4	3.48
Left Thalamus		22	20	8	3.34
	32698	2	-6	8	3.58

* FWE corrected ($p < 0.05$)

Table 6

Conjunction social pain: Self ∩ Other (Exclusion > Inclusion)

(cluster-level corrected, p < 0.05)

	Cluster Size	x	y	z	Z score
Left Mid Superior Frontal Gyrus	1417	-10	54	-12	3.82
Right subgenual Anterior Cingulate	1417	4	32	-6	3.19
Cortex		8	38	-6	3.15
Right Mid Orbitofrontal Cortex	1417	6	46	-8	3.08
		8	54	-10	3.05
		8	50	-8	3.04
Left Gyrus Rectus	1417	-10	46	-18	3.47
Right Gyrus Rectus	1417	6	48	-18	2.72
Left Posterior Insula	810	-46	-12	8	3.59
Right Mid/posterior Insula	1054	52	-4	6	3.75
Left Rolandic Operculum	810	-42	-18	24	3.04
Left Superior Temporal Gyrus	810	-56	-4	8	3.21
Right Superior Temporal Gyrus	1054	60	-10	2	3.94
		68	-14	-2	3.60
Left Mid Temporal Gyrus	810	-58	-16	-6	3.36

Table 7

Conjunction physical and social pain: Self (Pain > No Pain) ∩ Self (Exclusion > Inclusion)

(cluster-level corrected, p < 0.05)

	Cluster Size	x	y	z	Z score
Right subgenual Anterior Cingulate Cortex	1557	4	30	-6	3.40
Left Mid Orbitofrontal Cortex	1557	-4	52	-1	4.05
Left Posterior Insula	1189	-32	-16	20	5.43*****
Right Posterior Insula	1498	40	-18	14	4.15
Left Rolandic Operculum	1189	-56	-2	10	3.06
Right Superior Temporal Gyrus	1498	52	-12	4	3.96
		68	-14	-2	3.59
Left Mid Temporal Gyrus	1189	-58	-16	-6	3.59
Left Caudate	1557	-12	6	20	3.09
Right Caudate	1557	14	10	20	3.08
	1557	16	14	18	2.92

***** FWE corrected ($p < 0.05$)

Table 8

Conjunction physical and social pain: Self (Pain > No Pain) ∩ Self (Exclusion > Inclusion) ∩ Other (Pain > No Pain) ∩ Other (Exclusion > Inclusion)

(p < 0.001 uncorrected)

		MNI coordinates (mm)			
	Cluster Size	x	y	z	Z score
Right subgenual Anterior Cingulate Cortex	74	4	34	-6	3.11
Left Mid Orbitofrontal Gyrus	105	-4	58	-6	3.03

Table 9

Other (Pain > No Pain) > Other (Exclusion > Inclusion)

(cluster-level corrected, p < 0.05)

		MNI coordinates (mm)			
	Cluster Size	x	y	z	Z score
Left Mid Superior Frontal Gyrus	3387	-8	54	26	4.75*
		-12	36	60	4.27
Right Superior Frontal Gyrus	3387	16	46	46	4.02
Left Inferior Temporal Gyrus	731	-44	10	-40	3.63
Left Angular Gyrus	870	-44	-58	28	4.25
Left Temporo-Parietal Junction	870	-56	-68	34	4.20

* FWE corrected (p < 0.05)

Table 10

Other (Exclusion > Inclusion) > Other (Pain > No Pain)

(cluster-level corrected, p < 0.05)

		MNI coordinates (mm)			
	Cluster Size	x	y	z	Z score
Right Superior Frontal Gyrus	37970	26	2	56	4.01
Left Inferior Frontal Operculum	37970	-44	6	26	4.16
Left post Mid Cingulate Cortex	37970	-10	4	46	4.36
		-18	-30	42	4.21
Left Anterior Insula	37970	-26	24	6	3.82
		-30	14	4	3.76
Left Rolandic Operculum	37970	-46	0	10	5.09*
Right Rolandic Operculum	37970	48	2	12	5.34*
Right Supramarginal Gyrus	37970	62	-16	24	4.83*
		60	-22	42	4.63*
Left Postcentral Gyrus	37970	-58	-20	26	4.10
		-60	-16	16	3.80
Right Postcentral Gyrus	37970	26	-40	48	4.00
Right Superior Temporal Gyrus	37970	-56	-10	-2	4.67*
		66	-10	0	4.03
Left Inferior Temporal Gyrus	37970	-52	-54	-12	4.10
Left Fusiform Gyrus	37970	-32	-44	-16	4.32
		-36	-62	-6	4.08
Right Fusiform Gyrus	37970	28	-38	20	4.70*
		36	-54	-8	4.01
Left Inferior Parietal Gyrus	37970	-56	-28	46	4.29
		-40	-28	42	4.12
Left Calcarine Gyrus	37970	-20	-54	14	3.81
Left Precuneus	37970	-20	-62	34	4.53*

Left Mid Occipital Gyrus	37970	-30	-86	22	4.88*
		-36	-86	10	4.62*
Vermis	37970	6	-64	-14	3.87
Right Lingual Gyrus	37970	18	-80	-12	3.86

* FWE corrected ($p < 0.05$)

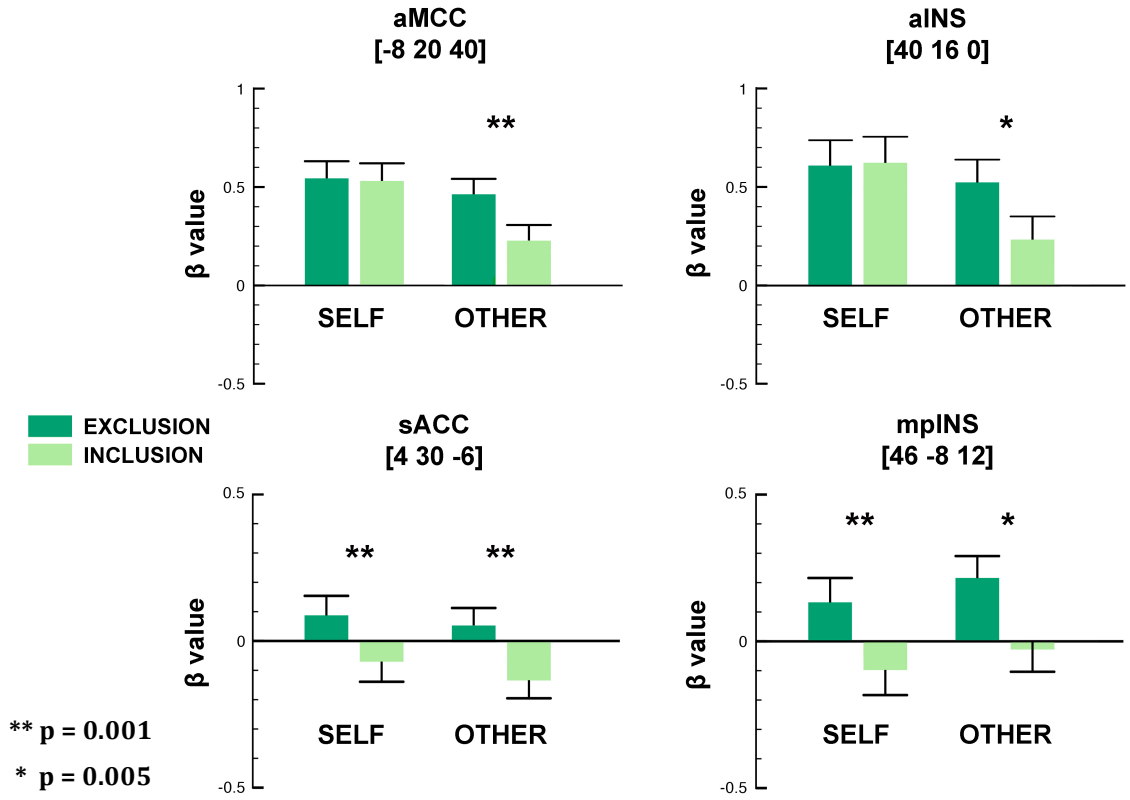

Figure 1 Patterns of activation and deactivation (negative and positive beta estimates for labeled peak coordinates) in left aMCC, right aINS (coordinates based on Eisenberger et al. 2003), right sACC (coordinate based on Premkumar 2012), and right mpINS (coordinate based on Kross et al. 2011). Beta estimates are plotted for the contrasts Self Exclusion, Self Inclusion, Other Exclusion, and Other Inclusion.

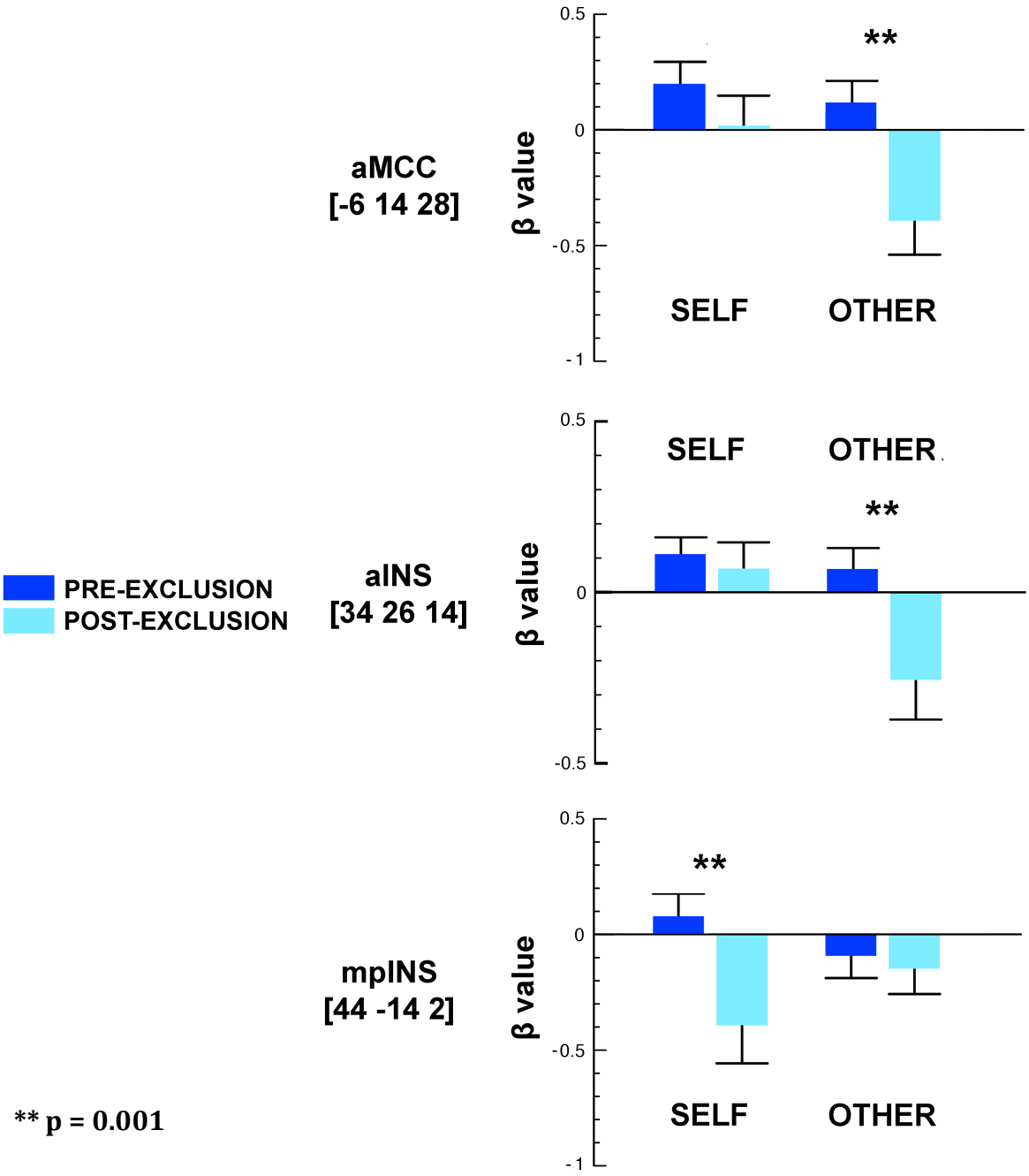

Figure 2 Patterns of activation and deactivation (negative and positive beta estimates for labeled peak coordinates) in left aMCC, right aINS, and right mpINS, for the two blocks of inclusion trials (pre-exclusion = first three inclusion trials; post-exclusion = last two inclusion trials).

Appendix II

Table 1 - Subjective rating (VAS) for the three scales evaluating the emotional state of the participants

	Tension		Sadness		Anxiety	
	Pre	Difference Post-Pre	Pre	Difference Post-Pre	Pre	Difference Post-Pre
SH group	-0.3 (2.6)	-1.8 (2.2)	-1.3 (1.2)	-0.5 (1.3)	-1.1 (2.9)	-1.8 (2.8)
NoH group	-1.0 (1.8)	-0.5 (2.4)	-1.3 (1.4)	0.3 (1.9)	-1.5 (2.4)	-0.4 (2.7)

Note. Assessments were performed before and after the experiment, however only the mean ratings reported at the beginning (Pre), and the difference between before and after the experiment (Difference Post-Pre) were computed and reported. SH = Successful Help; NoH = No Help. Standard deviations appear in parentheses.

Table 2 - Mean groups' scores for the four subscales of the Interpersonal Reactivity Index (IRI)

	Fantasy	Empathic concern	Perspective taking	Personal distress
SH group	17.4 (3.4)	19.9 (3.2)	18.0 (4.2)	12.1 (4.1)
NoH group	17.3 (5.5)	18.6 (3.5)	18.6 (3.7)	11.6 (6.1)

Note. SH = Successful Help; NoH = No Help. Standard deviations appear in parentheses.

Table 3 - Mean groups' scores for the five subscales of the Bermond-Vorst Alexithymia Questionnaire (BVAQ-B)

	Verbalizing	Fantasizing	Identifying	Emotionalizing	Analyzing
SH group	2.6 (0.5)	3.1 (0.3)	2.8 (0.6)	3.1 (0.6)	3.1 (0.4)
NoH group	2.8 (0.4)	3.4 (0.3)	2.8 (0.6)	3.0 (0.6)	2.9 (0.6)

Note. SH = Successful Help; NoH = No Help. Standard deviations appear in parentheses.

Table 4 - Mean groups' scores for the three subscales of the Igroup Presence Questionnaire (IPQ) and the general item G

	Involvement	Spatial presence	Experienced realism	General sense of experience
SH group	0.10 (1.3)	0.91 (1.1)	-0.56 (1.2)	1.06 (1.2)
NoH group	0.54 (1.3)	0.68 (1.3)	-0.76 (1.2)	0.11 (1.9)

Note. SH = Successful Help; NoH = No Help. Standard deviations appear in parentheses.

Table 5 - Multivariate tests on self-reported questionnaires and the three scales evaluating the emotional state of the participants

	Wilks λ	*F*	*df*	Error *df*	*p*	η_p^2
Emotional State	0.876	0.658	6	28	0.684	0.124
IRI	0.945	0.436	4	30	0.781	0.055
BVAQ-B	0.816	1.309	5	29	0.288	0.184
IPQ	0.779	2.130	4	30	0.102	0.221

Note. IRI = Interpersonal Reactivity Index; BVAQ-B = Bermond-Vorst Alexithymia Questionnaire, form B; IPQ = Igroup Presence Questionnaire.

Table 6 - Brain regions which were found in Independent Component 1.

Region	Cluster size	x	y	z	Z score
Left precentral gyrus	23115	-30	-4	56	65535
	23115	-34	-12	52	65535
	23115	-26	-18	64	65535
Right precentral gyrus	23115	28	-12	66	65535
	23115	20	-16	64	65535
	23115	20	-28	62	65535
Left postcentral gyrus	23115	-44	-22	50	65535
	23115	-34	-30	58	65535
	23115	-20	-34	68	65535
Right postcentral gyrus	23115	54	-14	46	65535
	23115	32	-34	52	65535
	23115	28	-42	62	65535
Left rolandic operculum	19	-44	-2	10	5.22
	315	-42	-26	16	5.8
	315	-46	-28	16	5.91
Right rolandic operculum	3	46	-20	14	5.13
Left superior frontal gyrus, dorsolateral part	23115	-22	-2	52	65535
Right superior frontal gyrus, dorsolateral part	23115	28	-6	62	65535
Right superior frontal gyrus, medial part	4	8	46	40	5.13
Left middle frontal gyrus	4	-34	40	34	5.02
	23115	-32	10	48	5.56
Right middle frontal gyrus	3	24	32	46	5.12
	23115	30	8	50	5.85
	23115	36	-4	56	65535
Left supplementary motor area	23115	0	-6	56	65535
	23115	-6	-10	64	65535
Right supplementary motor area	23115	12	0	62	65535
	23115	14	-4	52	65535
	23115	4	-6	66	65535
Left paracentral lobule	23115	-16	-14	66	65535
Right paracentral lobule	23115	8	-36	64	7.1
Left median cingulate and paracingulate gyri	23115	-6	22	36	5.33
	23115	-6	-2	42	65535
	23115	-2	-24	48	65535
Right median cingulate and paracingulate gyri	23115	4	10	44	65535
	23115	6	6	42	65535
	23115	2	-28	54	65535
Left insula	315	-38	-20	16	6.19
Left superior parietal gyrus	23115	-22	-48	62	65535
Right superior parietal gyrus	23115	16	-52	60	7.43
	23115	16	-56	58	7.56
Left inferior parietal cortex (except supramarginal and angular gyri)	23115	-30	-46	54	65535

Left precuneus	23115	-18	-40	68	65535
	23115	-12	-48	64	65535
	23115	-14	-60	56	65535
Right precuneus	23115	10	-42	52	7.42
	23115	12	-48	70	7.79
Left superior occipital gyrus	3	-22	-86	26	5.15
Left calcarine fissure and surrounding cortex	1	-8	-60	14	4.94
Right lingual gyrus	1	10	-66	-10	4.91
Left superior temporal gyrus	22	-56	-2	0	5.79
	315	-60	-20	12	6.16
	2	-56	-32	18	5.09
Left temporal pole (superior temporal gyrus)	71	-42	16	-22	5.94
Right temporal pole (superior temporal gyrus)	4	38	26	-30	5.02
Left caudate nucleus	214	-6	4	12	5.46
Right caudate nucleus	18	10	0	14	5.29
Left putamen	1	-30	-18	6	4.92
Left thalamus	214	-8	-6	6	6.31
	214	-14	-14	8	5.79
	214	-20	-22	10	5.36
Left cerebellum, lobules IV and V	318	-4	-56	-2	6.09
Right cerebellum, lobules IV and V	318	8	-40	-8	5.35
	318	8	-48	-10	5.86
	318	8	-50	-6	5.62
Vermis, lobules IV and V	318	2	-50	0	5.84
	318	4	-60	-8	5.07

Note. $p < 0.05$, corrected for multiple comparisons according to the family-wise error approach (FWE-corrected). Coordinates are in millimeters and in the MNI standard space.

Table 7 - Brain regions which were found in Independent Component 2.

Region	Cluster size	x	y	z	Z score
Left precentral gyrus	13545	-34	8	48	7.26
	13545	-36	0	54	65535
	13545	-44	0	44	7.54
Right precentral gyrus	3133	50	6	28	65535
	3133	46	4	44	6.64
	3133	34	2	50	7.64
Right postcentral gyrus	8	54	-14	40	5.12
	10529	52	-24	44	5.34
Left superior frontal gyrus, dorsolateral part	13545	-22	52	8	7.03
	13545	-14	40	32	5.04
	13545	-14	16	46	6.3
Left superior frontal gyrus, medial part	13545	0	32	34	7.59
	13545	2	24	42	65535
	13545	0	18	42	65535
Left superior frontal gyrus, orbital part	13545	-24	58	-4	6.48
	13545	-14	22	-18	6.55
Left middle frontal gyrus	13545	-28	54	16	65535
	13545	-32	52	16	65535
	13545	-22	10	52	65535
Right middle frontal gyrus	3133	40	50	18	6.53
	3133	36	36	28	6.36
	3133	28	6	58	6.75
Left middle frontal gyrus, orbital part	13545	-34	52	-6	5.36
Left inferior frontal gyrus, opercular part	13545	-44	8	30	65535
Right inferior frontal gyrus, opercular part	3133	34	6	30	6.1
Left inferior frontal gyrus, triangular part	13545	-48	22	30	65535
Right inferior frontal gyrus, triangular part	3133	44	32	28	6.19
	3133	46	30	24	6.21
	3133	44	26	24	6.26
Left gyrus rectus	13545	-12	18	-12	6.86
Right gyrus rectus	295	12	20	-12	5.31
Left supplementary motor area	13545	-2	20	56	7.26
	13545	-4	10	50	65535
	13545	0	4	52	65535
Left anterior cingulate and paracingulate gyri	13545	-8	36	22	6.66
	13545	-4	30	30	7.41
Right anterior cingulate and paracingulate gyri	13545	8	32	14	65535
	13545	6	16	26	65535
	13545	2	10	28	7.75
Left median cingulate and paracingulate gyri	13545	-4	22	36	7.84
	10529	-8	-34	42	6.32
	10529	-6	-42	46	6.99

Right median cingulate and paracingulate gyri	13545	4	14	46	65535
	13545	8	14	42	65535
Right median cingulate and paracingulate gyri	4	2	-16	46	5.11
Left insula	13545	-28	22	-8	6.6
	13545	-36	20	4	5.92
Right superior parietal gyrus	10529	20	-62	50	6.9
Left inferior parietal cortex (except supramarginal and angular gyri)	10529	-42	-36	40	65535
	10529	-36	-58	50	65535
	10529	-28	-60	42	65535
Right inferior parietal cortex (except supramarginal and angular gyri)	10529	32	-50	44	65535
Right angular gyrus	10529	34	-56	50	65535
	10529	32	-60	40	7.65
Right supramarginal gyrus	10529	50	-30	46	5.83
Left precuneus	10529	-10	-54	46	6.9
	10529	-8	-64	48	65535
	10529	-12	-74	46	65535
Right precuneus	10529	4	-54	46	6.82
	10529	8	-56	46	6.8
	10529	16	-64	48	7.18
Left superior occipital gyrus	10529	-26	-70	34	65535
Right superior occipital gyrus	10529	30	-64	42	7.58
	10529	32	-70	42	7.66
Left middle occipital gyrus	10529	-28	-78	34	65535
	10529	-38	-82	26	6.81
	10529	-38	-88	-2	6.69
Right middle occipital gyrus	10529	34	-74	36	7.55
	10529	44	-78	28	5.89
	1	48	-80	0	4.92
Left inferior occipital gyrus	10529	-48	-66	-16	7.54
	10529	-48	-76	-2	6.26
	10529	-46	-78	-6	6.31
Left cuneus	10529	-14	-72	32	6.02
Left calcarine fissure and surrounding cortex	19	-16	-60	16	5.25
Right calcarine fissure and surrounding cortex	6	14	-56	12	5.06
	14	8	-78	10	5.45
Left lingual gyrus	361	-10	-44	0	6.07
Right lingual gyrus	12	10	-44	6	5.4
Left fusiform gyrus	10529	-36	-40	-24	5.98
Left superior temporal gyrus	372	-66	-18	4	5.72
	372	-54	-18	2	6.77
Right superior temporal gyrus	24	62	-12	-2	5.68
Left middle temporal gyrus	372	-54	-16	-4	6.35
	372	-64	-26	0	6.08

	111	-58	-48	8	6.09
Left inferior temporal gyrus	10529	-56	-58	-8	6.12
Left olfactory cortex	13545	-8	12	-12	6.56
Left temporal pole (superior temporal gyrus)	22	-48	16	-16	5.29
Left temporal pole (middle temporal gyrus)	3	-28	12	-34	4.95
Left caudate nucleus	13545	-8	18	6	5.91
Right caudate nucleus	295	8	16	-10	5.17
	295	8	8	4	7.1
Left putamen	13545	-28	14	2	5.73
	13545	-18	12	2	5.64
Right putamen	295	22	18	-8	6.19
Left globus pallidus	13545	-10	4	2	5.54
Left thalamus	1	-8	-18	8	5.17
Left cerebellum, lobule VI	10529	-42	-48	-26	6.57

Note. $p < 0.05$, corrected for multiple comparisons according to the family-wise error approach (FWE-corrected). Coordinates are in millimeters and in the MNI standard space.

Table 8 - Brain regions which were found in Independent Component 3.

Region	Cluster size	x	y	z	Z score
Right superior frontal gyrus, dorsolateral part	10228	32	56	12	65535
	10228	18	30	46	65535
	10228	20	26	50	65535
Left superior frontal gyrus, medial part	10228	2	34	40	65535
Right superior frontal gyrus, medial part	10228	12	36	48	65535
Right superior frontal gyrus, medial orbital part	1	8	50	-6	4.95
Left middle frontal gyrus	105	-42	56	4	5.27
	30	-40	20	40	5.26
	73	-28	10	56	6.4
Right middle frontal gyrus	10228	28	26	48	65535
	10228	46	22	40	65535
	10228	38	10	56	65535
Left middle frontal gyrus, orbital part	105	-32	50	-8	5.02
	105	-42	48	-8	5.91
Right middle frontal gyrus, orbital part	10228	30	58	-6	65535
	10228	42	50	-8	65535
	10228	46	48	-14	7.8
Right inferior frontal gyrus, opercular part	10228	54	20	4	5.44
Right inferior frontal gyrus, triangular part	10228	48	36	18	65535
	10228	50	30	30	65535
	10228	58	22	16	6.3
Right inferior frontal gyrus, orbital part	10228	46	44	-8	7.51
	10228	32	42	-18	7.38
	10228	40	40	-2	7.09
Right anterior cingulate and paracingulate gyri	10228	6	46	6	7.19
	10228	6	40	28	65535
	537	6	-34	38	7.6
Right insula	10228	34	16	-14	5.09
	1	34	-16	10	5.03
Left inferior parietal cortex (except supramarginal and angular gyri)	782	-50	-46	48	7.55
	782	-44	-56	48	6.41
	782	-38	-62	52	5.83
Right inferior parietal cortex (except supramarginal and angular gyri)	4438	44	-46	52	65535
	4438	46	-46	46	65535
	4438	42	-56	44	65535
Left angular gyrus	782	-48	-62	50	6.35
Right angular gyrus	4438	56	-52	38	65535
	4438	48	-52	30	65535
	4438	56	-54	30	65535
Right supramarginal gyrus	4438	56	-44	44	65535

Right precuneus	537	6	-58	42	6.62
	18	8	-66	32	4.92
	19	6	-78	50	5.35
Right cuneus	2	14	-62	22	4.92
	18	8	-68	24	5.26
Right superior temporal gyrus	109	46	-4	-8	5.64
	109	46	-6	-12	5.6
Right inferior temporal gyrus	787	66	-30	-18	6.4
	787	64	-40	-10	65535
Right temporal pole (superior temporal gyrus)	1	30	26	-30	5.17
Right parahippocampal gyrus	1	22	16	-30	5.05
Vermis, lobules IV and V	3	4	-46	-6	5.01
	1	0	-46	-12	4.98

Note. $p < 0.05$, corrected for multiple comparisons according to the family-wise error approach (FWE-corrected). Coordinates are in millimeters and in the MNI standard space.

Table 9 - Brain regions which were found in Independent Component 4.

Region	Cluster size	x	y	z	Z score
Right precentral gyrus	92	54	-2	48	5.93
Left postcentral gyrus	59	-54	-12	46	6.19
	45	-40	-14	36	5.6
	9	-22	-28	60	5.21
Right postcentral gyrus	7947	58	-6	28	5.6
Left rolandic operculum	9012	-60	-2	12	7.05
Left middle frontal gyrus	6	-26	46	26	5.35
Left inferior frontal gyrus, triangular part	233	-40	16	26	6.82
Left gyrus rectus	35	-10	54	-16	4.97
	35	0	52	-20	5.64
Right median cingulate and paracingulate gyri	491	10	-38	52	5.09
Left insula	9012	-40	-2	10	6.08
Left precuneus	491	-2	-52	46	6.99
Right precuneus	1	8	-56	22	4.92
Right calcarine fissure and surrounding cortex	54	12	-86	10	5.61
	54	8	-90	12	4.97
Left superior temporal gyrus	9012	-60	4	-8	65535
	9012	-42	-30	8	65535
	9012	-66	-38	12	65535
Right superior temporal gyrus	7947	58	0	-8	65535
	7947	48	-14	0	65535
	7947	62	-16	4	65535
Left rolandic operculum (Heschl gyrus)	9012	-46	-18	8	65535
Right rolandic operculum (Heschl gyrus)	7947	44	-20	6	65535
Left middle temporal gyrus	9012	-58	-4	-16	65535
	9012	-56	-28	4	65535
	9012	-56	-48	12	7.65
Right middle temporal gyrus	7947	56	-2	-14	65535
	7947	64	-4	-10	65535
	7947	66	-14	-10	65535
Left temporal pole (superior temporal gyrus)	9012	-54	8	-10	65535
Right temporal pole (superior temporal gyrus)	7947	54	10	-12	65535
Left cerebellum. lobules IV and V	4	-6	-48	-18	5.02
Vermis, lobules IV and V	1	-2	-52	-10	5.02
	1	0	-54	-8	4.97

Note. $p < 0.05$, corrected for multiple comparisons according to the family-wise error approach (FWE-corrected). Coordinates are in millimeters and in the MNI standard space.

Table 10 - Brain regions which were found in Independent Component 5.

Region	Cluster size	x	y	z	Z score
Right middle frontal gyrus	1	40	44	10	4.97
Right supplementary motor area	2	4	20	62	5.06
Left precuneus	38	-4	-50	46	5.6
	38	-10	-52	42	5.05
Left cuneus	6636	-8	-78	34	65535
	6636	4	-90	18	65535
	6636	-6	-94	18	65535
Right cuneus	6636	4	-80	26	65535
	6636	14	-90	24	65535
Left calcarine fissure and surrounding cortex	6636	-6	-94	6	65535
Right calcarine fissure and surrounding cortex	6636	6	-82	10	65535
	6636	8	-90	4	65535

Note. $p < 0.05$, corrected for multiple comparisons according to the family-wise error approach (FWE-corrected). Coordinates are in millimeters and in the MNI standard space.

Table 11 - Brain regions which were found in Independent Component 6.

Region	Cluster size	x	y	z	Z score
Right precentral gyrus	503	40	-18	62	5.83
	503	38	-20	54	5.72
Left postcentral gyrus	87	-42	-32	58	5.47
	87	-40	-32	48	5.86
	87	-36	-32	46	5.67
Right postcentral gyrus	503	56	-18	52	6.74
	503	56	-24	54	6.67
	503	48	-26	56	7.6
Right superior frontal gyrus, dorsolateral part	1	18	66	14	5.01
Left superior frontal gyrus, medial part	372	-2	58	34	5.47
Right superior frontal gyrus, medial part	372	4	70	8	7.17
	372	4	66	20	6.05
	372	4	64	28	5.84
Left superior parietal gyrus	14987	-26	-66	48	6.51
Left inferior parietal cortex (except supramarginal and angular gyri)	7	-56	-20	50	5.13
Right inferior parietal cortex (except supramarginal and angular gyri)	14987	28	-54	54	5.1
Right angular gyrus	14987	26	-58	44	5.81
	14987	26	-62	48	5.89
Left precuneus	7	-4	-50	18	5
Right precuneus	60	18	-50	20	6.32
Left superior occipital gyrus	14987	-26	-68	32	6.24
	14987	-14	-96	8	65535
Right superior occipital gyrus	14987	28	-64	34	5.26
Left middle occipital gyrus	14987	-42	-80	2	65535
	14987	-32	-92	8	65535
	14987	-18	-102	6	65535
Right middle occipital gyrus	14987	36	-84	6	65535
	14987	40	-88	2	65535
	14987	34	-96	0	65535
Left inferior occipital gyrus	14987	-48	-66	-12	65535
	14987	-44	-78	-4	65535
Right inferior occipital gyrus	14987	42	-68	-10	65535
	14987	44	-76	-6	65535
	14987	36	-82	-6	7.67
Left calcarine fissure and surrounding cortex	14987	-4	-82	-8	65535
	14987	4	-86	0	65535
	14987	4	-96	0	65535
Right calcarine fissure and surrounding cortex	14987	6	-92	10	65535
	14987	16	-96	2	65535
Left lingual gyrus	14987	-28	-82	-12	65535

Right lingual gyrus	14987	8	-78	-4	65535
	14987	16	-88	-4	65535
	14987	10	-90	-4	65535
Left fusiform gyrus	14987	-30	-62	-16	65535
	14987	-28	-66	-12	7.8
	14987	-24	-82	-10	65535
Right fusiform gyrus	14987	34	-56	-12	65535
	14987	32	-64	-12	65535
	14987	28	-70	-10	65535
Right inferior temporal gyrus	14987	50	-42	-20	6.4
	14987	50	-64	-10	7.14
	14987	44	-72	-8	65535
Left hippocampus	17	-24	-6	-22	5.48
Left thalamus	83	-14	-16	8	5.51
Right thalamus	1	10	-8	2	5.01
Left cerebellum, lobules IV and V	14987	-22	-50	-16	7.23
Left cerebellum, lobule VI	14987	-40	-54	-22	65535
	14987	-18	-68	-16	7.16
Vermis, lobules VI	14987	-2	-64	-16	5.16

Note. $p < 0.05$, corrected for multiple comparisons according to the family-wise error approach (FWE-corrected). Coordinates are in millimeters and in the MNI standard space.

Table 12 - Brain regions which were found in Independent Component 7.

Region	Cluster size	x	y	z	Z score
Left rolandic operculum	27	-42	-24	18	5.59
Right rolandic operculum	3488	56	14	0	65535
Right superior frontal gyrus, medial part	3492	6	60	4	5.23
Right superior frontal gyrus, medial orbital part	3492	6	60	-2	4.95
Left inferior frontal gyrus, orbital part	3608	-46	16	-4	65535
Right inferior frontal gyrus, orbital part	3488	52	28	-2	65535
	3488	34	26	-10	65535
	3488	38	22	-18	65535
Left supplementary motor area	3492	-2	12	60	5.69
	3492	-4	12	56	5.68
Right supplementary motor area	2	6	22	52	4.94
Left anterior cingulate and paracingulate gyri	3492	-6	44	6	7.64
	3492	-4	38	18	7.75
	3492	-2	32	26	65535
Right anterior cingulate and paracingulate gyri	3492	6	48	4	7.47
	3492	4	40	12	7.81
	3492	2	34	22	7.78
Left median cingulate and paracingulate gyri	3492	0	20	36	7.54
Right median cingulate and paracingulate gyri	3492	6	10	44	6.24
Left insula	3608	-34	22	-8	65535
	3608	-36	20	-12	65535
	3608	-42	10	-4	65535
Right insula	3488	34	18	2	65535
	3488	42	8	0	6.86
	13	32	-18	12	5.75
Right angular gyrus	248	58	-50	28	5.95
	248	56	-54	38	5.53
Left supramarginal gyrus	3	-60	-46	28	5.08
Right supramarginal gyrus	248	62	-40	34	6.2
	248	60	-44	32	5.95
	248	64	-44	30	6.33
Left precuneus	22	-4	-62	64	5.45
Right middle temporal gyrus	130	62	-22	-14	5.88
	130	52	-30	-8	5.76
Right inferior temporal gyrus	130	60	-22	-18	5.58
Left temporal pole (superior temporal gyrus)	3608	-42	18	-14	65535
	3608	-32	18	-30	6.82
Right temporal pole (superior temporal gyrus)	3488	50	18	-10	65535
	3488	52	8	-4	7.6
Left putamen	3608	-30	4	-6	7.14
	3	-28	-12	10	5.11
Right putamen	4	22	12	-4	5.06

Left thalamus	1961	-16	-14	6	6.56
	1961	-6	-16	0	65535
Right thalamus	1961	6	-14	8	7.19
	1961	6	-20	0	65535
	1961	10	-28	0	6.73
Right cerebellum, lobules IV and V	357	16	-50	-20	6.79
Left cerebellum, lobule VI	39	-36	-54	-26	5.27
	39	-30	-56	-24	5.07
	39	-24	-60	-20	5.6
Right cerebellum, lobule VI	357	10	-60	-16	6.99
Vermis, lobules IV and V	357	0	-54	-18	5.95

Note. $p < 0.05$, corrected for multiple comparisons according to the family-wise error approach (FWE-corrected). Coordinates are in millimeters and in the MNI standard space.

Table 13 - Brain regions which were found in Independent Component 8.

Region	Cluster size	x	y	z	Z score
Right precentral gyrus	36	22	-30	68	5.63
Left postcentral gyrus	3	-50	-12	38	5.17
Right postcentral gyrus	25	50	-4	32	5.21
Right postcentral gyrus	25	54	-6	34	5.35
Left superior frontal gyrus, dorsolateral part	16528	-24	58	18	65535
	16528	-20	46	24	65535
	16528	-14	24	58	65535
Right superior frontal gyrus, dorsolateral part	16528	18	56	30	65535
	16528	16	52	32	65535
	16528	16	42	50	65535
Left superior frontal gyrus, medial part	16528	-2	58	24	65535
	16528	-8	50	42	65535
	16528	-8	42	44	65535
Right superior frontal gyrus, medial part	16528	2	58	8	65535
	16528	4	52	40	65535
	16528	4	46	50	65535
Left middle frontal gyrus	16528	-32	48	24	65535
	16528	-28	34	44	65535
	16528	-24	30	50	65535
Right middle frontal gyrus	16528	26	52	26	65535
	16528	24	46	34	65535
	16528	30	34	38	65535
Left gyrus rectus	16528	0	58	-16	7.01
Left supplementary motor area	16528	0	22	62	7.49
	16528	-2	16	64	7.32
Right supplementary motor area	6	12	4	64	5.09
	11	4	-14	70	5.15
Left anterior cingulate and paracingulate gyri	16528	-2	48	10	65535
	16528	2	46	18	65535
	16528	-4	30	28	65535
Right anterior cingulate and paracingulate gyri	16528	2	40	20	65535
Left median cingulate and paracingulate gyri	16528	-2	6	40	5.04
	16528	0	-16	40	6.89
Right median cingulate and paracingulate gyri	16528	2	24	38	7.45
	16528	10	24	34	7.01
	16528	2	-26	42	7.55
Left posterior cingulate gyrus	377	-4	-46	34	6.76
Right inferior parietal cortex (except supramarginal and angular gyri)	221	58	-58	40	6.17
Left angular gyrus	163	-48	-58	32	6.09
	163	-52	-62	34	5.68
Right angular gyrus	221	52	-54	32	5.56
Left precuneus	377	-2	-54	32	6.76

Right precuneus	42	2	-54	60	6.18
Right superior occipital gyrus	14	22	-84	38	5.59
	139	24	-84	18	5.11
	139	24	-94	20	5.09
Right middle occipital gyrus	139	40	-84	16	5.39
	139	30	-88	20	5.88
Left lingual gyrus	170	-6	-74	-2	5.6
Left middle temporal gyrus	24	-66	-20	-14	5.16
	24	-66	-22	-10	5.12
	23	-58	-26	-2	5.64
Left inferior temporal gyrus	9	-38	14	-38	5.29
	3	-46	6	-32	5.01
	73	-64	-16	-26	6.34
Left temporal pole (superior temporal gyrus)	18	-50	18	-10	5.53
Right caudate nucleus	86	16	16	12	5.93

Note. $p < 0.05$, corrected for multiple comparisons according to the family-wise error approach (FWE-corrected). Coordinates are in millimeters and in the MNI standard space.

Table 14 - Brain regions which were found in Independent Component 9.

Region	Cluster size	x	y	z	Z score
Right postcentral gyrus	134	46	-22	60	5.84
	134	48	-24	54	6.02
Left superior frontal gyrus, dorsolateral part	137	-22	60	10	6.05
Left superior frontal gyrus, medial part	137	-12	66	14	5.47
Right superior frontal gyrus, medial part	2138	6	56	6	7.11
	2138	4	54	16	6.2
	2138	2	54	8	6.98
Left superior frontal gyrus, orbital part	137	-22	60	-4	5.82
Left superior frontal gyrus, medial orbital part	2138	0	56	-8	7.21
	2138	-6	50	-6	7.61
Right superior frontal gyrus, medial orbital part	2138	4	62	-2	7.02
	2138	2	60	-12	7.27
	2138	4	52	-12	7.3
Left middle frontal gyrus	2	-22	34	44	4.96
	2	-28	22	50	4.98
	1	-30	20	52	4.94
Left gyrus rectus	2138	-2	58	-14	7.27
Left anterior cingulate and paracingulate gyri	2138	0	42	12	6.71
	2138	0	32	18	6.27
Right anterior cingulate and paracingulate gyri	2138	4	48	16	6.36
	2138	4	44	14	6.48
Left median cingulate and paracingulate gyri	8842	0	-22	34	65535
	8842	-6	-32	40	65535
Right median cingulate and paracingulate gyri	8842	6	-46	34	65535
Left posterior cingulate gyrus	8842	-6	-42	32	65535
	8842	-4	-48	28	65535
Left inferior parietal cortex (except supramarginal and angular gyri)	2870	-50	-44	42	5.85
Left angular gyrus	2870	-44	-60	30	65535
	2870	-40	-64	40	65535
	2870	-46	-64	32	65535
Right angular gyrus	2478	56	-60	28	65535
	2478	42	-64	38	65535
	2478	44	-66	46	65535
Left precuneus	8842	-6	-54	22	65535
	8842	0	-62	22	65535
	8842	-4	-66	34	65535
Right precuneus	8842	4	-52	22	65535
	8842	8	-56	28	65535
Right inferior occipital gyrus	6	32	-90	-4	5.28
Left middle temporal gyrus	29	-66	-42	-10	5.37

Right middle temporal gyrus	12	64	-12	-22	5.53
	126	66	-30	-6	6.06
	126	62	-32	-6	5.76
Left parahippocampal gyrus	59	-26	-22	-20	6.07
Left thalamus	42	-6	-22	6	5.93
Vermis, lobules IV and V	8842	-6	-46	4	7.73

Note. $p < 0.05$, corrected for multiple comparisons according to the family-wise error approach (FWE-corrected). Coordinates are in millimeters and in the MNI standard space.

Table 15 - Brain regions of IC 7 which were found significant in the contrast SH group < NoH group

Region	Cluster size	x	y	z	Z score
Left superior frontal gyrus, dorsolateral part	18	-16	42	30	5,19
	408	-12	22	48	6,16
Right superior frontal gyrus, dorsolateral part	4	24	32	56	5,17
	11	20	28	48	5,1
	11	16	26	46	5,13
	5	14	16	50	5,18
Left superior frontal gyrus, medial part	18	-10	46	34	5,37
	408	-4	36	52	5,89
	408	-8	26	44	5,37
Right superior frontal gyrus, medial part	408	4	42	44	5,77
	11	12	28	46	5,13
Right middle frontal gyrus	12	40	14	58	5,88
Right inferior frontal gyrus, orbital part	122	36	24	-16	6,41
Left supplementary motor area	408	-10	18	58	5,41
Left anterior cingulate and paracingulate gyri	28	-8	36	20	5,8
	408	-2	22	38	5,67
Right median cingulate and paracingulate gyri	4	8	20	38	4,99
Left insula	142	-40	20	-4	5,25
	142	-32	20	-12	5,38
	142	-36	18	-2	5,27
	142	-44	18	-2	5,71
	142	-46	16	2	5,72
Right insula	1	36	12	-6	5,09
	9	46	-4	4	5,34
Right superior parietal gyrus	1	34	-74	54	5,16
Right angular gyrus	20	50	-66	48	5,3
	20	42	-68	54	5,22
	20	38	-74	52	5,39
Left middle occipital gyrus	2	-18	-92	6	5,08
Right superior temporal gyrus	7	56	-14	-6	5,24
Left putamen	38	-28	6	-2	5,65

Note. $p < 0.05$, corrected for multiple comparisons according to the family-wise error approach (FWE-corrected). Coordinates are in millimeters and in the MNI standard space.

Table 16 - Brain regions of IC 7 which were found significant in the contrast SH group > NoH group

Region	Cluster size	x	y	z	Z score
Left precentral gyrus	38	-60	8	38	6,52
	38	-58	2	44	6,34
	1	-54	-2	52	5,45
Left postcentral gyrus	38	-58	-2	46	6,24
	38	-60	-2	42	5,89
Right postcentral gyrus	597	54	-20	36	5,94
Right rolandic operculum	597	62	-18	16	5,85
Left middle frontal gyrus	212	-26	56	34	6,03
	212	-46	44	28	7,69
	212	-44	38	38	7,35
Right middle frontal gyrus	2	30	52	36	5,07
	285	44	52	14	6,42
	285	46	48	22	6,27
Right inferior frontal gyrus, triangular part	285	52	44	4	5,32
	285	52	42	8	5,32
	285	56	38	6	5,48
Left inferior parietal cortex (except supramarginal and angular gyri)	1	-56	-38	48	4,97
Left supramarginal gyrus	172	-60	-26	38	5,98
	172	-54	-26	32	5,4
	172	-50	-32	36	5,04
Right supramarginal gyrus	597	66	-18	30	5,83
	597	68	-24	30	5,88
	597	66	-30	28	5,97
Right superior occipital gyrus	6	22	-76	40	5,31
Left middle occipital gyrus	1	-34	-66	40	4,94
Right inferior occipital gyrus	2967	46	-72	-14	7,01
Right fusiform gyrus	2967	30	-74	-16	6,66
Left superior temporal gyrus	172	-58	-30	24	5,27
Right superior temporal gyrus	597	68	-26	16	5,6
	597	64	-32	18	5,95
Left middle temporal gyrus	2	-56	-64	-2	5,08
Right inferior temporal gyrus	2967	62	-58	-8	5,34
	2967	56	-66	-12	6,1
Right temporal pole (superior temporal gyrus)	2	22	16	-32	5,47

Note. $p < 0.05$, corrected for multiple comparisons according to the family-wise error approach (FWE-corrected). Coordinates are in millimeters and in the MNI standard space.

Table 17 - Brain regions of IC 8 which were found significant in the contrast SH group > NoH group

Region	Cluster size	x	y	z	Z score
Right rolandic operculum	1	52	2	6	5
	2	50	0	12	5,07
	1	38	-20	18	4,96
Left superior frontal gyrus, dorsolateral part	96	-22	68	10	7,19
	96	-28	62	18	6,18
Right superior frontal gyrus, dorsolateral part	1	16	68	12	5,01
	2	16	62	26	5,02
	1241	18	56	2	5,92
Left superior frontal gyrus, medial part	141	-2	70	12	6,59
	141	0	66	22	6,9
	6	-12	56	16	5,04
Right superior frontal gyrus, medial part	141	10	72	8	5,7
	141	10	68	18	5,84
	1241	10	60	4	5,4
Left superior frontal gyrus, orbital part	52	-26	58	-4	5,96
Left superior frontal gyrus, medial orbital part	1	-14	60	-2	4,97
	1241	-10	44	-8	6,22
Right superior frontal gyrus, medial orbital part	1241	4	56	-10	5,27
	1241	4	42	-4	7,08
Right middle frontal gyrus	3	32	54	30	5,1
	1	36	46	8	4,96
Right inferior frontal gyrus, triangular part	55	42	32	2	5,01
	55	46	28	6	5,4
	55	50	22	2	5,85
Left gyrus rectus	1241	-6	34	-20	5,04
Right gyrus rectus	1241	6	48	-14	5,57
Left anterior cingulate and paracingulate gyri	1241	-4	44	10	5,8
	1241	-6	40	-6	6,57
	10	-8	24	26	5,33
Right anterior cingulate and paracingulate gyri	8	4	34	22	5,16
Left median cingulate and paracingulate gyri	4	-8	14	36	5,22
Left insula	4	-34	18	4	5,13
Right insula	31	36	28	2	5,11
Right precuneus	108	10	-66	30	6,39
Left cuneus	78	-8	-72	28	5,68
Right inferior temporal gyrus	3	32	8	-42	5,23

	20	48	6	-34	6,38
	4	48	-2	-40	5,46
Left caudate nucleus	11	-16	20	6	5,42
Right caudate nucleus	2	14	22	10	5,01
	9	10	20	12	5,22

Note. $p < 0.05$, corrected for multiple comparisons according to the family-wise error approach (FWE-corrected). Coordinates are in millimeters and in the MNI standard space.

Table 18 - Brain regions of IC 8 which were found significant in the contrast SH group < NoH group

Region	Cluster size	x	y	z	Z score
Left precentral gyrus	290	-54	12	42	6,31
	290	-46	8	50	6,36
	3	-42	0	64	5,47
Left superior frontal gyrus, dorsolateral part	1	-14	54	44	5,05
	344	-16	42	54	6,22
	344	-16	28	62	5,45
Left superior frontal gyrus, medial part	27	2	56	40	5,22
	344	-6	26	62	5,3
Right superior frontal gyrus, medial part	27	2	52	46	5,13
	344	4	34	60	6,98
	344	4	26	62	6,02
Right superior frontal gyrus, orbital part	33	16	32	-22	5,3
	33	12	26	-22	5,49
Left middle frontal gyrus	1	-50	32	34	5,09
	290	-40	10	58	6,09
	290	-38	8	62	6,04
Right middle frontal gyrus	7	48	46	20	5,13
	7	52	44	16	5,24
Right middle frontal gyrus, orbital part	57	46	52	-14	7,35
Left inferior frontal gyrus, triangular part	2	-52	30	32	5,51
	1	-54	28	30	5,26
Left supplementary motor area	344	-10	18	64	5,69
	344	-10	12	66	5,52
	344	-4	10	68	5,01
Right supplementary motor area	344	4	18	64	6,32
Left inferior temporal gyrus	7	-42	-26	-20	5,22
	1	-52	-34	-26	5,12

Note. $p < 0.05$, corrected for multiple comparisons according to the family-wise error approach (FWE-corrected). Coordinates are in millimeters and in the MNI standard space.

Appendix III

Table 1 **Self pain: controls > responders**

Abbreviation: FWE = family wise error correction. k = cluster size
*SVC = small volume correction. *placebo-induced reductions ROIs, **placebo-induced increases ROIs*

Region	Side	MNI coordinates			Z	k	pvalue (corrected)
Superior orbitofrontal gyrus	L	-14	68	-10	5.68	378	0.05 cluster-level
	L	-12	36	-26	4.46	418	0.05 cluster-level
Middle orbitofrontal gyrus	R	28	58	-16	5.76	642	0.05 FWE
Medial orbitofrontal gyrus	R	4	42	-14	3.83	41	0.002 SVC**
(vmPFC)	R	4	40	-10	3.75		0.003 SVC**
Superior frontal gyrus	R	-28	2	66	3.30	1295	0.05 FWE
Superior medial frontal gyrus	R	10	32	60	3.45	1295	0.05 FWE
Rectal gyrus		0	38	-18	5.49	418	0.05 cluster-level
	R	2	34	-18	4.47	47	0.000 SVC**
	L	-2	36	-14	4.20		0.001 SVC**
	R	2	36	-14	4.82	57	0.000 SVC**
	R	4	42	-14	3.83	41	0.002 SVC**
Superior temporal pole	R	48	30	-20	4.46	335	0.05 cluster-level
	R	44	28	-22	4.29		0.05 cluster-level
	R	56	16	-20	3.56		0.05 cluster-level
	R	52	22	-22	3.46		0.05 cluster-level
Middle temporal gyrus	L	-60	-32	0	6.39	1667	0.05 FWE
	L	-50	-28	-6	4.89		0.05 FWE
	R	54	-32	-12	5.06	389	0.05 cluster-level
	R	72	-24	-10	3.93		0.05 cluster-level
	R	62	4	-18	3.20	335	0.05 cluster-level
Supplementary motor area	R	4	6	76	6.36	1295	0.05 FWE
	R	14	18	70	6.12		0.05 FWE
	R	0	2	76	5.71		0.05 FWE
	L	-8	12	74	5.25		0.05 FWE
	L	-6	0	78	5.22		0.05 FWE
Paracentral lobule	L	-2	-14	76	3.36		0.05 FWE
Postcentral gyrus (S1)	R	16	-38	66	3.14	8	0.018 SVC*
Anterior cingulate cortex (rostral part)	L	-2	30	22	3.12	798	0.05 FWE
	L	-4	34	18	2.89	12	0.035 SVC**
	R	2	22	18	3.03	21	0.025 SVC**

	L	-2	32	18	3.01	24	0.026 SVC**
(dorsal part)	R	2	28	30	3.86	202	0.002 SVC**
Middle cingulate cortex	L	-4	2	26	5.74		0.05 FWE
	R	8	10	26	5.17		0.05 FWE
	R	6	28	32	4.43		0.05 FWE
Inferior frontal gyrus	L	-46	30	-8	2.94	24	0.031 SVC**
(pars orbitalis)	L	-50	26	-8	2.92		0.032 SVC**
	R	50	28	-8	4.82	10	0.023 SVC**
Anterior insular cortex	L	-46	12	-18	3.20	15	0.015 SVC*
	L	-42	10	12	2.80	7	0.044 SVC*
Posterior insular cortex	L	-44	-14	2	3.17	36	0.017 SVC*
	L	-44	-14	0	3.11	14	0.020 SVC*
Precuneus	L	-6	-66	56	4.51	361	0.05 cluster-level
	R	8	-64	58	4.01		0.05 cluster-level
Fusiform gyrus	L	-24	-76	-4	4.60	1663	0.05 FWE
Inferior occipital gyrus	R	32	-88	-12	5.82	878	0.05 FWE
Calcarine gyrus	L	-4	-96	-8	5.06	1663	0.05 FWE
Thalamus	L	-20	-24	2	5.08	780	0.05 FWE
	L	-18	-24	14	3.75		0.05 FWE
	L	-10	22	-2	3.68	7	0.001 SVC**
Hippocampus	L	-24	-38	2	4.35		0.05 FWE
Pallidum	L	-18	-2	-2	3.68		0.05 FWE
Putamen	L	-26	-14	-2	3.50	24	0.002 SVC*
Amygdala	L	-24	2	-8	3.43	33	0.002 SVC*
	L	-18	10	-14	3.42	780	0.05 FWE
	L	-22	6	-10	3.20	33	0.005 SVC*

Table 2 **Self pain: responders > controls**

Abbreviation: FWE = family wise error correction. k = cluster size
*SVC = small volume correction. *placebo-induced reductions ROIs, **placebo-induced increases ROIs*

Region	Side	MNI coordinates			Z	k	pvalue (corrected)
Middle frontal gyrus	R	26	26	40	3.40	48	0.021 SVC**
(DLPFC)	R	28	24	38	3.08	14	0.049 SVC**
Anterior cingulate cortex (rostral part)	L	-12	34	-6	3.29	10	0.054 SVC**
Anterior insular cortex	R	36	28	10	4.31	56	0.000 SVC**
	L	-32	30	14	3.29	15	0.012 SVC**
	R	34	22	10	3.12	11	0.019 SVC**
Inferior frontal gyrus	R	42	28	16	4.70	503	0.05 cluster-level
(pars triangularis)	R	38	24	10	3.69	15	0.003 SVC**
Inferior temporal gyrus	R	54	-50	12	4.53	341	0.05 cluster-level
Precuneus	L	-16	-52	20	4.23	1058	0.05 FWE
Calcarine gyrus	L	-12	-66	16	4.70		0.05 FWE
	L	-24	-54	14	4.30		0.05 FWE
Cerebellum	R	28	-74	-38	6.66	1533	0.05 FWE
	L	-48	-44	-42	5.66		0.05 FWE
	L	-42	-66	-42	4.98		0.05 FWE
	L	-52	-42	-34	3.21		0.05 FWE
	R	54	-56	-46	5.45	1341	0.05 FWE
	R	36	-48	-50	5.05		0.05 FWE
	R	26	-70	-40	4.92		0.05 FWE
Periaqueductal gray matter	R	2	-32	-10	4.15	78	0.000 SVC**
Ventral striatum	R	6	-4	12	2.90	6	0.011 SVC**

Table 3 **Self no-pain: controls > responders**

Abbreviation: FWE = family wise error correction. k = cluster size
*SVC = small volume correction. *placebo-induced reductions ROIs, **placebo-induced increases ROIs*

Region	Side	MNI coordinates			Z	k	pvalue (corrected)
Middle frontal gyrus (DLPFC)	L	-50	30	36	3.44	32	0.018 SVC**
Inferior frontal gyrus (pars orbitalis)	R	36	36	-8	3.76	338	0.05 cluster-level
Superior temporal gyrus	L	-50	-10	4	3.41	2032	0.05 FWE
	R	64	-12	4	3.81	554	0.05 FWE
	R	66	-32	12	3.65		0.05 FWE
Middle temporal gyrus	L	-62	-32	0	5.12	2032	0.05 FWE
	L	-58	-18	-6	4.93		0.05 FWE
	R	60	-50	16	3.61	554	0.05 FWE
Anterior insular cortex	R	42	12	8	2.83	15	0.003 SVC**
Middle insular cortex	R	42	12	8	2.83	22	0.041 SVC*
Posterior insular cortex	L	-44	-14	0	3.05	144	0.023 SVC*
	L	-46	-10	-4	2.71		0.047 SVC*
	L	-34	-14	-2	2.85	175	0.039 SVC*
Rolandic operculum	L	-54	-6	14	3.37	2032	0.05 FWE
Inferior occipital gyrus	R	34	-86	-12	3.64	334	0.05 cluster-level
Thalamus	L	-10	-22	-2	3.30	15	0.003 SVC**
Putamen	L	-28	-14	-2	3.49	52	0.002 SVC*

Table 4 **Self no-pain: responders > controls**

Abbreviation: FWE = family wise error correction. k= cluster size

*SVC = small volume correction. *placebo-induced reductions ROIs, **placebo-induced increases ROIs*

Region	Side	MNI coordinates			Z	k	pvalue (corrected)
Inferior frontal gyrus (pars triangularis)	R	32	28	14	3.33	21	0.011 SVC**
Periaqueductal gray matter	R	2	-32	-8	4.15	8	0.016 SVC**

Table 5 **Other pain: controls > responders**

Abbreviation: FWE = family wise error correction. k= cluster size
*SVC = small volume correction. *placebo-induced reductions ROIs, **placebo-induced increases ROIs*

Region	Side	MNI coordinates			Z	k	pvalue (corrected)
Medial orbitofrontal gyrus (Rectal gyrus)	L	-4	38	-20	2.76	31	0.048 SVC**
Superior temporal gyrus	L	-46	-12	-8	3.21	2440	0.05 FWE
	R	42	-38	8	3.33	373	0.05 cluster-level
Middle temporal gyrus	L	-54	-22	-8	5.47	2440	0.05 FWE
	L	-60	-32	-8	5.28		0.05 FWE
	R	42	-70	12	4.02	1302	0.05 FWE
	R	62	-52	16	4.31	373	0.05 cluster-level
Posterior insular cortex	L	-48	-10	2	2.86	18	0.038 SVC*
	L	-50	-6	6	3.00		0.051 SVC*
Precentral gyrus	L	-56	-10	52	4.07	602	0.05 FWE
Postcentral gyrus (S1)	L	-64	-4	30	4.33		0.05 FWE
	L	-48	-8	38	3.73		0.05 FWE
	L	-56	-24	56	3.57		0.05 FWE
	L	-48	-14	26	3.17		0.05 FWE
Precuneus	L	-6	-62	54	4.53	656	0.05 FWE
	L	-14	-54	46	4.23		0.05 FWE
	L	-10	-56	56	3.20		0.05 FWE
Cuneus	R	10	-80	24	4.41	390	0.05 FWE
Fusiform gyrus	L	-40	-50	-10	4.32	2440	0.05 FWE
	R	38	-22	-30	5.39	768	0.05 FWE
	R	36	-36	-14	4.69		0.05 FWE
	R	40	-50	-10	4.09		0.05 FWE
	R	28	-68	-2	3.74	1302	0.05 FWE
Lingual gyrus	R	22	-76	-2	4.81	332	0.05 cluster-level
	L	-18	-86	-10	4.03		0.05 cluster-level
Calcarine gyrus	R	14	-84	8	3.81	390	0.05 cluster-level
Superior occipital gyrus	R	22	-80	44	3.87	332	0.05 cluster-level
Middle occipital gyrus	R	30	-84	32	3.30		0.05 cluster-level
Inferior occipital gyrus	R	30	-86	-12	4.57	1302	0.05 FWE
Thalamus	L	-10	-22	-2	3.33	6	0.003 SVC**
Putamen	L	-28	-14	-2	2.92	9	0.011 SVC*
Amygdala	L	-24	-10	-8	3.85	36	0.001 SVC*

Table 6 **Other pain: responders > controls**

Abbreviation: FWE = family wise error correction. k = cluster size
*SVC = small volume correction. *placebo-induced reductions ROIs, **placebo-induced increases ROIs*

Region	Side	MNI coordinates			Z	k	pvalue (corrected)
Middle orbitofrontal gyrus	L	-12	36	-24	2.98	31	0.028 SVC**
– Rectal gyrus	L	-4	38	-20	2.76		0.012 SVC**
Thalamus	L	-10	-22	-2	3.33	6	0.003 SVC**

Table 7 **Other no-pain: controls > responders.**

Abbreviation: FWE = family wise error correction. k = cluster size
*SVC = small volume correction. *placebo-induced reductions ROIs, **placebo-induced increases ROIs*

Region	Side	MNI coordinates			Z	k	pvalue (corrected)
Posterior insular cortex	L	-46	-16	-2	2.82	72	0.041 SVC*
Rolandic operculum (S2)	L	-54	-8	10	3.03	41	0.025 SVC*
	L	-50	-6	6	2.72	15	0.052 SVC*

Table 8 **Other no-pain: responders > controls**

Abbreviation: FWE = family wise error correction. k = cluster size
*SVC = small volume correction. *placebo-induced reductions ROIs, **placebo-induced increases ROIs*

Region	Side	MNI coordinates			Z	k	pvalue (corrected)
Inferior frontal gyrus	R	36	24	14	3.51	145	0.006 SVC**
(pars triangularis)	R	40	26	14	3.50		0.006 SVC**
Putamen	R	28	16	-6	3.17	8	0.005 SVC*

Table 9 **Self pain: controls > non-responders**

Abbreviation: FWE = family wise error correction. k = cluster size
*SVC = small volume correction. *placebo-induced reductions ROIs, **placebo-induced increases ROIs*

Region	Side	MNI coordinates			Z	k	pvalue (corrected)
Anterior insular cortex	L	-38	12	10	2.78	10	0.046 SVC*
Middle occipital gyrus	R	24	-92	-6	4.38	711	0.05 FWE
Inferior occipital gyrus	R	32	-84	-6	4.60		0.05 FWE
Calcarine gyrus	L	-10	-100	-4	4.71		0.05 FWE

Table 10 **Self pain: non-responders > controls**

Abbreviation: FWE = family wise error correction. k = cluster size
*SVC = small volume correction. *placebo-induced reductions ROIs, **placebo-induced increases ROIs*

Region	Side	MNI coordinates			Z	k	pvalue (corrected)
Superior frontal gyrus	R	20	22	44	4.83	2571	0.05 FWE
	R	18	34	36	4.62		0.05 FWE
	R	18	42	36	4.34		0.05 FWE
	R	14	60	24	4.84	355	0.05 cluster-level
Superior orbitofrontal gyrus	R	24	42	-14	3.52	610	0.05 FWE
Superior medial frontal gyrus	R	2	32	50	4.74	2571	0.05 FWE
	L	-8	38	40	3.84		0.05 FWE
Middle frontal gyrus	R	44	32	24	4.37		0.05 FWE
(DLPFC)	R	32	20	36	4.39	604	0.001 SVC**
	L	-34	18	32	3.24	237	0.032 SVC**
Anterior cingulate cortex	R	12	48	20	3.27	26	0.013 SVC**
(rostral part)	R	10	36	2	3.42	10	0.008 SVC**
	R	12	32	6	4.35	35	0.000 SVC**
	R	14	36	8	3.55	13	0.005 SVC**
	L	-12	34	-2	3.20	10	0.015 SVC**
Inferior frontal gyrus	L	-40	28	10	3.17	13	0.017 SVC**
– anterior insular cortex	L	-42	28	16	4.05	126	0.001 SVC**
	R	44	32	-2	2.84	10	0.039 SVC**
Anterior insular cortex	R	36	10	-6	3.03	12	0.024 SVC*
Middle insular cortex	L	-36	-4	-4	2.96	37	0.029 SVC*
Inferior frontal gyrus (pars opercularis)	R	52	22	30	4.76	2571	0.05 FWE
Supplementary motor area	R	4	20	58	4.50	2571	0.05 FWE
Lingual gyrus	L	-18	-70	-10	5.31	1229	0.05 FWE
	L	-26	-52	-8	5.21		0.05 FWE
	L	-20	-64	4	4.87		0.05 FWE
Cerebellum	L	-40	-70	-50	> 8	5315	0.05 FWE
	L	-36	-68	-48	> 8		0.05 FWE
	R	52	-64	-44	7.56		0.05 FWE
	L	-48	-74	-40	7.24		0.05 FWE
	R	8	-72	-42	6.57		0.05 FWE
	R	4	-84	-40	5.88		0.05 FWE
	R	38	-40	-46	5.73		0.05 FWE
	R	28	-66	-44	5.63		0.05 FWE

Parahippocampal gyrus	L	-14	-2	18	5.90	827	0.05 FWE
Putamen	L	24	-4	8	3.61	2571	0.05 FWE
Amygdala	R	26	10	-18	3.21	621	0.05 FWE
	R	20	-2	-16	4.68		0.05 FWE
	L	-28	2	-16	4.88	48	0.000 SVC*
	L	-24	-4	-14	4.00	24	0.000 SVC*
	L	-28	-4	-14	3.68		0.001 SVC*

Table 11 **Self no-pain: controls > non-responders**

Abbreviation: FWE = family wise error correction. k = cluster size
*SVC = small volume correction. *placebo-induced reductions ROIs, **placebo-induced increases ROIs*

Region	Side	MNI coordinates			Z	k	pvalue (corrected)
Middle frontal gyrus	L	-40	30	46	3.35	44	0.024 SVC**
(DLPFC)	L	-44	32	44	3.19		0.037 SVC**
	L	-48	32	38	3.12		0.044 SVC**
Anterior insular cortex	L	-38	8	10	4.08	120	0.001 SVC*
(rostral part)	L	-34	10	4	3.29	21	0.012 SVC*
Middle insular cortex	L	-40	4	6	3.24	16	0.014 SVC*
Middle occipital gyrus	L	-20	-102	8	4.61	1622	0.05 FWE
Inferior occipital gyrus	L	-22	-94	-8	4.78		0.05 FWE
	R	32	-86	-6	4.29		0.05 FWE
	L	-24	-98	-10	3.62		0.05 FWE
Calcarine gyrus	L	-10	-100	-4	5.83		0.05 FWE
Fusiform gyrus	L	-24	-80	-8	3.90		0.05 FWE

Table 12 **Self no-pain: non-responders > controls**

Abbreviation: FWE = family wise error correction (cluster level). k = cluster size
*SVC = small volume correction. *placebo-induced reductions ROIs, **placebo-induced increases ROIs*

Region	Side	MNI coordinates			Z	k	pvalue (corrected)
Middle frontal gyrus (DLPFC)	R	30	28	38	3.45	1001	0.05 FWE
	L	-24	34	34	3.16	13	0.040 SVC**
	L	-34	16	32	3.11	85	0.045 SVC**
Anterior cingulate cortex	L	-14	38	0	3.19	14	0.016
	R	14	32	8	3.18	13	0.016
Inferior frontal gyrus	R	52	24	30	5.06	1001	0.05 FWE
(pars triangularis)	L	-42	28	16	4.23	140	0.024 SVC**
	R	44	28	20	3.41	13	0.008 SVC**
	L	-42	28	10	3.21	10	0.015 SVC**
(pars opercularis)	R	46	8	20	3.28	1001	0.05 FWE
Anterior insular cortex	R	28	10	-16	3.96	316	0.05 cluster-level
Lingual gyrus	L	-26	-54	-6	5.19	567	0.05 FWE
Calcarine gyrus	L	-18	-70	10	4.63		0.05 FWE
Cerebellum	L	-40	-70	-50	> 8	4584	0.05 FWE
	R	28	-66	-44	6.32		0.05 FWE
	R	38	-52	-44	6.00		0.05 FWE
	R	6	-82	-40	5.72		0.05 FWE
	R	8	-76	-40	5.58		0.05 FWE
	L	-50	-72	-40	5.50		0.05 FWE
	R	52	-66	-44	5.46		0.05 FWE
	L	-56	-60	-42	5.00		0.05 FWE
	R	20	-58	-50	4.96		0.05 FWE
	L	-40	-42	-48	3.69		0.05 FWE
Parahippocampal gyrus	L	-12	-4	-16	5.05	328	0.05 cluster-level
	R	14	-4	-18	4.40	316	0.05 cluster-level
Amygdala	R	24	0	-14	3.56	70	0.001 SVC*
	L	24	-4	-14	3.21	12	0.001 SVC*
	L	-22	2	-14	3,21	17	0.001 SVC*

Table 13 **Other pain: controls > non-responders**

Abbreviation: FWE = family wise error correction (cluster level). k = cluster size
*SVC = small volume correction. *placebo-induced reductions ROIs, **placebo-induced increases ROIs*

Region	Side	MNI coordinates			Z	k	pvalue (corrected)
Middle frontal gyrus	L	-40	30	46	3.38	123	0.022 SVC**
(DLPFC)	L	-52	26	38	3.06		0.052 SVC**
	L	-40	28	44	3.12	39	0.054 SVC**
Medial orbitofrontal gyrus	R	10	30	-10	3.55	36	0.005 SVC**
(vmPFC)							
Anterior insular cortex	L	-46	8	8	2.71	13	0.054 SVC*
Inferior occipital gyrus	R	30	-82	-8	3.60	1582	0.05 FWE
Calcarine gyrus	L	-10	-102	-4	6.47		0.05 FWE
Fusiform gyrus	R	40	-66	-20	3.38		0.05 FWE
Lingual gyrus	R	20	-94	-8	4.82		0.05 FWE
Cerebellum	R	32	-72	-20	3.66		0.05 FWE
	R	26	-60	-20	3.61		0.05 FWE

Table 14 **Other pain: non-responders > controls**

Abbreviation: FWE = family wise error correction (cluster level). k = cluster size
*SVC = small volume correction. *placebo-induced reductions ROIs, **placebo-induced increases ROIs*

Region	Side	MNI coordinates			Z	k	pvalue (corrected)
Middle frontal gyrus (DLPFC)	L	-26	32	34	3.12	32	0.044 SVC**
Inferior frontal gyrus	L	-40	26	14	4.51	155	0.000 SVC**
(pars triangularis)	L	-42	28	10	3.35	10	0.010 SVC**
Lingual gyrus	L	-26	-54	-6	4.57	798	0.05 FWE
Calcarine gyrus	L	-18	-70	10	4.75		0.05 FWE
Fusiform gyrus	L	-20	-42	-10	4.65	334	0.05 cluster-level
Cerebellum	L	-24	-80	-46	> 8	1600	0.05 FWE
	L	-56	-58	-42	4.64		0.05 FWE
	R	44	-56	-46	5.87	669	0.05 FWE
	R	52	-66	-44	4.87		0.05 FWE
	R	36	-48	-44	4.71		0.05 FWE
	R	20	-68	-46	4.65	334	0.05 cluster-level
Amygdala	R	24	-6	-14	4.28	26	0.000 SVC*
	R	24	0	-14	3.31	27	0.003 SVC*

Table 15 **Other no-pain: non-responders > controls**

Abbreviation: FWE = family wise error correction (cluster level). k = cluster size
*SVC = small volume correction. *placebo-induced reductions ROIs, **placebo-induced increases ROIs*

Region	Side	MNI coordinates			Z	k	pvalue (corrected)
Superior frontal gyrus	R	18	40	36	6.06	7771	0.05 FWE
	R	22	16	42	5.11		0.05 FWE
	L	-26	34	36	5.04		0.05 FWE
	R	18	56	22	4.47		0.05 FWE
	L	-14	48	22	3.62		0.05 FWE
Superior medial frontal gyrus	L	-6	42	38	4.38		0.05 FWE
	L	-4	26	42	3.42		0.05 FWE
Middle frontal gyrus	R	32	42	12	3.80		0.05 FWE
(DLPFC)	L	-26	34	36	5.04	880	0.000 SVC**
Superior orbitofrontal gyrus	L	-24	52	-4	3.97		0.05 FWE
Middle orbitofrontal gyrus	R	32	58	-4	4.34	8268	0.05 FWE
	R	34	56	-2	4.30	7771	0.05 FWE
	R	28	44	-12	3.91		0.05 FWE
	L	-34	44	-8	3.19		0.05 FWE
Medial orbitofrontal gyrus	R	6	54	-10	2.95	54	0.030 SVC**
(vmPFC)	R	8	54	-14	2.89		0.035 SVC**
Inferior frontal gyrus	R	-42	28	16	6.18	7771	0.05 FWE
(pars triangularis)	L	-36	14	28	4.74		0.05 FWE
	R	44	32	20	4.56		0.05 FWE
	L	-50	38	8	4.05		0.05 FWE
	L	-42	28	16	6.19	320	0.000 SVC**
	L	-42	28	10	4.99	188	0.000 SVC**
	L	-40	32	12	4.76		0.000 SVC**
	L	-46	38	6	3.84		0.002 SVC**
	L	-36	40	-2	3.15		0.018 SVC**
	L	-42	28	8	3.86	28	0.002 SVC**
	L	-46	24	10	3.72		0.003 SVC**
	R	44	30	8	4.20	85	0.001 SVC**
(pars orbitalis)	L	-34	42	-16	3.50		0.05 FWE
	L	-36	40	-2	3.14		0.05 FWE
(pars opercularis)	R	46	16	36	5.99		0.05 FWE
Anterior insular cortex	L	-26	32	6	3.45	21	0.007 SVC**
	L	-32	36	6	3.15	188	0.018 SVC**
	R	42	-6	-8	3.04	135	0.024 SVC*

Anterior cingulate cortex	L	-14	34	24	2.94		0.031 SVC**
(rostral part)	R	14	32	8	3.56	84	0.005 SVC**
	R	12	34	6	3.38	23	0.009 SVC**
(dorsal part)	L	-12	24	30	2.98	75	0.028 SVC**
Middle insular cortex	L	-34	-4	-8	3.91	30	0.002 SVC*
	R	36	2	-8	2.82	161	0.042 SVC*
	R	44	-6	-8	3.16	176	0.017 SVC*
Posterior insular cortex	L	-34	-14	-2	3.05	177	0.024 SVC*
Precentral gyrus	L	-48	8	40	3.80	7771	0.05 FWE
Inferior temporal gyrus	R	34	0	-42	4.75	3109	0.05 FWE
	R	46	0	-36	3.71	3745	0.05 FWE
Supramarginal gyrus	L	-50	-42	36	3.98	631	0.05 FWE
Middle temporal gyrus	L	-58	-56	22	4.04		0.05 FWE
	L	-54	-54	2	3.25		0.05 FWE
Fusiform gyrus	R	32	-10	-32	4.28	3745	0.05 FWE
	R	34	-24	-22	3.33		0.05 FWE
	R	30	-54	-6	4.47	8268	0.05 FWE
Lingual gyrus	R	14	-52	-8	4.41		0.05 FWE
	L	-26	-52	-8	5.92	3109	0.05 FWE
	L	-20	-64	2	4.95		0.05 FWE
	L	-20	-42	-8	4.71		0.05 FWE
Precuneus		0	-70	42	4.53		0.05 FWE
	L	-2	-60	20	4.28		0.05 FWE
Cuneus	L	-10	-80	40	3.15		0.05 FWE
Superior occipital gyrus	L	-12	-92	32	4.89		0.05 FWE
Calcarine gyrus	L	-18	-68	12	5.05		0.05 FWE
Cerebellum	L	-40	-70	-50	> 8	8268	0.05 FWE
	R	44	-56	-44	7.22		0.05 FWE
	R	50	-68	-44	6.62		0.05 FWE
	R	40	-46	-42	6.15		0.05 FWE
	L	-50	-72	-40	6.11		0.05 FWE
	R	30	-68	-40	5.88		0.05 FWE
	L	-20	-88	-30	5.21		0.05 FWE
	R	6	-86	-38	5.02		0.05 FWE
	L	-20	-48	-40	4.61		0.05 FWE
	R	12	-70	-36	4.56		0.05 FWE
	L	-56	-58	-42	3.98		0.05 FWE
	R	16	-46	-20	3.86		0.05 FWE
	L	-18	-54	-50	3.18		0.05 FWE

	R	6	-56	-50	7.56	361	0.05 cluster-level
Vermis	L	-4	-60	0	3.82	3109	0.05 FWE
Hippocampus	R	22	-6	-16	5.55	3745	0.05 FWE
Pallidum	L	-16	2	4	3.37		0.05 FWE
Ventral striatum	L	-8	2	-4	2.68	8	0.020 SVC**
Putamen	R	24	16	-6	5.62	3745	0.05 FWE
	R	26	-4	4	4.15		0.05 FWE
	L	-20	18	2	3.98		0.05 FWE
Amygdala	L	-30	-4	-16	5.02		0.05 FWE
	R	24	-6	-14	5.39	81	0.000 SVC*

Table 16 **Self pain: non-responders > responders**

Abbreviation: FWE = family wise error correction (cluster level). k = cluster size
*SVC = small volume correction. *placebo-induced reductions ROIs, **placebo-induced increases ROIs*

Region	Side	MNI coordinates			Z	k	pvalue (corrected)
Superior orbitofrontal gyrus	R	26	52	-2	4.47	1120	0.05 FWE
	L	-14	68	-10	5.24	587	0.05 FWE
	L	-20	70	-2	4.07		0.05 FWE
Middle orbitofrontal gyrus	R	30	54	-16	5.54	1120	0.05 FWE
Superior medial frontal gyrus	R	8	30	56	4.79	7292	0.05 FWE
	L	-8	72	2	3.38	587	0.05 FWE
Rectal gyrus		0	36	-18	5.05	348	0.05 FWE
Superior frontal gyrus	R	20	60	26	4.96	7292	0.05 FWE
	R	18	20	48	3.95		0.05 FWE
	R	18	34	48	3.52		0.05 FWE
Middle frontal gyrus (DLPFC)	L	-26	48	38	5.34	381	0.05 FWE
	L	-30	56	14	4.06	587	0.05 FWE
	L	-28	38	34	3.05	11	0.044 SVC**
	R	42	40	24	3.14	116	0.042 SVC**
	R	36	14	38	3.75	83	0.007 SVC**
	R	42	38	24	3.13	37	0.044 SVC**
Anterior cingulate cortex	R	10	26	32	5.44	196	0.000 SVC**
(dorsal part)	R	2	28	30	3.94	137	0.001 SVC**
	L	-10	24	32	3.39		0.009 SVC**
	L	-2	34	-14	3.93	26	0.001 SVC**
(rostral part)	R	14	36	6	3.58	73	0.005 SVC**
	R	8	36	2	3.53	123	0.006 SVC**
	R	10	38	4	3.31	22	0.011 SVC**
Middle cingulate cortex	R	8	28	34	5.46	7292	0.05 FWE
	L	-12	16	40	4.82		0.05 FWE
Inferior frontal gyrus	R	48	30	-6	3.78	3.78	0.003 SVC**
(pars orbitalis)	L	-44	30	-4	3.42	91	0.008 SVC**
Anterior insular cortex	L	-38	2	-2	3.21	11	0.015 SVC*
	L	-34	2	-8	3.91	57	0.002 SVC*
	L	-36	2	-6	3.88	48	0.002 SVC**
	R	48	14	-8	2.87	96	0.037 SVC**
	R	40	12	-4	2.87	12	0.037 SVC**
Middle insular cortex	L	-34	-2	-6	4.53	7292	0.05 FWE
	L	-32	-2	-8	4.49	87	0.000 SVC*

	L	-36	-2	-6	4.26	159	0.000 SVC*
	L	-36	-2	-2	3.77	141	0.003 SVC*
Posterior insular cortex	L	-40	-18	0	4.48	314	0.006 SVC*
	L	-44	-14	2	3.93	141	0.001 SVC*
Rolandic operculum (S2)	R	44	-8	20	3.02	11	0.025 SVC*
Precentral gyrus	R	44	10	50	3.97	7292	0.05 FWE
Middle temporal gyrus	L	-46	-22	0	5.66	1069	0.05 FWE
	L	-62	-32	0	5.42		0.05 FWE
	L	-60	24	0	5.25		0.05 FWE
Precuneus	R	12	-78	48	4.70	858	0.05 FWE
	L	-6	-62	58	3.90		0.05 FWE
	R	2	-68	48	3.58		0.05 FWE
Superior parietal gyrus	L	-22	-72	52	3.93		0.05 FWE
Lingual gyrus	L	-18	-76	4	7.22	739	0.05 FWE
	R	28	-64	0	5.52	405	0.05 cluster-level
Inferior occipital gyrus	R	32	-90	-16	4.81	437	0.05 cluster-level
Cerebellum	L	-40	-70	-50	7.41	517	0.05 cluster-level
	L	-24	-90	-24	5.73	692	0.05 FWE
Thalamus	L	-18	-24	12	4.81	7292	0.05 FWE
	L	-20	-18	8	4.54		0.05 FWE
Pallidum	R	22	-2	6	4.62		0.05 FWE
	L	-18	0	-2	4.09		0.05 FWE
Ventral striatum	L	-12	0	-4	3.15	7	0.003 SVC**
Putamen	L	-20	6	12	4.02	7292	0.05 FWE
Amygdala	L	-20	6	-16	5.98		0.05 FWE
	R	22	8	-16	5.38		0.05 FWE
	L	-22	4	-14	5.64	81	0.000 SVC*
	R	24	6	-16	5.19	81	0.000 SVC*
	L	-24	-2	-12	4.90	81	0.000 SVC*
	R	24	-2	-12	3.91	25	0.000 SVC*

Table 17 **Self pain: responders > non-responders**

Abbreviation: FWE = family wise error correction (cluster level). k = cluster size
*SVC = small volume correction. *placebo-induced reductions ROIs, **placebo-induced increases ROIs*

Region	Side	MNI coordinates			Z	k	pvalue (corrected)
Anterior cingulate cortex (rostral part)	R	14	34	-8	4.01	21	0.001 SVC**
Inferior frontal gyrus	R	36	24	12	4.72	277	0.000 SVC**
	R	38	24	10	4.49	69	0.000 SVC**
	R	36	28	10	4.18	45	0.001 SVC**
	R	40	26	10	4.15		0.001 SVC**
	R	40	24	8	3.69	12	0.003 SVC**
Anterior insular cortex	R	34	24	6	3.54	21	0.006 SVC**
	L	-34	16	12	3.03	10	0.024 SVC**
Middle temporal pole	R	36	4	-34	3.87	373	0.05 cluster-level
Inferior temporal gyrus	R	52	-54	-12	4.11	2817	0.05 FWE
	R	46	-58	-16	4.08		0.05 FWE
Fusiform gyrus	R	20	-34	-18	4.39		0.05 FWE
Inferior occipital gyrus	R	32	-74	-8	3.71		0.05 FWE
Cerebellum	R	8	-66	-12	4.88		0.05 FWE
	R	16	-56	-18	4.03		0.05 FWE
	R	42	-46	-30	3.53		0.05 FWE
	R	50	-40	-34	3.14		0.05 FWE
	L	-40	-44	-32	4.68	421	0.05 cluster-level
	L	-46	-42	-40	4.49		0.05 cluster-level
Thalamus	R	2	-22	-2	3.43	20	0.002 SVC**
	L	-2	-22	-2	3.25	8	0.004 SVC**
Periaqueductal gray matter	R	2	-32	-10	4.66	81	0.000 SVC**
	R	2	-34	-16	4.53		0.000 SVC**

Table 18 **Self no-pain: non-responders > responders**

Abbreviation: FWE = family wise error correction (cluster level). k = cluster size
*SVC = small volume correction. *placebo-induced reductions ROIs, **placebo-induced increases ROIs*

Region	Side	MNI coordinates			Z	k	**pvalue (corrected)**
Middle frontal gyrus	R	56	24	34	4.68	778	0.000 SVC**
(DLPFC)	L	-34	16	32	3.09	60	0.048 SVC**
Middle orbitofrontal gyrus	R	36	52	-2	4.42	475	0.05 cluster-level
Superior frontal gyrus	R	20	16	42	3.79	853	0.05 FWE
Inferior frontal gyrus	R	34	12	36	5.51		0.05 FWE
(pars opercularis)	R	56	26	34	4.76		0.05 FWE
	R	44	10	24	3.77		0.05 FWE
(pars triangularis)	L	-44	28	4	3.07	52	0.022 SVC**
	L	-44	30	14	2.92		0.033 SVC**
Anterior cingulate cortex	R	12	28	32	3.24	13	0.014 SVC**
(rostral part)	R	12	36	4	3.11	22	0.020 SVC**
Anterior insular cortex	R	44	20	-6	3.51	529	0.05 cluster-level
	R	36	10	-6	3.43	81	0.008 SVC*
	R	42	16	-6	3.36		0.010 SVC*
	R	38	14	-6	3.32		0.011 SVC*
Middle temporal gyrus	L	-60	-34	-2	4.54	878	0.05 FWE
	L	-60	-20	-2	4.25		0.05 FWE
Inferior temporal gyrus	L	-70	-24	-18	3.91	475	0.05 FWE
Precuneus	R	12	-46	16	3.32	775	0.05 FWE
Lingual gyrus	L	-18	-76	4	6.76	1159	0.05 FWE
	R	28	-66	0	5.76	775	0.05 FWE
Calcarine gyrus	R	18	-46	8	3.56	775	0.05 FWE
Cerebellum	R	6	-56	-50	7.59	476	0.05 cluster-level
	R	34	-58	-42	4.52		0.05 cluster-level
	R	30	-64	-50	4.49		0.05 cluster-level
	R	18	-56	-50	4.47		0.05 cluster-level
	L	-40	-70	-50	7.54		0.05 cluster-level
	L	-18	-74	-40	3.38		0.05 cluster-level
Pallidum	R	22	-6	4	3.61	529	0.05 cluster-level
Putamen	R	14	14	-6	3.53		0.05 cluster-level
	R	28	2	-8	3.82	81	0.001 SVC*
	R	24	-2	-10	3.42	37	0.002 SVC*
Amygdala	L	-22	-4	-10	2.78	6	0.015 SVC*

Table 19 **Self no-pain: responders > non-responders**

Abbreviation: FWE = family wise error correction (cluster level). k = cluster size
*SVC = small volume correction. *placebo-induced reductions ROIs, **placebo-induced increases ROIs*

Region	Side	MNI coordinates			Z	k	pvalue (corrected)
Anterior insular cortex	R	32	24	14	2.94	11	0.031 SVC**
Periaqueductal gray matter	R	2	-34	-10	3.60	56	0.001 SVC**

Table 20 **Other pain: non-responders > responders**

Abbreviation: FWE = family wise error correction (cluster level). k = cluster size
*SVC = small volume correction. *placebo-induced reductions ROIs, **placebo-induced increases ROIs*

Region	Side	MNI coordinates			Z	k	pvalue (corrected)
Inferior frontal gyrus (pars opercularis)	R	50	16	32	4.37	717	0.05 FWE
Middle insular cortex	L	-42	-2	-4	3.21	44	0.015 SVC*
	L	-42	0	-10	3.02	98	0.025 SVC*
Posterior insular cortex	L	-46	-6	-2	3.79	45	0.002 SVC*
Superior temporal gyrus	L	-46	-6	-8	4.25	4451	0.05 FWE
Middle temporal gyrus	L	-56	-20	-6	5.55		0.05 FWE
	L	-56	-34	-2	4.77		0.05 FWE
	L	-52	6	-20	4.49		0.05 FWE
	L	-50	-54	2	3.44	1115	0.05 FWE
Inferior temporal gyrus	L	-50	-42	14	4.03	4451	0.05 FWE
	R	46	-40	-16	3.95		0.05 FWE
Fusiform gyrus	R	36	-26	-22	4.95		0.05 FWE
Precuneus	L	-2	-62	48	3.70	327	0.05 cluster-level
	L	-6	-58	58	3.68		0.05 cluster-level
Lingual gyrus	R	28	-66	0	5.43	641	0.05 FWE
	L	-22	-66	2	5.42	1115	0.05 FWE
	L	-20	-54	0	4.94		0.05 FWE
	R	18	-50	-4	4.21	641	0.05 FWE
Calcarine gyrus	L	-20	-76	6	6.03	1115	0.05 FWE
Superior occipital gyrus	R	22	-78	44	4.50	782	0.05 FWE
	R	28	-82	40	4.37		0.05 FWE
	R	26	-68	24	3.44		0.05 FWE
Middle occipital gyrus	R	38	-70	20	4.23		0.05 FWE
Cerebellum	L	-40	-70	-50	7.08	821	0.05 FWE
	L	-24	-80	-48	6.73		0.05 FWE
	L	-24	-90	-26	5.12		0.05 FWE
	R	28	-34	-32	3.33	4451	0.05 FWE
Hippocampus	L	-30	-26	-10	5.24		0.05 FWE
	R	22	-10	-14	4.76		0.05 FWE
Thalamus	R	8	-8	18	5.29		0.05 FWE
	L	-18	-24	14	3.47		0.05 FWE
Amygdala	L	30	-4	-18	4.40		0.05 FWE
	R	22	-8	-12	4.41	41	0.000 SVC*

	L	-26	-6	-14	3.96	65	0.000 SVC*
	L	-28	0	-14	2.98	6	0.009 SVC*
	R	24	2	-16	2.94	9	0.010 SVC*

Table 21 **Other pain: responders > non-responders**

Abbreviation: FWE = family wise error correction (cluster level). k = cluster size
*SVC = small volume correction. *placebo-induced reductions ROIs, **placebo-induced increases ROIs*

Region	Side	MNI coordinates			Z	k	pvalue (corrected)
Aanterior cingulate cortex (rostral part)	R	8	28	-8	3.28	44	0.012 SVC**
Inferior frontal gyrus (pars triangularis)	R	32	30	12	3.63	46	0.004 SVC**

Table 22 **Other no-pain: non-responders > responders**

Abbreviation: FWE = family wise error correction (cluster level). k = cluster size
*SVC = small volume correction. *placebo-induced reductions ROIs, **placebo-induced increases ROIs*

Region	Side	MNI coordinates			Z	k	pvalue (corrected)
Superior frontal gyrus	R	18	40	30	5.16	2371	0.05 FWE
	R	20	16	42	4.66		0.05 FWE
	L	-24	38	36	4.86	782	0.05 FWE
	L	-14	56	20	3.49		0.05 FWE
Superior medial frontal gyrus	R	8	36	52	3.65	2371	0.05 FWE
	L	-2	42	44	3.39		0.05 FWE
Middle frontal gyrus (DLPFC)	L	-32	62	20	4.21	782	0.05 FWE
	R	52	32	34	3.38	2371	0.05 FWE
Inferior frontal gyrus	R	30	12	34	4.87		0.05 FWE
(pars opercularis)	L	-52	18	22	4.16	634	0.05 FWE
	R	48	14	32	3.77	2731	0.05 FWE
	R	56	26	34	3.29		0.05 FWE
Inferior frontal gyrus	R	58	32	30	3.75		0.05 FWE
(pars triangularis)	L	-44	26	16	3.46	634	0.05 FWE
	L	-46	22	18	3.53	151	0.006 SVC**
Supplementary motor area	R	8	22	62	4.24	2731	0.05 FWE
Precentral gyrus	L	-48	-4	38	3.68	634	0.05 FWE
	L	-50	12	34	3.59		0.05 FWE
	L	-50	-14	36	3.17		0.05 FWE
Postcentral gyrus (S1)	L	-60	-8	30	3.17		0.05 FWE
Anterior cingulate cortex (rostral part)	R	10	34	30	3.01	42	0.026 SVC**
	R	14	24	28	2.96		0.029 SVC**
	R	12	28	32	2.88		0.036 SVC**
Anterior insular cortex	R	42	22	-6	2.85	10	0.039 SVC**
Posterior insular cortex	L	-34	-12	2	2.81	83	0.042 SVC*
Middle temporal gyrus	L	-58	-34	-2	4.53	14736	0.05 FWE
Superior parietal gyrus	L	-18	-74	48	4.51		0.05 FWE
	L	-26	-70	52	4.40		0.05 FWE
Fusiform gyrus	R	38	-26	-24	4.43		0.05 FWE
Precuneus	L	-4	-66	48	4.19		0.05 FWE
Cuneus	R	20	-78	44	5.12		0.05 FWE
	L	-12	-90	30	4.95		0.05 FWE

	R	10	-84	24	4.41		0.05 FWE
Lingual gyrus	L	-18	-76	4	6.44		0.05 FWE
	R	28	-66	0	6.43		0.05 FWE
	L	-20	-56	0	5.60		0.05 FWE
	R	18	-50	-2	5.14		0.05 FWE
Calcarine gyrus	R	12	-82	8	4.09		0.05 FWE
Cerebellum	L	-40	-70	-50	> 8		0.05 FWE
	L	-36	-68	-50	> 8		0.05 FWE
	R	8	-88	-38	5.44		0.05 FWE
	R	30	-88	-38	5.31		0.05 FWE
	R	52	-66	-44	5.19		0.05 FWE
	R	38	-36	-42	4.69		0.05 FWE
	R	38	-56	-44	4.46		0.05 FWE
Hippocampus	R	24	-14	-12	4.78		0.05 FWE
	L	-34	-26	-10	4.16		0.05 FWE
Thalamus	L	-14	-26	0	4.62		0.05 FWE
	L	-10	-22	-2	2.85	10	0.039 SVC**
Amygdala	R	24	-10	-12	4.35	65	0.000 SVC*
	R	26	6	-16	3.43	68	0.002 SVC*
	L	-24	-4	-12	3.23	58	0.004 SVC*
	L	-24	0	-12	2.78	6	0.015 SVC*